

# **Supplementary Information**

## **Benzobisthiadiazole-based high-spin donor-acceptor conjugated polymers with localized spin distribution**

Md Abdus Sabuj,<sup>†</sup> Md Masrul Huda,<sup>†,‡</sup> Chandra Shekar Sarap,<sup>†,‡</sup> and Neeraj  
Rai<sup>\*,†</sup>

*†Dave C. Swalm School of Chemical Engineering, and Center for Advanced Vehicular  
Systems, Mississippi State University, Mississippi State, MS 39762, USA.*

*‡These authors contributed equally*

E-mail: neerajrai@che.msstate.edu

**Table S1:** Calculated electronic properties of CPDT-BBT dimer ( $N = 2$ ) at different functional and 6-31G(d,p) basis set. The computed singlet–triplet energy gap ( $\Delta E_{ST}$ ), diradical character index ( $y_0$ ), tetraradical character index ( $y_1$ ), spin-squared values of broken-symmetry (BS) singlet ( $\langle S_{BS}^2 \rangle$ ) and triplet state  $\langle S_T^2 \rangle$ . Calculated properties are on fully optimized geometries at all the functional.

Functional	$\Delta E_{ST}$	$y_0$	$y_1$	$\langle S_{BS}^2 \rangle$	$\langle S_T^2 \rangle$
BYLP	-0.123	0.033	0.000	0.001	2.000
B3YLP	-0.078	0.604	0.000	1.134	2.007
PBE1PBE	-0.113	0.580	0.000	1.658	2.020
BHandHLYP	-0.108	0.825	0.290	6.192	2.420
M062X	-0.098	0.770	0.130	4.358	2.152
CAM-B3LYP	-0.071	0.615	0.238	1.950	2.008
$\omega$ B97XD	-0.123	0.707	0.250	4.091	2.153

**Table S2:** Computed singlet–triplet energy gap and diradical index for the CPDS-BBT and CPDS-iso-BBT using OT-(S)RSH (with LC- $\omega$ HPBE) functional at 6-31G(d,p) basis set, along with the tuned range-separating parameter ( $\omega$ ) (Bohr<sup>-1</sup>). For comparison, B3LYP values are also shown.

Polymer	$N$	$\Delta E_{ST}$			$y_0$	OT-RSH	OT-SRSH	$\omega$
		(U)B3LYP	OT-RSH	OT-SRSH				
CPDS-BBT	2	$-4.88 \times 10^{-2}$	$-8.38 \times 10^{-2}$	$-7.85 \times 10^{-2}$	0.700	0.750	0.890	0.75
	4	$-7.51 \times 10^{-4}$	$-20.70 \times 10^{-4}$	$-18.90 \times 10^{-4}$	0.984	0.987	0.981	0.42
CPDS-iso-BBT	2	$-9.20 \times 10^{-1}$	$-12.84 \times 10^{-1}$	$-11.47 \times 10^{-1}$	0.000	0.000	0.000	0.10
	4	$-7.90 \times 10^{-1}$	$-11.53 \times 10^{-1}$	$-10.16 \times 10^{-1}$	0.000	0.000	0.000	0.75

**Table S3:** Calculated electronic properties at (U)B3LYP/6-31G(d,p) level of theory and basis set for the CPDS-BBT heptamer ( $N = 7$ ) with BBT (A) and CPDS (D) end groups. The computed singlet–triplet energy gap ( $\Delta E_{ST}$ ), population ( $P_T$ ) of the triplet ( $S = 1$ ) state at room temperature, energy of the FMOs, energetic difference between the FMOs ( $E_g$ ), and diradical character index ( $y_0$ ) of the polymers. Energy values are provided in eV, and  $y_0$  is a dimensionless quantity.

Polymer	End groups	$\Delta E_{ST}$	$P_T$	HOMO	LUMO	$E_g$	$y_0$
CPDS-BBT	D	$-2.72 \times 10^{-6}$	74.99	-4.42	-3.31	1.11	1.00
	A	$-2.45 \times 10^{-5}$	74.99	-4.62	-3.54	1.08	1.00

**Table S4:** Electronic properties at (U)B3LYP/6-31G(d,p) level of theory and basis set for the BBT- and iso-BBT-based polymers, provided as a function of chain length ( $N$ ). The singlet–triplet energy gap ( $\Delta E_{\text{ST}}$ ), population ( $P_{\text{T}}$ ) of the triplet ( $S = 1$ ) state at room temperature, energy of the FMOs, energetic difference between the FMOs ( $E_g$ ), and diradical character index ( $y_0$ ) of the polymers. Energy values are provided in eV, and  $y_0$  is a dimensionless quantity.

Polymer	$N$	$\Delta E_{\text{ST}}$	$P_{\text{T}}$	HOMO	LUMO	$E_g$	$y_0$
CPDT-BBT	1	$-4.09 \times 10^{-1}$	0.00	-5.02	-3.36	1.66	0.040
	2	$-7.85 \times 10^{-2}$	14.37	-4.61	-3.43	1.18	0.604
	3	$-1.62 \times 10^{-2}$	62.31	-4.50	-3.48	1.02	0.879
	4	$-3.37 \times 10^{-3}$	72.61	-4.44	-3.50	0.95	0.966
	5	$-6.99 \times 10^{-4}$	74.52	-4.42	-3.51	0.91	0.990
	6	$-1.44 \times 10^{-4}$	74.90	-4.40	-3.51	0.89	0.997
	7	$-2.99 \times 10^{-5}$	74.98	-4.39	-3.52	0.88	0.999
	8	$-5.44 \times 10^{-6}$	74.99	-4.39	-3.52	0.88	1.000
CPDT-iso-BBT	1	$-13.80 \times 10^{-1}$	0.00	-5.37	-2.81	2.56	0.000
	2	$-10.50 \times 10^{-1}$	0.00	-5.08	-3.07	2.01	0.000
	3	$-9.70 \times 10^{-1}$	0.00	-4.98	-3.18	1.80	0.000
	4	$-9.50 \times 10^{-1}$	0.00	-4.93	-3.24	1.69	0.000
	5	$-9.40 \times 10^{-1}$	0.00	-4.91	-3.27	1.64	0.000
	6	$-9.40 \times 10^{-1}$	0.00	-4.89	-3.29	1.60	0.000
	7	$-9.40 \times 10^{-1}$	0.00	-4.88	-3.30	1.58	0.000
	8	$-9.40 \times 10^{-1}$	0.00	-4.88	-3.31	1.57	0.000
CPDS-BBT	1	$-3.76 \times 10^{-1}$	0.00	-5.03	-3.38	1.64	0.070
	2	$-4.88 \times 10^{-2}$	33.26	-4.61	-3.46	1.16	0.700
	3	$-6.13 \times 10^{-3}$	70.54	-4.51	-3.50	1.02	0.931
	4	$-7.51 \times 10^{-4}$	74.48	-4.47	-3.51	0.96	0.984
	5	$-9.25 \times 10^{-5}$	74.94	-4.45	-3.52	0.93	0.996
	6	$-1.09 \times 10^{-5}$	74.99	-4.44	-3.52	0.91	0.999
	7	$-0.00 \times 10^0$	75.00	-4.43	-3.52	0.90	1.000
	8	$-0.00 \times 10^0$	75.00	-4.43	-3.53	0.89	1.000
CPDS-iso-BBT	1	$-12.70 \times 10^{-1}$	0.00	-5.32	-2.87	2.45	0.000
	2	$-9.20 \times 10^{-1}$	0.00	-5.00	-3.17	1.83	0.000
	3	$-8.20 \times 10^{-1}$	0.00	-4.89	-3.29	1.60	0.000
	4	$-7.90 \times 10^{-1}$	0.00	-4.84	-3.36	1.48	0.000
	5	$-7.80 \times 10^{-1}$	0.00	-4.81	-3.39	1.42	0.000
	6	$-7.80 \times 10^{-1}$	0.00	-4.79	-3.41	1.38	0.000
	7	$-7.80 \times 10^{-1}$	0.00	-4.78	-3.43	1.35	0.000
	8	$-7.80 \times 10^{-1}$	0.00	-4.77	-3.44	1.33	0.000

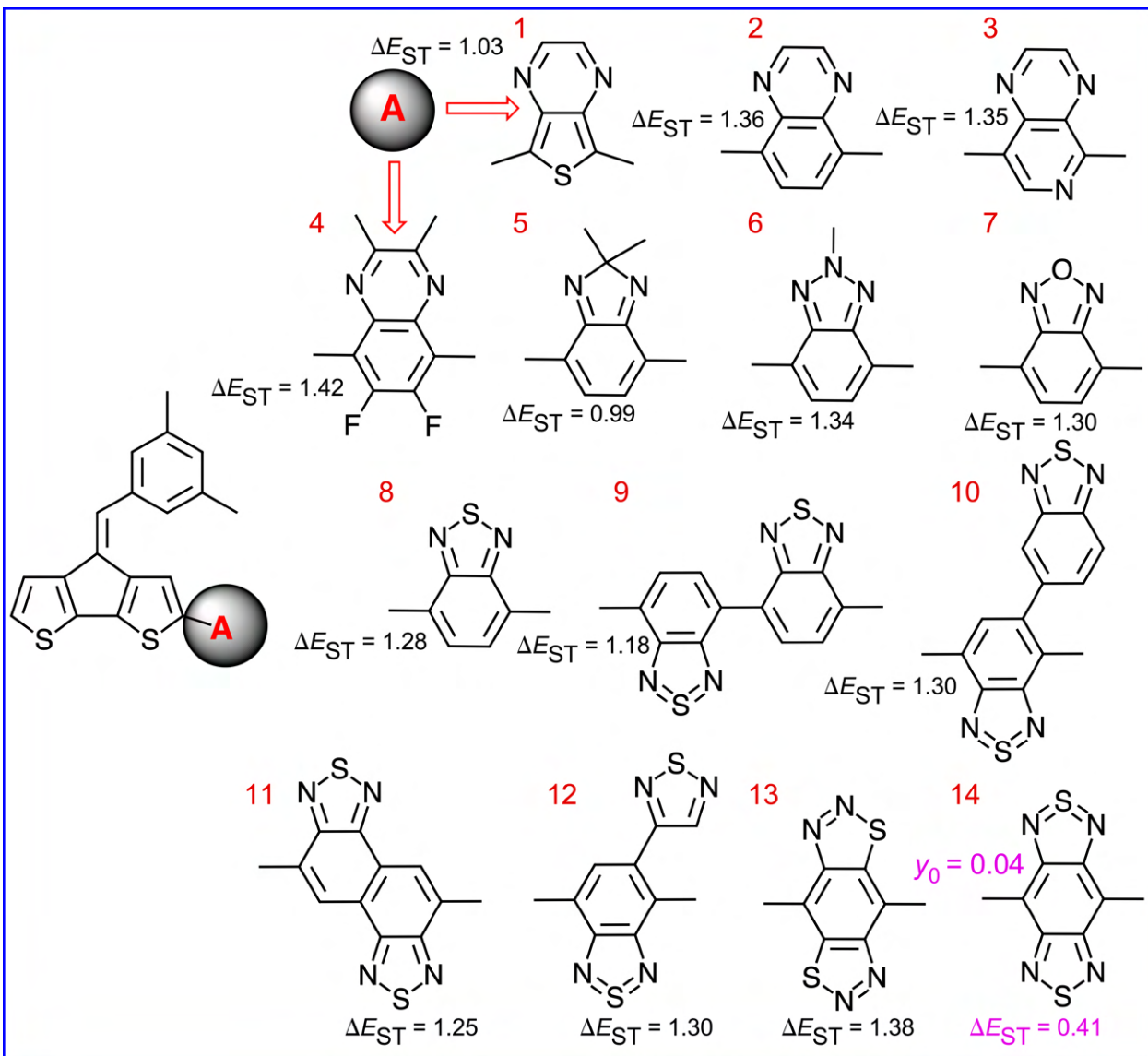


**Figure S1:** Selected acceptors from an extensive screening study are provided with  $\Delta E_{ST}$  and  $y_0$  at  $N = 1$ . Except the CPDT-BBT ( $N = 1$ ) combination, all other donor-acceptor show a closed-shell ( $y_0 = 0.0$ ) configuration. Calculations are performed with (U)B3LYP/6-31G(d,p) theory and basis set. Energy values are provided in eV, and  $y_0$  is a dimensionless quantity.

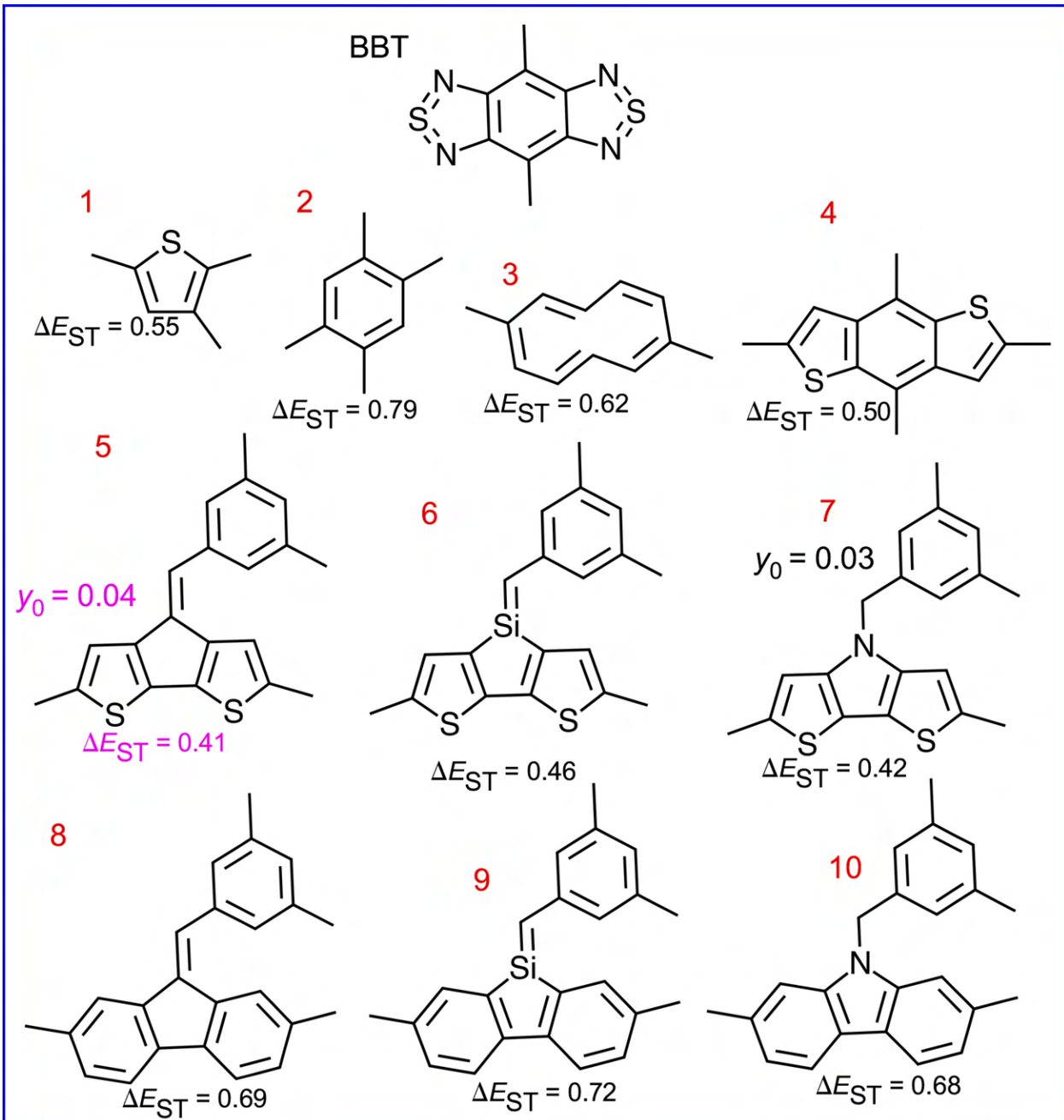


**Figure S2:** The calculated  $\Delta E_{ST}$  and  $y_0$  with different donors and BBT (top) acceptor. The CPDT-BBT ( $N = 1$ ) provides smallest  $\Delta E_{ST}$  and a larger  $y_0$  than the other D–A combinations. Calculations are performed with (U)B3LYP/6-31G(d,p) theory and basis set. Energy values are provided in eV, and  $y_0$  is a dimensionless quantity.

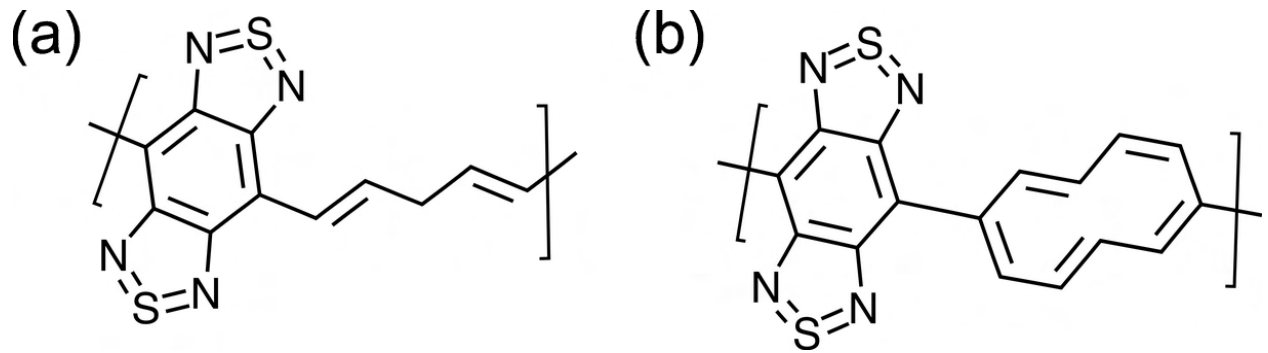


**Figure S3:** Non-aromatic donors (A) pentadiene and (b) [10]annulene  $\pi$ -conjugated with the BBT acceptor.

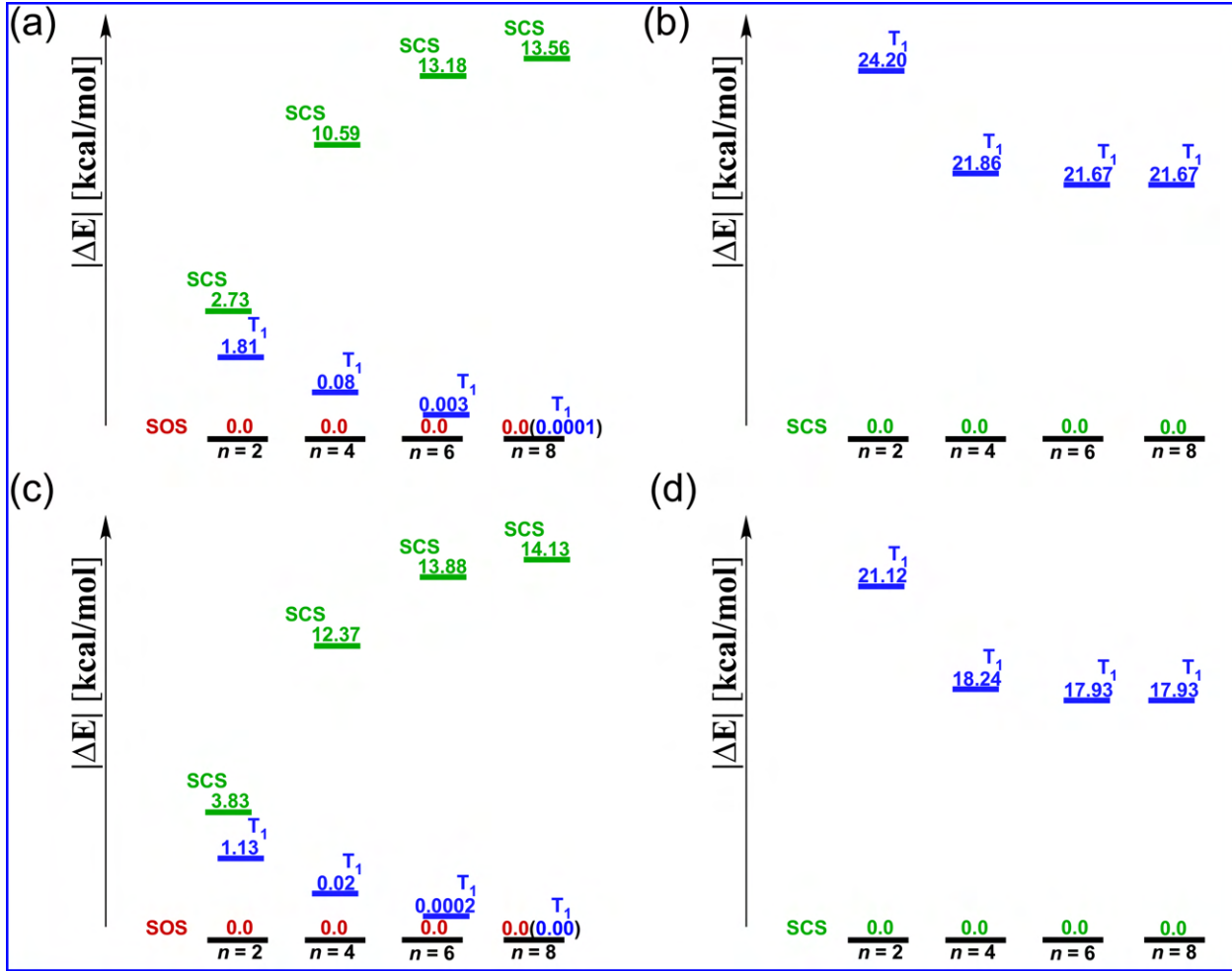


**Figure S4:** Absolute value of  $\Delta E_{ST}$  of the polymers as a function of  $N$  showing the change in relative energies of the various spin states with reference to singlet open-shell (SOS) state. As the number of monomer increases, the energy gap between SOS and triplet state ( $T_1$ ) decreases rapidly, increasing the gap with singlet closed-shell (SCS) state. The singlet open-shell and triplet states are nearly degenerate in the CPDT-BBT octamer ( $N = 8$ ) ( $\Delta E_{ST} = 1 \times 10^{-4}$  kcal/mol) and degenerate in the CPDS-BBT octamer ( $N = 8$ ) ( $\Delta E_{ST} = 0.00$  kcal/mol). However, the iso-BBT based polymers have a large  $\Delta E_{ST}$  in reference to the ground-state SCS, becomes constant at  $N = 6$ .

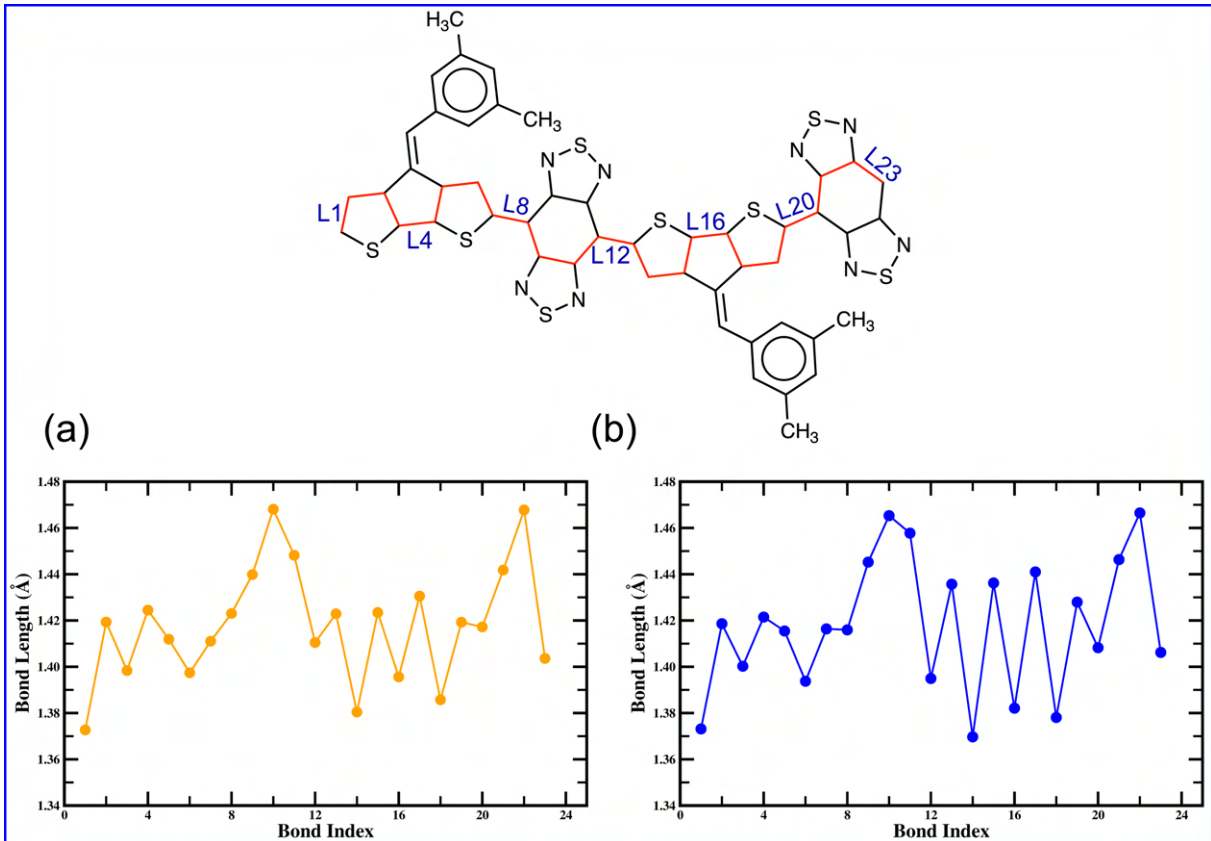


**Figure S5:** Calculated bond lengths ( $\text{\AA}$ ) of the CPDT-BBT dimer ( $N = 2$ ) for (a) singlet ( $S = 0$ ) and (b) triplet states ( $S = 1$ ).

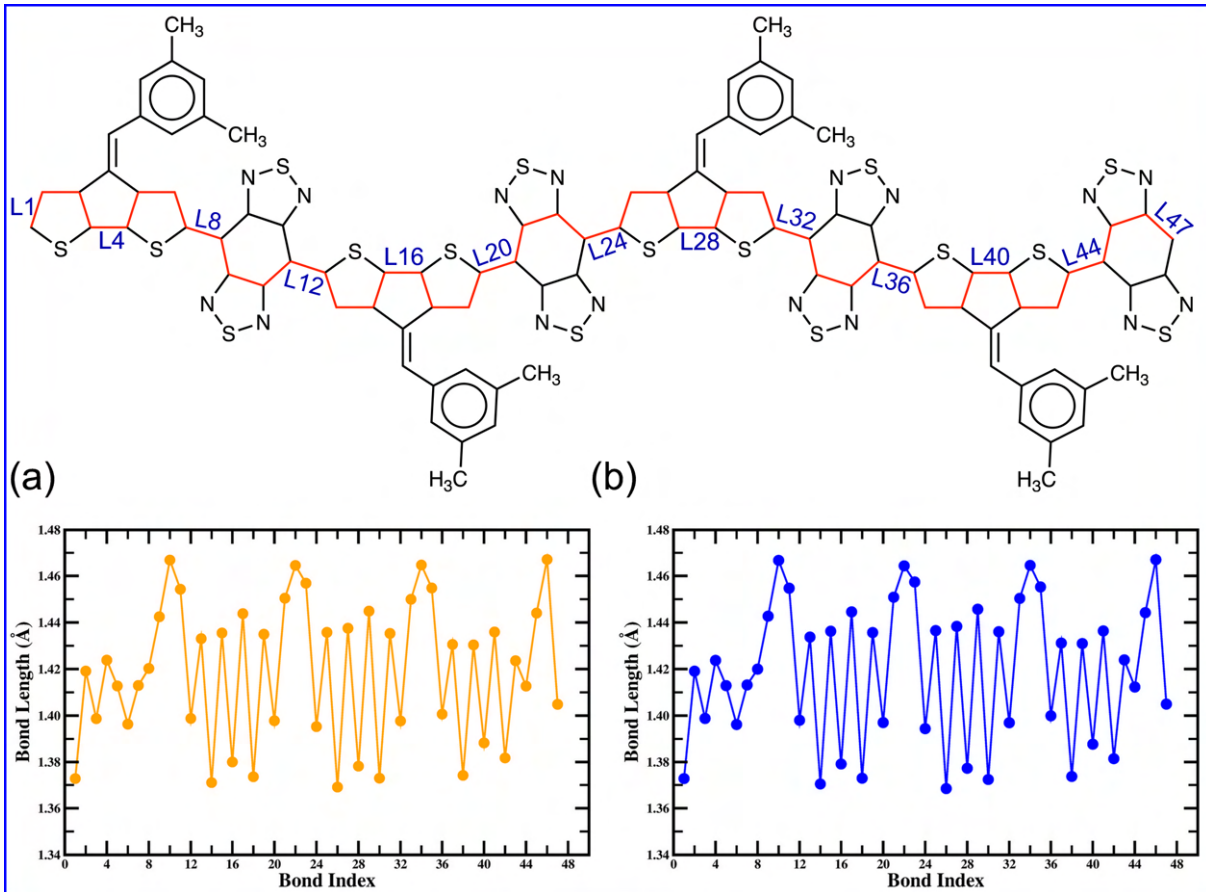


**Figure S6:** Calculated bond lengths ( $\text{\AA}$ ) of the CPDT-BBT tetramer ( $N = 4$ ) for (a) singlet ( $S = 0$ ) and (b) triplet states ( $S = 1$ ).

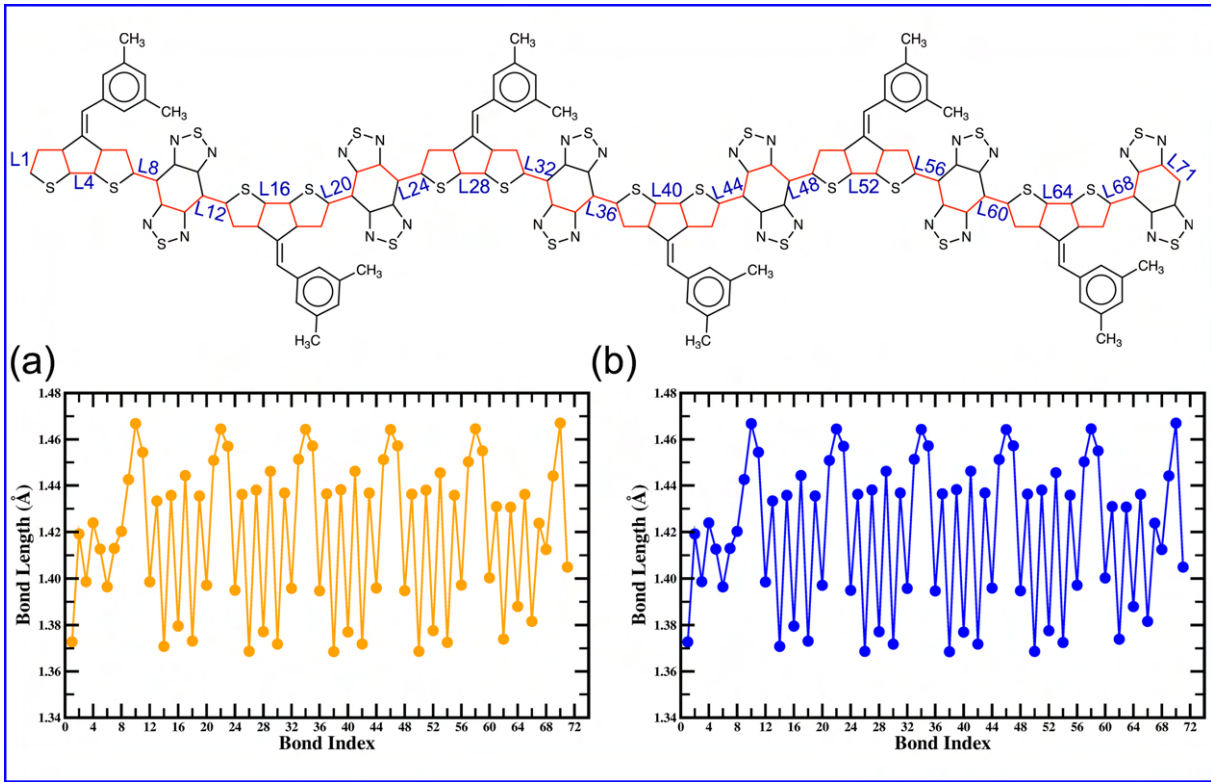


**Figure S7:** Calculated bond lengths ( $\text{\AA}$ ) of the CPDT-BBT hexamer ( $N = 6$ ) for (a) singlet ( $S = 0$ ) and (b) triplet states ( $S = 1$ ).

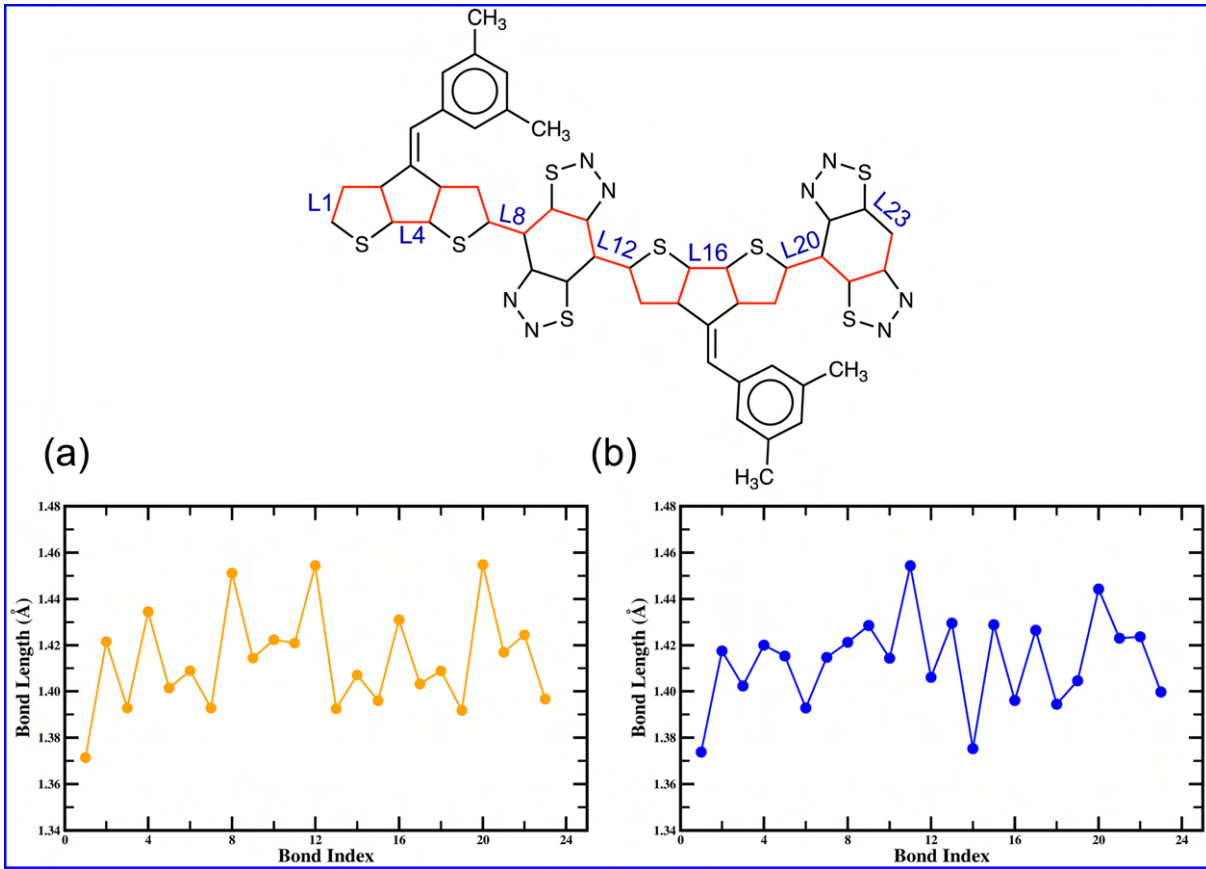


**Figure S8:** Calculated bond lengths ( $\text{\AA}$ ) of the CPDT-iso-BBT dimer ( $N = 2$ ) for (a) singlet ( $S = 0$ ) and (b) triplet states ( $S = 1$ ).

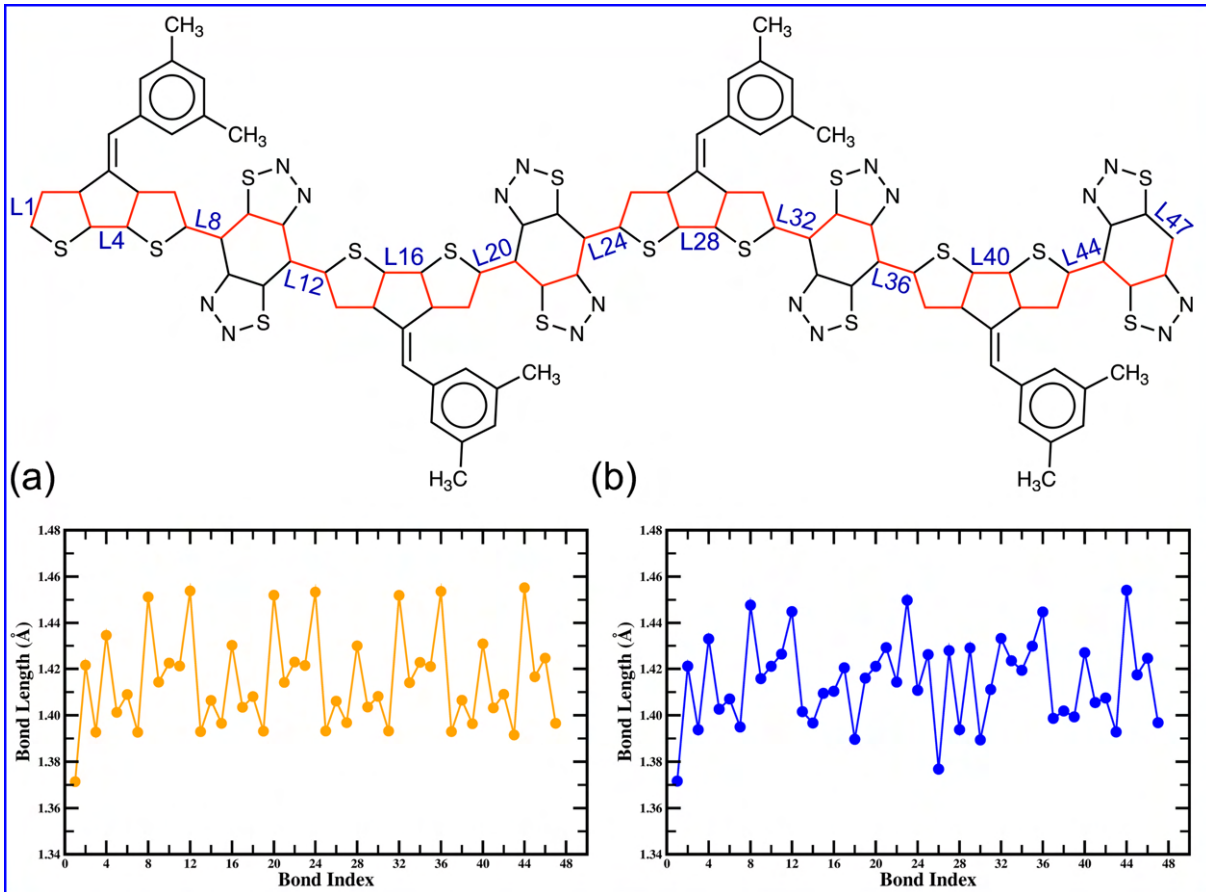


**Figure S9:** Calculated bond lengths ( $\text{\AA}$ ) of the CPDT-iso-BBT tetramer ( $N = 4$ ) for (a) singlet ( $S = 0$ ) and (b) triplet states ( $S = 1$ ).

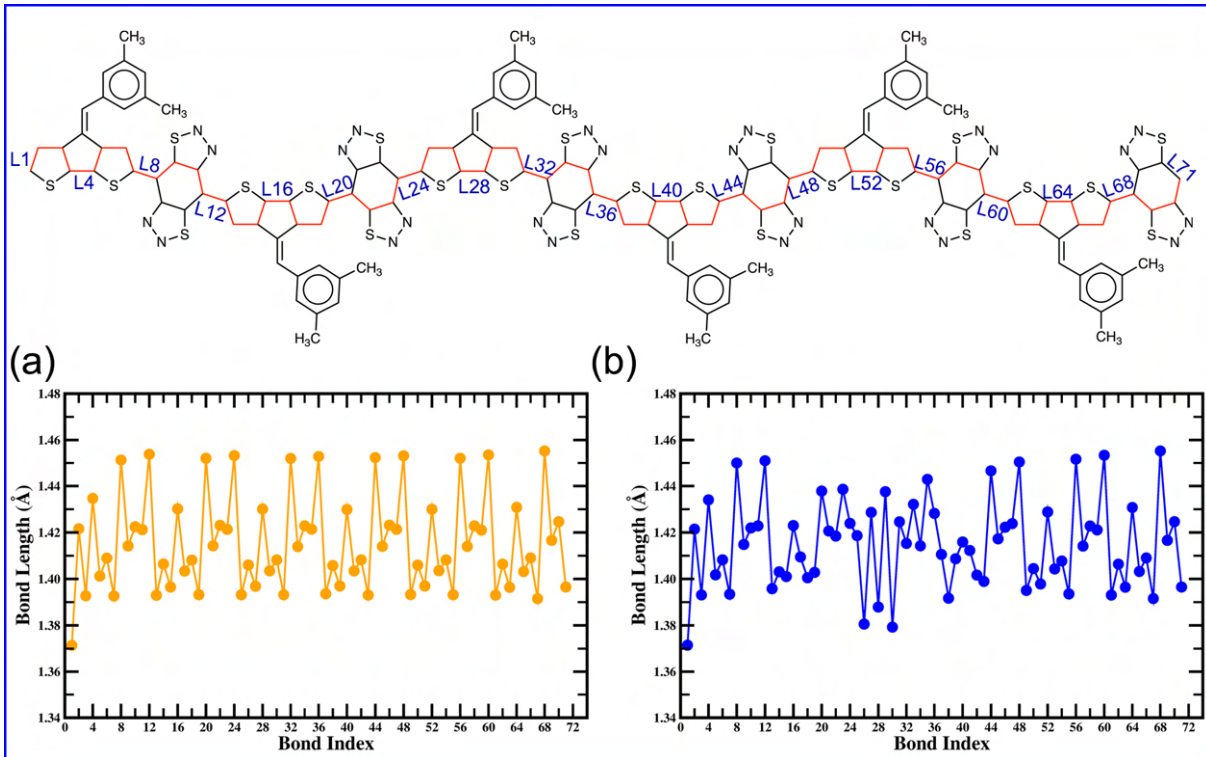


**Figure S10:** Calculated bond lengths ( $\text{\AA}$ ) of the CPDT-iso-BBT hexamer ( $N = 6$ ) for (a) singlet ( $S = 0$ ) and (b) triplet states ( $S = 1$ ).

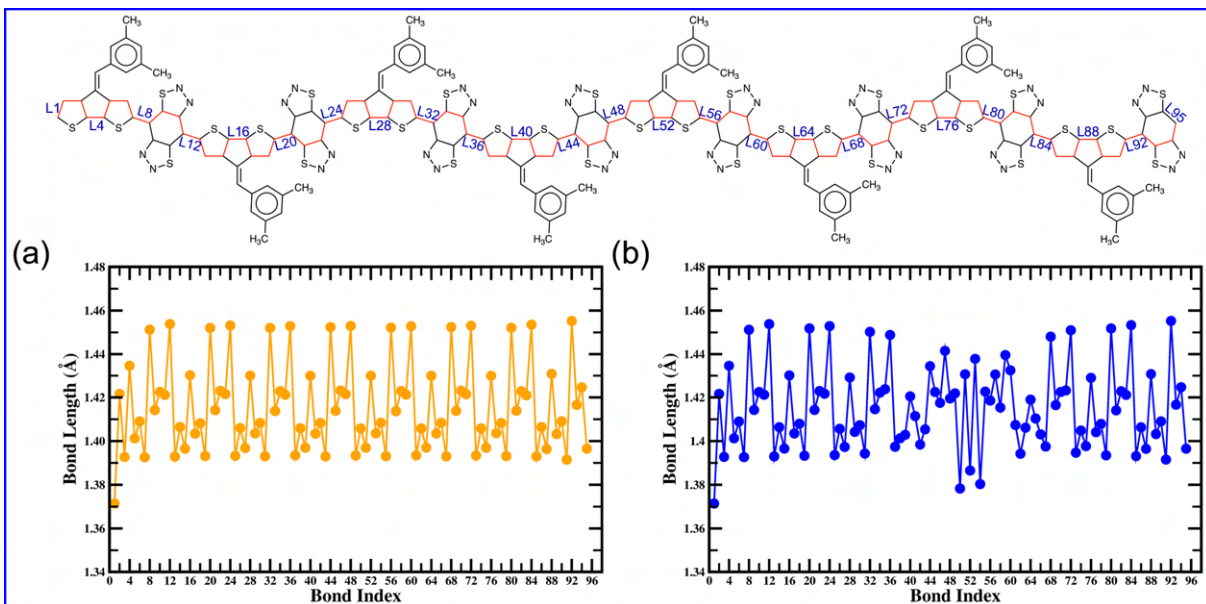


**Figure S11:** Calculated bond lengths ( $\text{\AA}$ ) of the CPDT-iso-BBT octamer ( $N = 8$ ) for (a) singlet ( $S = 0$ ) and (b) triplet states ( $S = 1$ ).

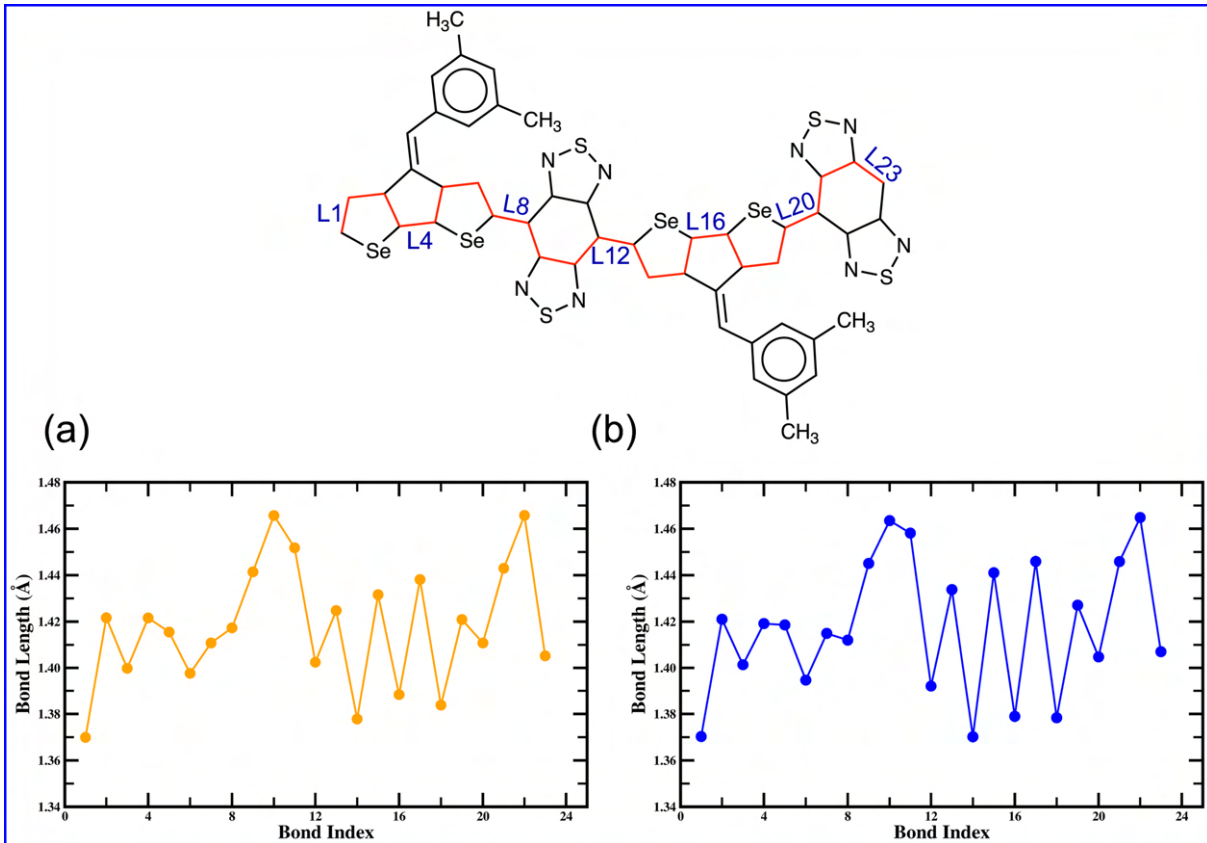


**Figure S12:** Calculated bond lengths ( $\text{\AA}$ ) of the CPDS-BBT dimer ( $N = 2$ ) for (a) singlet ( $S = 0$ ) and (b) triplet states ( $S = 1$ ).

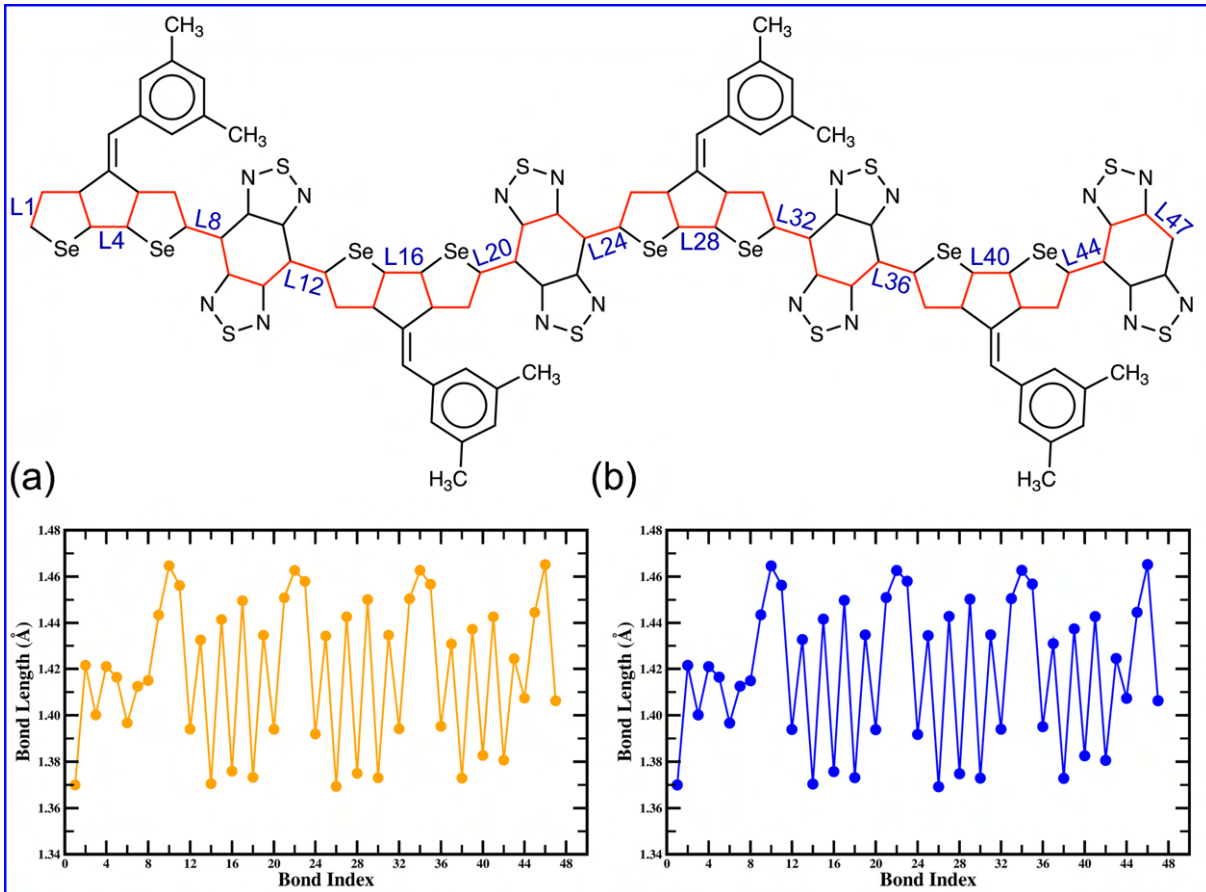


**Figure S13:** Calculated bond lengths ( $\text{\AA}$ ) of the CPDS-BBT tetramer ( $N = 4$ ) for (a) singlet ( $S = 0$ ) and (b) triplet states ( $S = 1$ ).

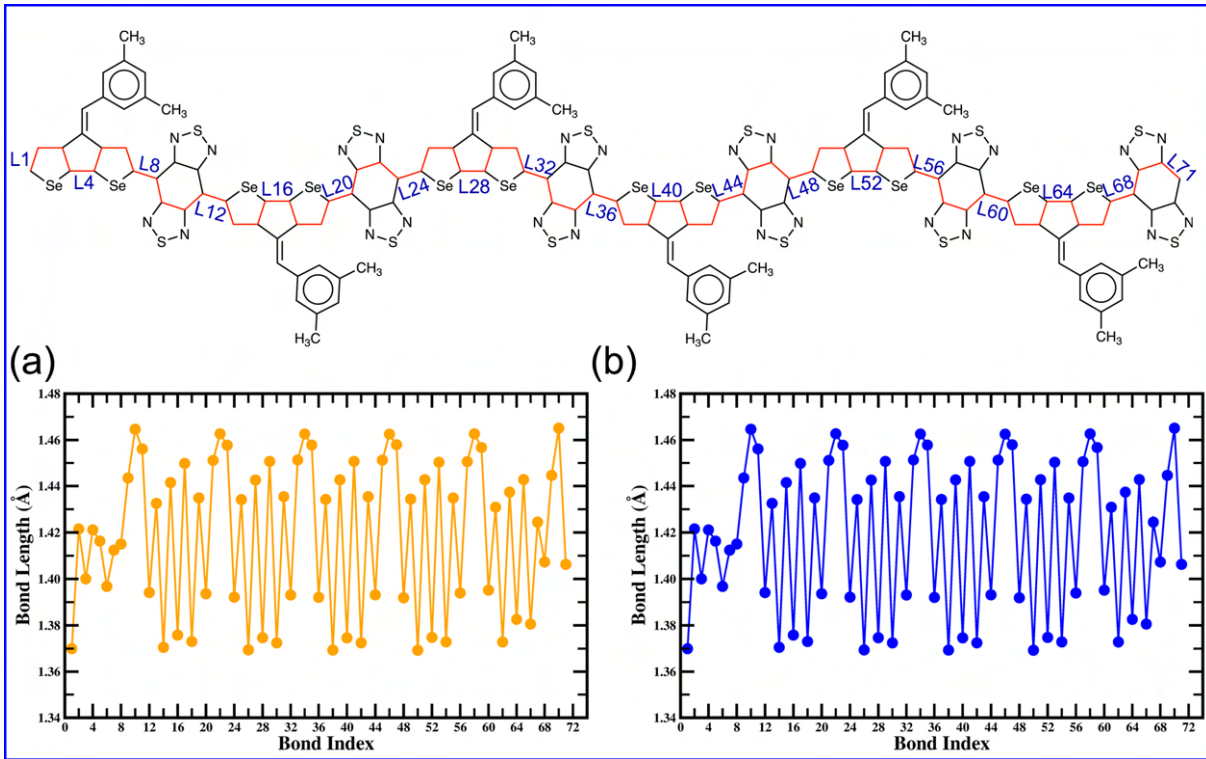


**Figure S14:** Calculated bond lengths ( $\text{\AA}$ ) of the CPDS-BBT hexamer ( $N = 6$ ) for (a) singlet ( $S = 0$ ) and (b) triplet states ( $S = 1$ ).

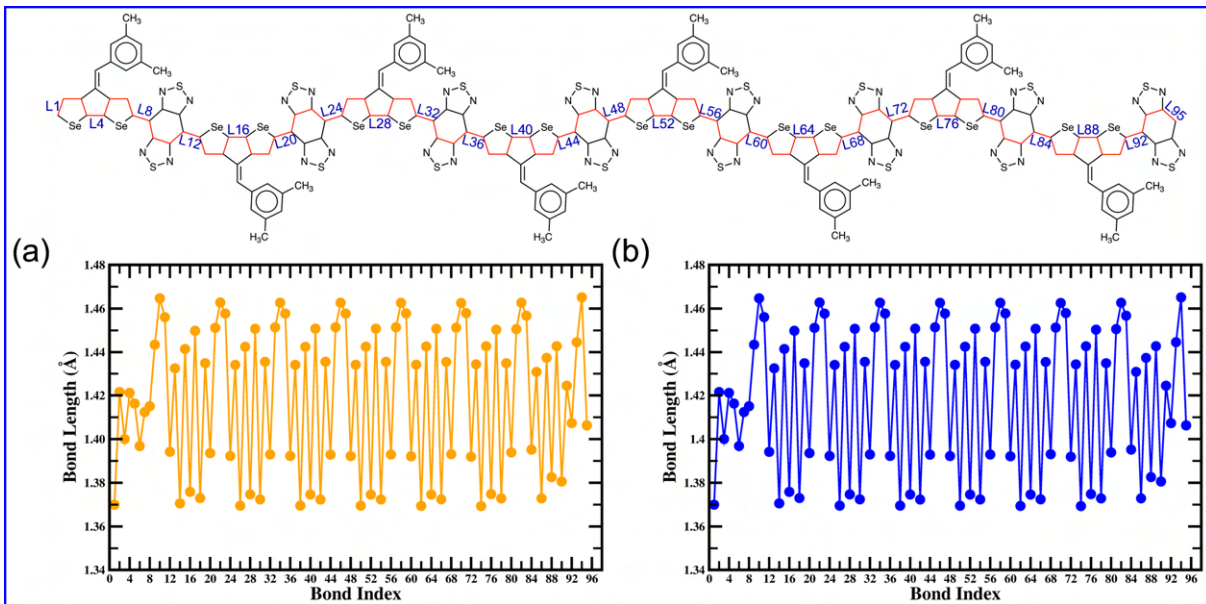


**Figure S15:** Calculated bond lengths ( $\text{\AA}$ ) of the CPDS-BBT octamer ( $N = 8$ ) for (a) singlet ( $S = 0$ ) and (b) triplet states ( $S = 1$ ).

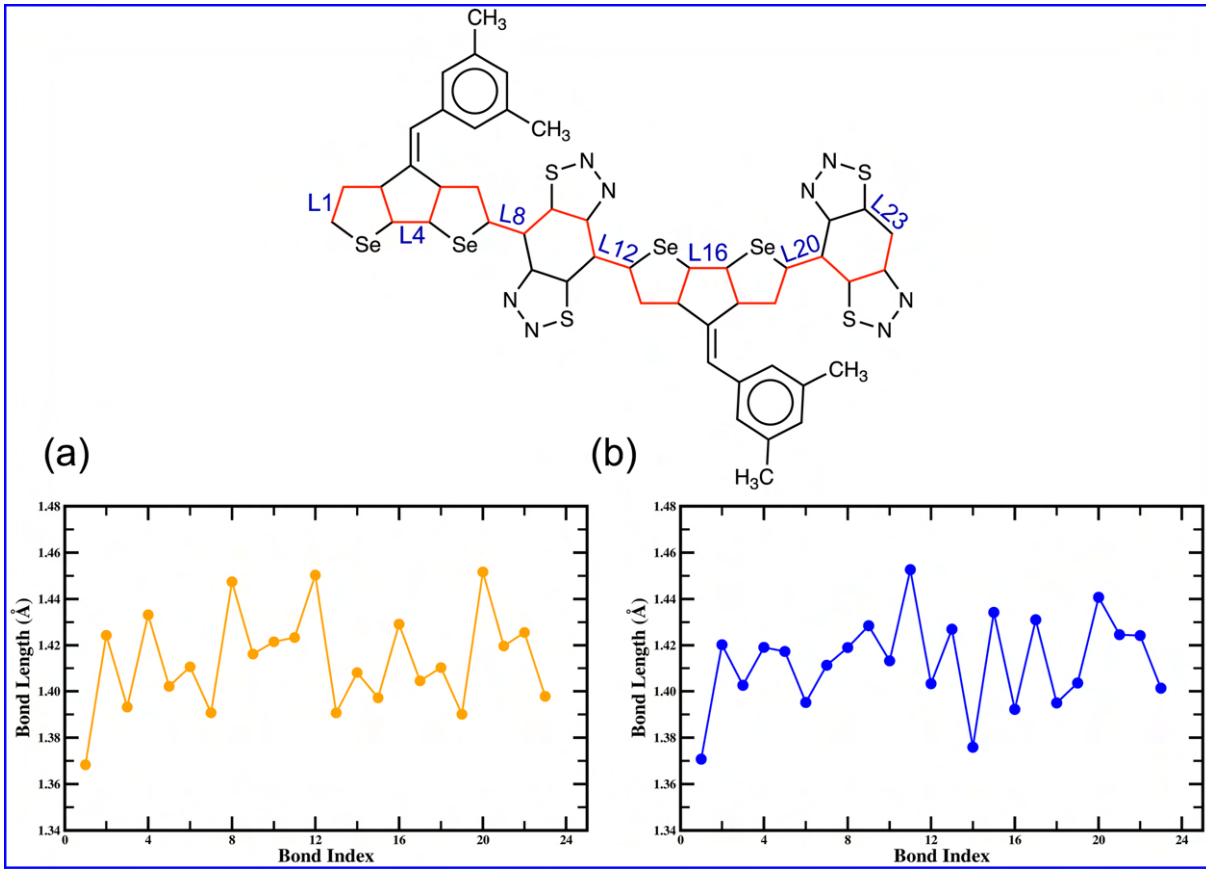


**Figure S16:** Calculated bond lengths ( $\text{\AA}$ ) of the CPDS-iso-BBT dimer ( $N = 2$ ) for (a) singlet ( $S = 0$ ) and (b) triplet states ( $S = 1$ ).

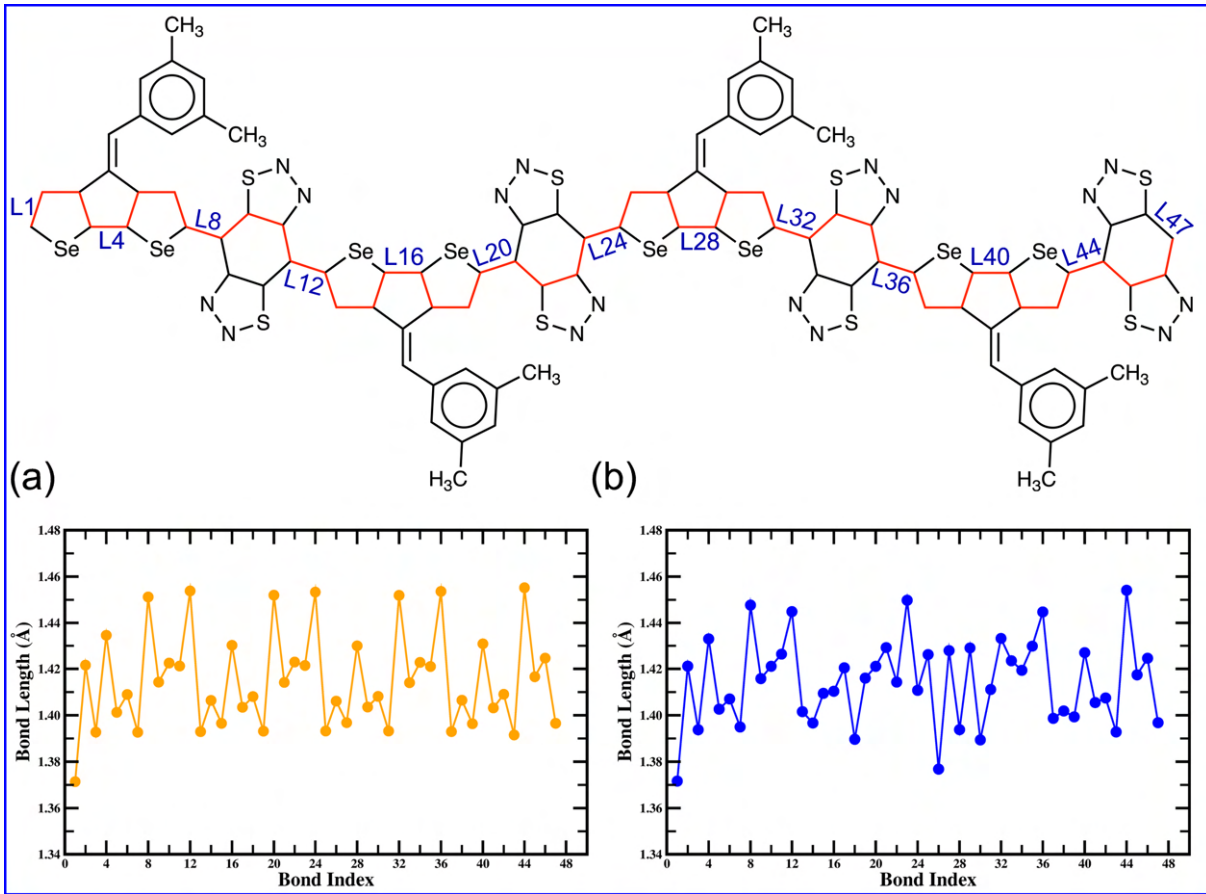


**Figure S17:** Calculated bond lengths ( $\text{\AA}$ ) of the CPDS-iso-BBT tetramer ( $N = 4$ ) for (a) singlet ( $S = 0$ ) and (b) triplet states ( $S = 1$ ).

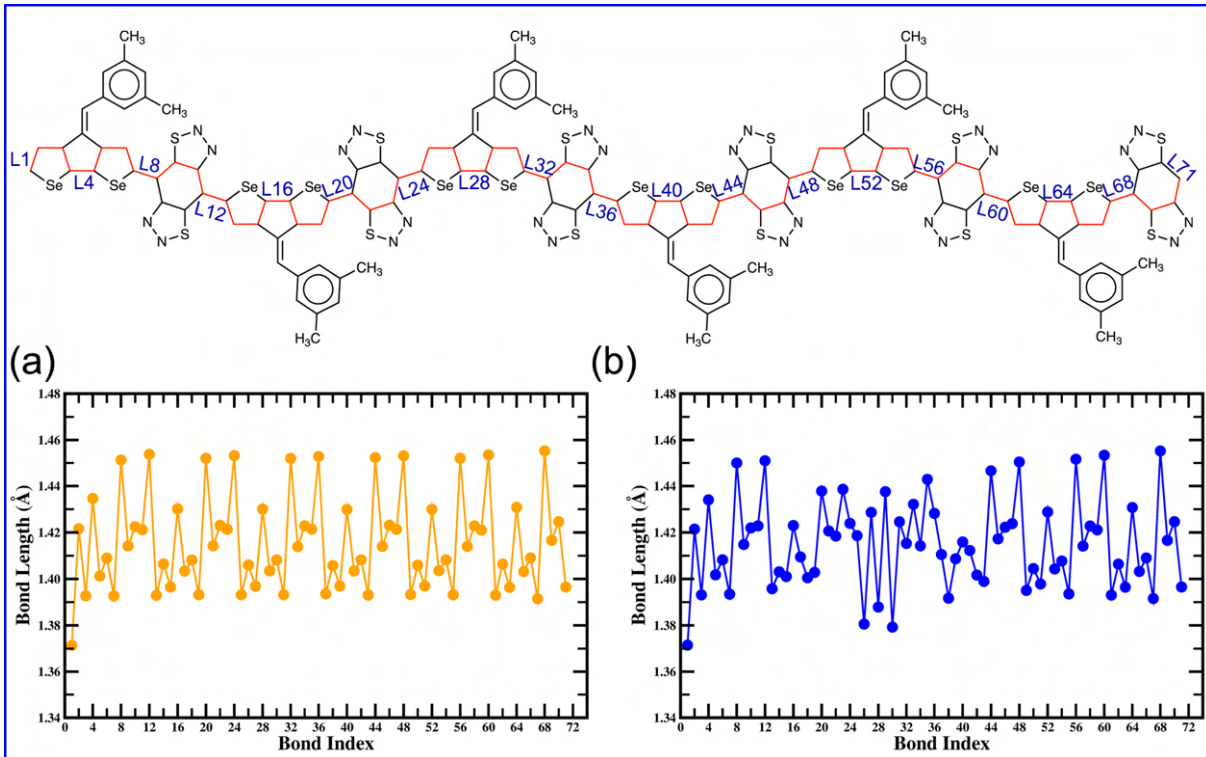


**Figure S18:** Calculated bond lengths ( $\text{\AA}$ ) of the CPDS-iso-BBT hexamer ( $N = 6$ ) for (a) singlet ( $S = 0$ ) and (b) triplet states ( $S = 1$ ).

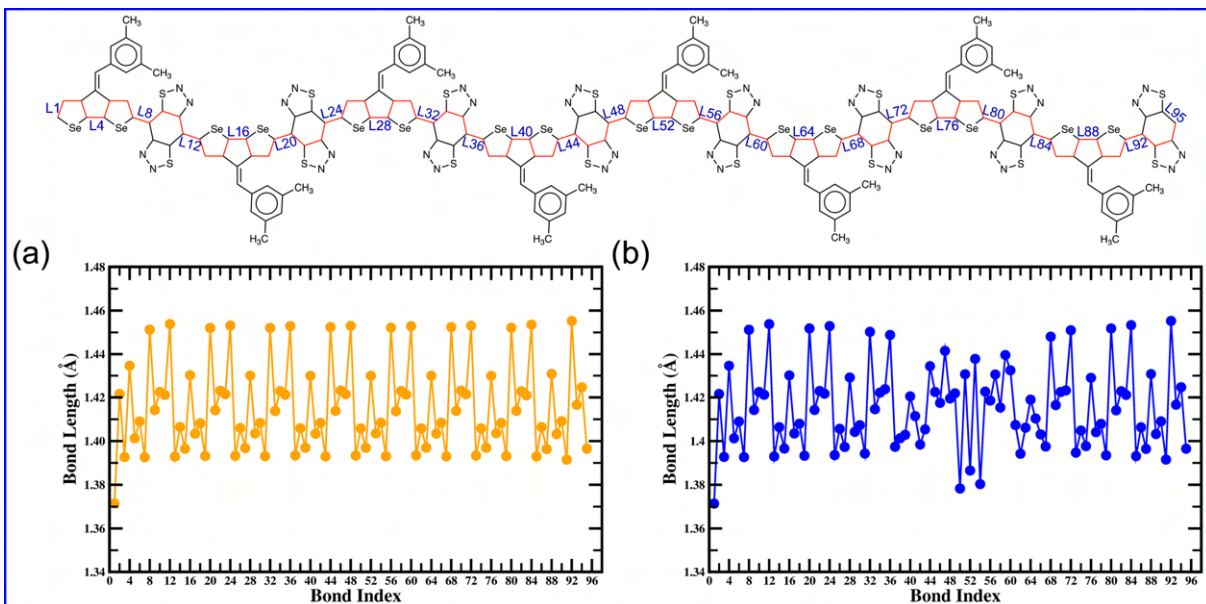


**Figure S19:** Calculated bond lengths ( $\text{\AA}$ ) of the CPDS-iso-BBT octamer ( $N = 8$ ) for (a) singlet ( $S = 0$ ) and (b) triplet states ( $S = 1$ ).

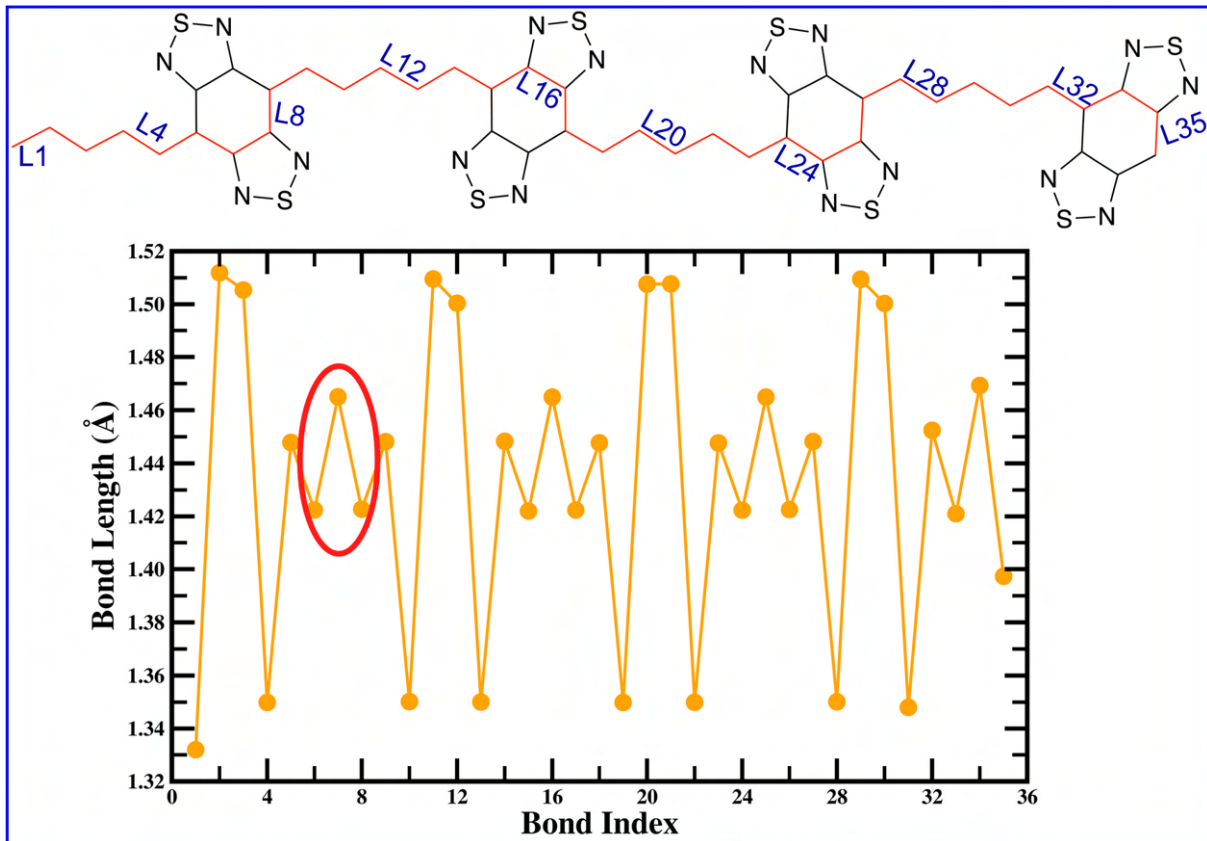


**Figure S20:** Calculated bond lengths ( $\text{\AA}$ ) of the pentadiene-BBT tetramer ( $N = 4$ ) for the singlet ( $S = 0$ ) state. Inclusion of the non-aromatic donor reduces the BLA at the core of the BBT acceptor (red circle), reducing the quinoidal character.

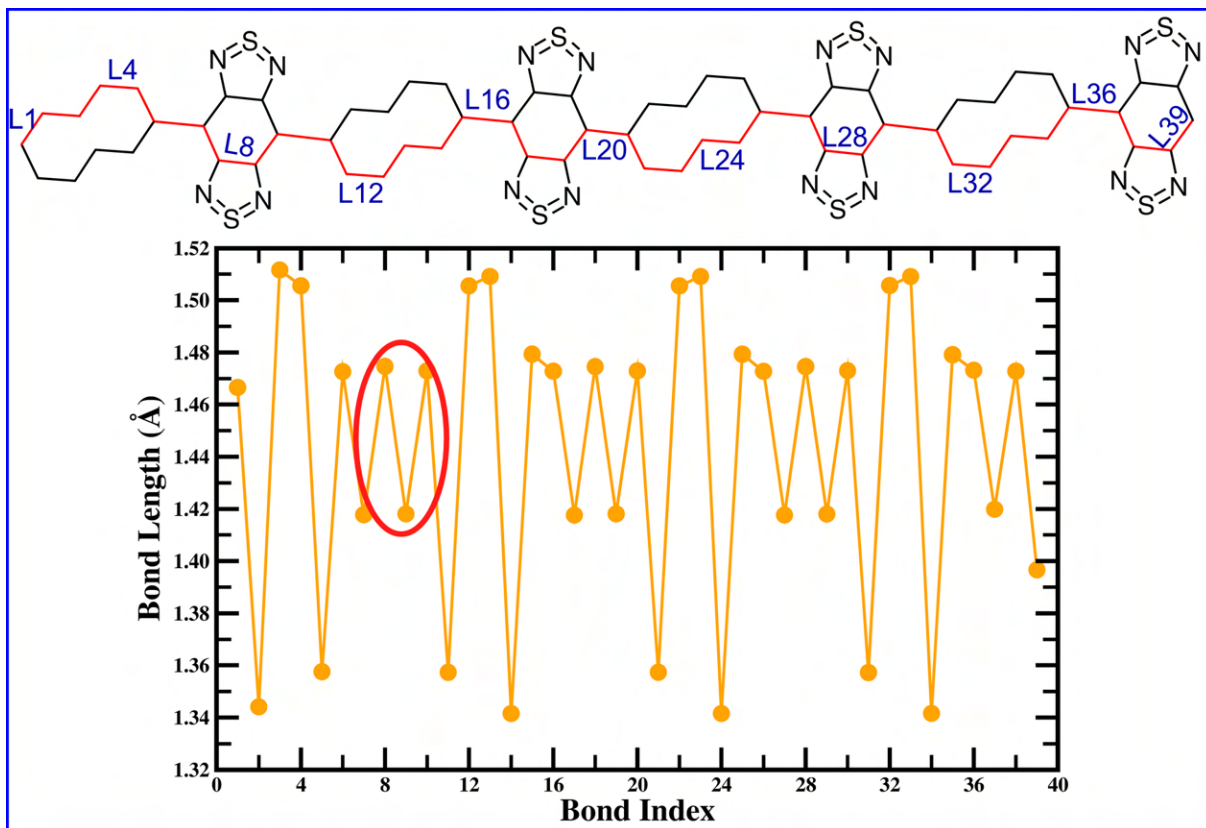


**Figure S21:** Calculated bond lengths ( $\text{\AA}$ ) of the [10]Annulene-BBT tetramer ( $N = 4$ ) for the singlet ( $S = 0$ ) state. Inclusion of the non-aromatic donor reduces the BLA at the core of the BBT acceptor (red circle), reducing the quinoidal character.

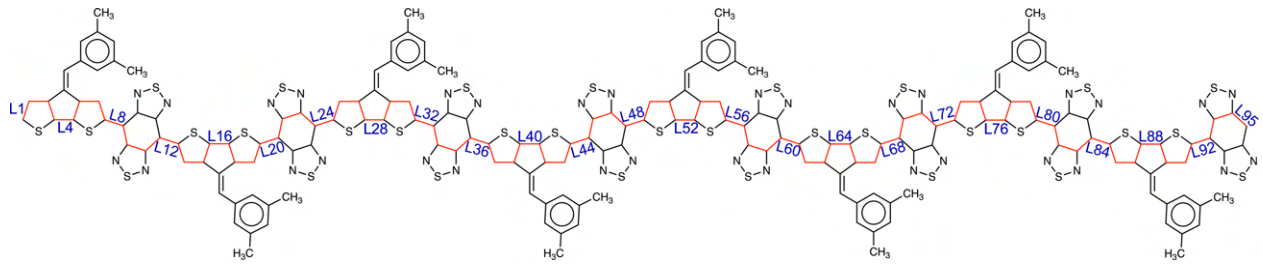


**Table S5:** Calculated bond lengths ( $\text{\AA}$ ) of CPDT-BBT octamer ( $N = 8$ ) in the singlet and triplet states.

Bond index	singlet ( $S = 0$ )	triplet ( $S = 1$ )	Bond index	singlet ( $S = 0$ )	triplet ( $S = 1$ )
1	1.37276	1.37276	49	1.43631	1.43631
2	1.41917	1.41917	50	1.36867	1.36867
3	1.39863	1.39863	51	1.43812	1.43812
4	1.42398	1.42398	52	1.37699	1.37699
5	1.41263	1.41263	53	1.44634	1.44634
6	1.39647	1.39647	54	1.37169	1.37169
7	1.41291	1.41291	55	1.43694	1.43694
8	1.42033	1.42032	56	1.39561	1.39561
9	1.44253	1.44253	57	1.45686	1.45144
10	1.46688	1.46687	58	1.46468	1.46431
11	1.45437	1.45437	59	1.45125	1.45714
12	1.39861	1.39860	60	1.39476	1.39475
13	1.43330	1.43330	61	1.43639	1.43639
14	1.37088	1.37088	62	1.36860	1.36860
15	1.43573	1.43573	63	1.43818	1.43818
16	1.37958	1.37958	64	1.37700	1.37700
17	1.44434	1.44434	65	1.44624	1.44624
18	1.37308	1.37308	66	1.37181	1.37181
19	1.43553	1.43553	67	1.43684	1.43684
20	1.39707	1.39707	68	1.39585	1.39585
21	1.45091	1.45091	69	1.45127	1.45126
22	1.46453	1.46453	70	1.46425	1.46425
23	1.45691	1.45691	71	1.45720	1.45720
24	1.39510	1.39510	72	1.39479	1.39479
25	1.43613	1.43614	73	1.43626	1.43626
26	1.36881	1.36880	74	1.36870	1.36870
27	1.43795	1.43795	75	1.43801	1.43802
28	1.37715	1.37715	76	1.37758	1.37758
29	1.44621	1.44621	77	1.44552	1.44552
30	1.37176	1.37176	78	1.37252	1.37251
31	1.43687	1.43687	79	1.43586	1.43587
32	1.39566	1.39566	80	1.39713	1.39713
33	1.45144	1.45144	81	1.45030	1.45030
34	1.46438	1.46438	82	1.46458	1.46458
35	1.45703	1.45703	83	1.45501	1.45501
36	1.39493	1.39493	84	1.40030	1.40030
37	1.43628	1.43628	85	1.43092	1.43093
38	1.36871	1.36871	86	1.37396	1.37396
39	1.43804	1.43804	87	1.43069	1.43069
40	1.37701	1.37701	88	1.38798	1.38798
41	1.44635	1.44635	89	1.43621	1.43621
42	1.37169	1.37169	90	1.38158	1.38159
43	1.43698	1.43698	91	1.42382	1.42382
44	1.39559	1.39559	92	1.41246	1.41246
45	1.45147	1.45147	93	1.44412	1.44412
46	1.46434	1.46434	94	1.46704	1.46704
47	1.45706	1.45706	95	1.40493	1.40493
48	1.39489	1.39489			

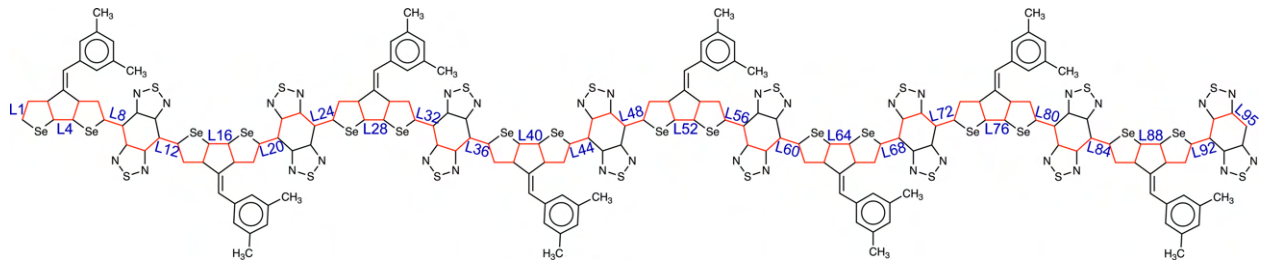


**Table S6:** Calculated bond lengths ( $\text{\AA}$ ) of CPDS-BBT octamer ( $N = 8$ ) in the singlet and triplet states.

Bond index	singlet ( $S = 0$ )	triplet ( $S = 1$ )	Bond index	singlet ( $S = 0$ )	triplet ( $S = 1$ )
1	1.36994	1.36994	49	1.43411	1.43412
2	1.42153	1.42153	50	1.36948	1.36948
3	1.40000	1.40000	51	1.44253	1.44253
4	1.42114	1.42115	52	1.37461	1.37461
5	1.41626	1.41626	53	1.45078	1.45077
6	1.39680	1.39681	54	1.37235	1.37235
7	1.41236	1.41237	55	1.43552	1.43552
8	1.41503	1.41503	56	1.39292	1.39292
9	1.44344	1.44344	57	1.45139	1.45139
10	1.46467	1.46467	58	1.46260	1.4626
11	1.45606	1.45607	59	1.45776	1.45776
12	1.39417	1.39416	60	1.39210	1.39210
13	1.43247	1.43248	61	1.43418	1.43418
14	1.37057	1.37056	62	1.36939	1.36939
15	1.44142	1.44143	63	1.44262	1.44263
16	1.37581	1.37581	64	1.37461	1.37461
17	1.44981	1.44982	65	1.45073	1.45073
18	1.37299	1.37299	66	1.37242	1.37242
19	1.43487	1.43487	67	1.43543	1.43542
20	1.39356	1.39356	68	1.39307	1.39307
21	1.45114	1.45114	69	1.45126	1.45126
22	1.46275	1.46275	70	1.46254	1.46254
23	1.45766	1.45767	71	1.45791	1.45791
24	1.39225	1.39224	72	1.39190	1.39189
25	1.43407	1.43407	73	1.43432	1.43432
26	1.36951	1.36950	74	1.36930	1.36930
27	1.44248	1.44248	75	1.44271	1.44271
28	1.37467	1.37467	76	1.37479	1.37479
29	1.45071	1.45071	77	1.45034	1.45033
30	1.37238	1.37239	78	1.37285	1.37285
31	1.43549	1.43549	79	1.43487	1.43487
32	1.39293	1.39294	80	1.39389	1.39389
33	1.45139	1.45138	81	1.45057	1.45057
34	1.46266	1.46266	82	1.46266	1.46266
35	1.45768	1.45768	83	1.45672	1.45671
36	1.39225	1.39225	84	1.39517	1.39518
37	1.43407	1.43407	85	1.43086	1.43085
38	1.36950	1.36950	86	1.37285	1.37286
39	1.44249	1.44249	87	1.43733	1.43732
40	1.37463	1.37463	88	1.38257	1.38258
41	1.45080	1.45080	89	1.44277	1.44275
42	1.37233	1.37233	90	1.38056	1.38056
43	1.43554	1.43554	91	1.42443	1.42442
44	1.39287	1.39287	92	1.40729	1.40729
45	1.45142	1.45142	93	1.44460	1.44459
46	1.46264	1.46263	94	1.46513	1.46512
47	1.45768	1.45769	95	1.40625	1.40625
48	1.39222	1.39222			

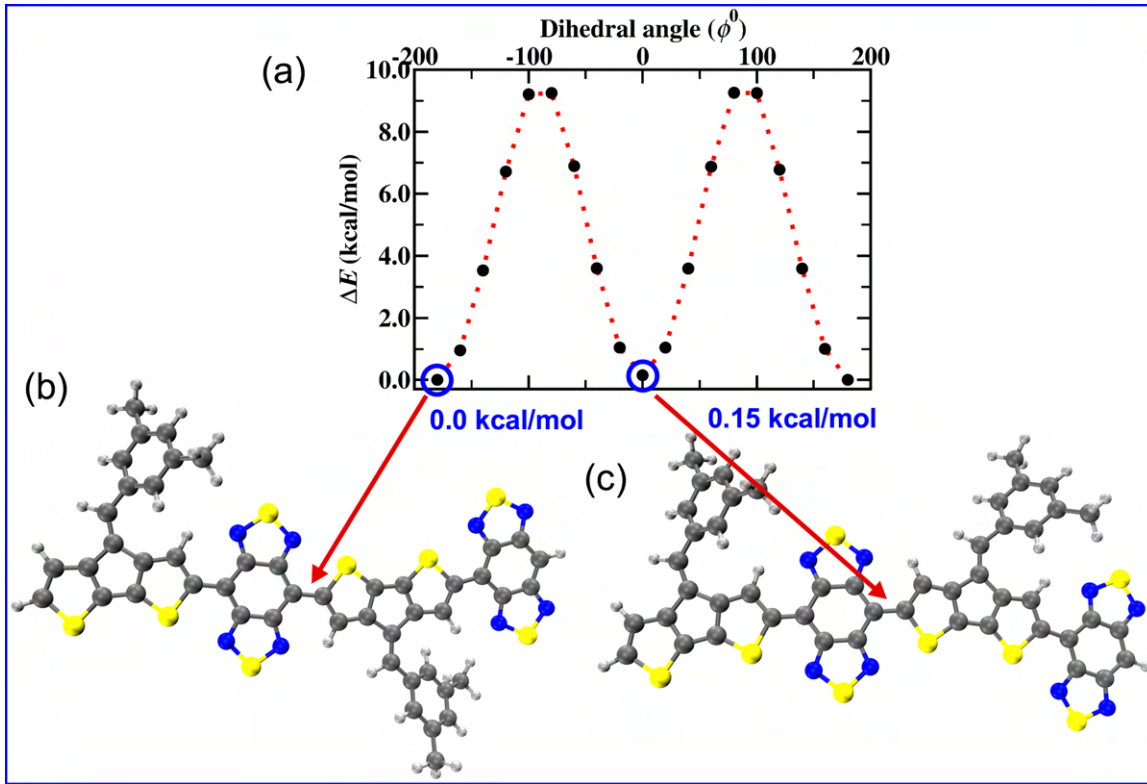


**Figure S22:** (a) The relative energies of CPDT-BBT dimer ( $N = 2$ ) as a function of the dihedral angle between the two repeat units for the singlet closed-shell state ( $S = 0$ ), (b) trans- and (c) cis-conformational geometries. The trans- (where the two olefin groups are at the opposite sides) is 0.15 kcal/mol lower in energy than the cis-conformation. Therefore, all calculations are performed on the trans-conformation of the BBT- and iso-BBT-based polymers.

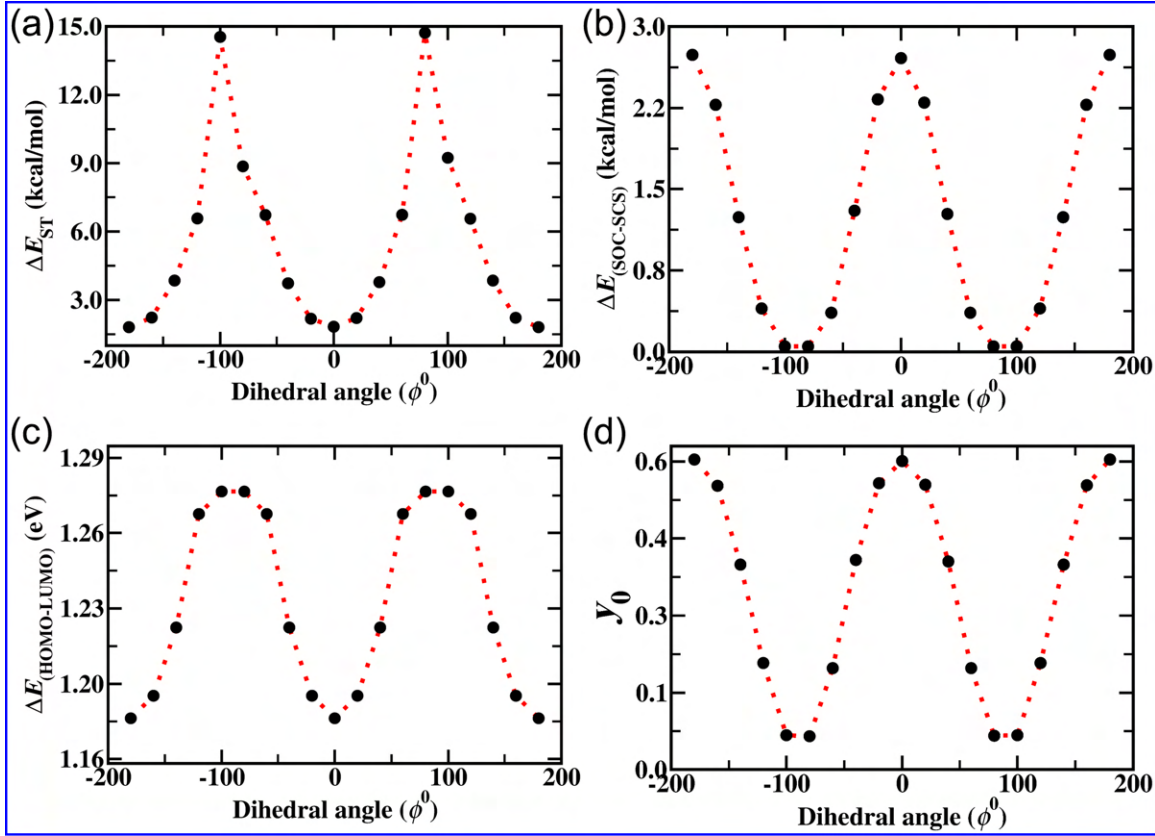


**Figure S23:** Calculated different properties of the CPDT-BBT dimer ( $N = 2$ ) as a function of the dihedral angle between the adjacent two repeat units. (a) singlet and triplet energy gaps ( $\Delta E_{ST}$ ), (b) energy of the singlet closed-shell (SCS) state with reference to the singlet open-shell (SOS) state, (c) the HOMO–LUMO energy gaps, and (d) diradical character ( $y_0$ ) at different conformations.

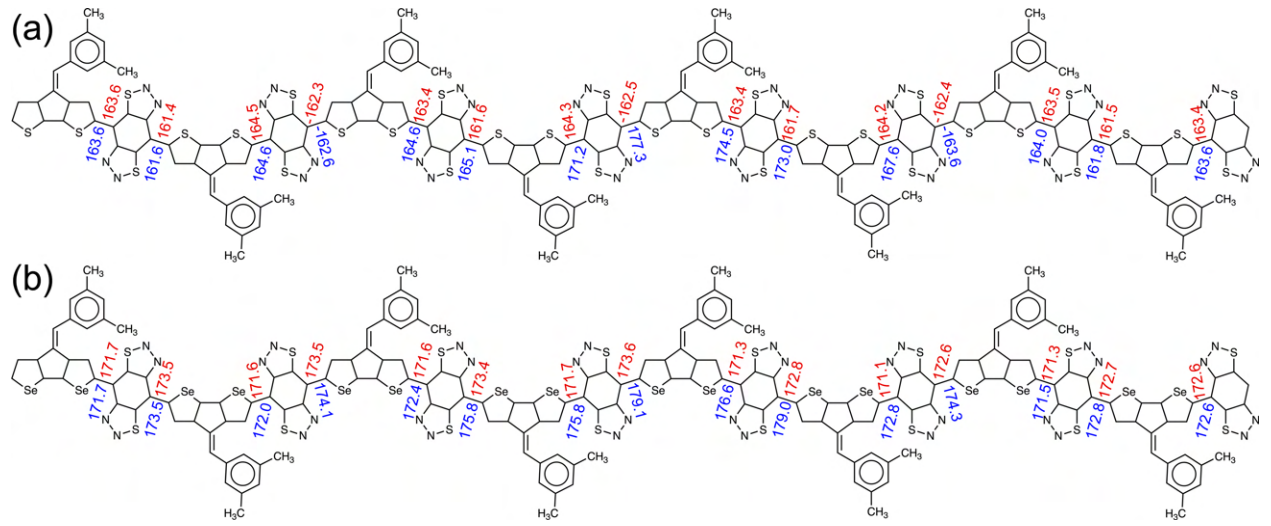


**Figure S24:** Calculated dihedral angles between adjacent donor and acceptor units of octamer ( $N = 8$ ) for (a) CPDT-iso-BBT and (b) CPDS-iso-BBT in their singlet (red) and triplet states (blue).

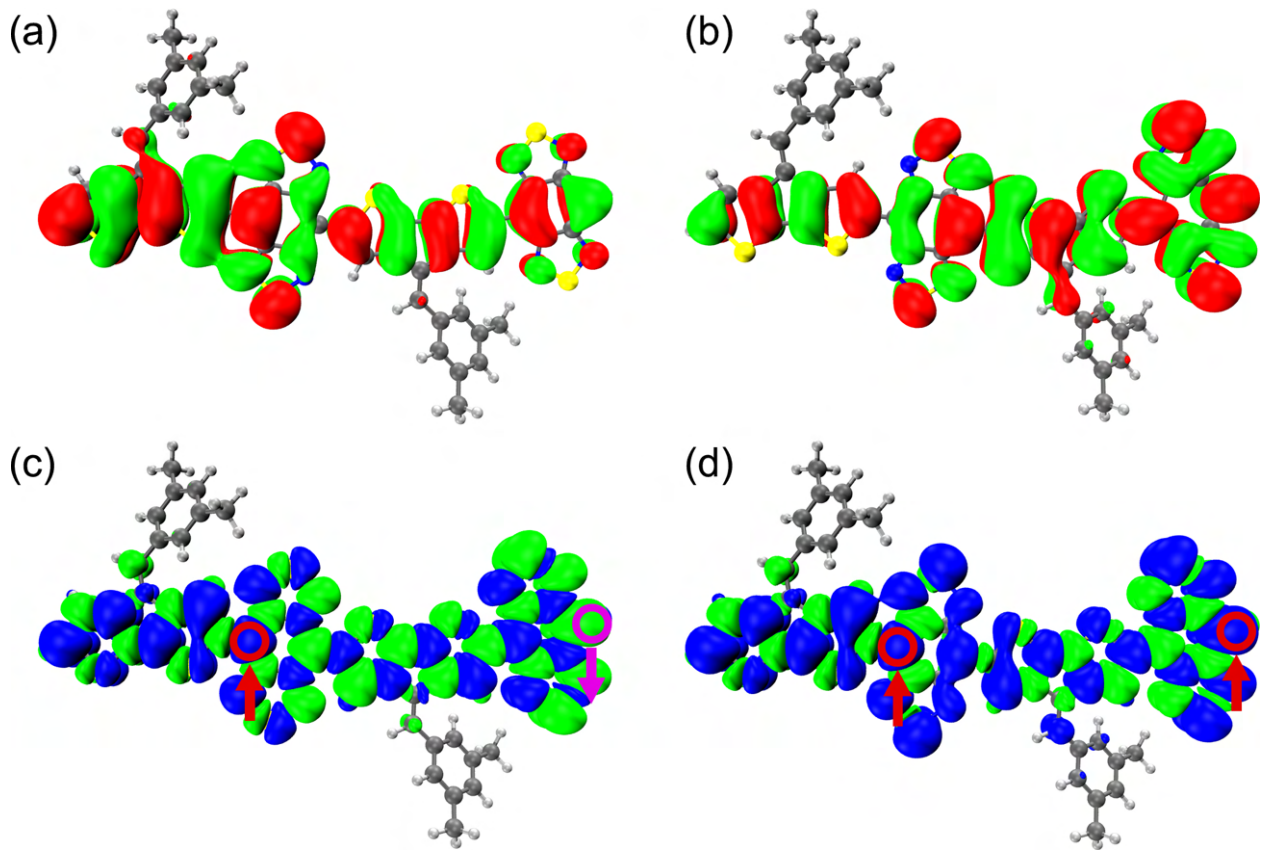


**Figure S25:** Optimized ground-state geometric structures for the CPDT-BBT dimer ( $N = 2$ ) and pictorial representations of the frontier MOs and spin density distribution. (a)  $\alpha$ -SOMO and (b)  $\beta$ -SOMO of the open-shell singlet ( $S = 0$ ), (c) spin density distribution of the singlet and (d) triplet states ( $S = 1$ ). The green and red surfaces represent positive and negative signs of the MO at isovalue = 0.01 au, respectively. The blue and green surfaces represent positive and negative contributions of the spin density at an isovalue = 0.0002 au. The most probable locations for the unpaired electrons are indicated with up (alpha spin) and down (beta spin) arrows and open circles, respectively. Color codes for the atoms are: gray for C, blue for N, and yellow for S.

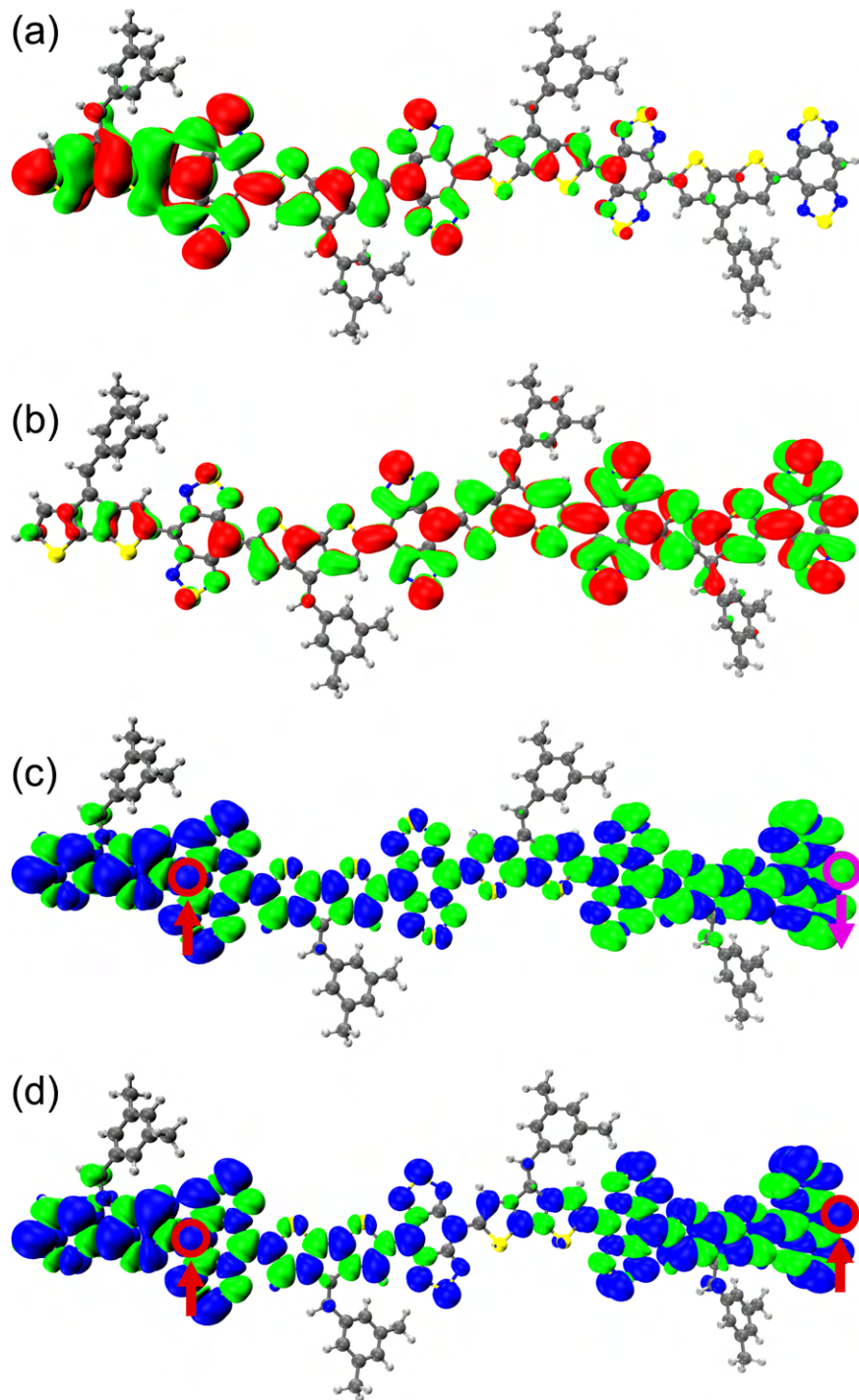


**Figure S26:** Optimized ground-state geometric structures for the CPDT-BBT tetramer ( $N = 4$ ) and pictorial representations of the frontier MOs and spin density distribution. (a)  $\alpha$ -SOMO and (b)  $\beta$ -SOMO of the open-shell singlet ( $S = 0$ ), (c) spin density distribution of the singlet and (d) triplet states ( $S = 1$ ). The green and red surfaces represent positive and negative signs of the MO at isovalue = 0.01 au, respectively. The blue and green surfaces represent positive and negative contributions of the spin density at an isovalue = 0.0002 au. The most probable locations for the unpaired electrons are indicated with up (alpha spin) and down (beta spin) arrows and open circles, respectively. Color codes for the atoms are: gray for C, blue for N, and yellow for S.

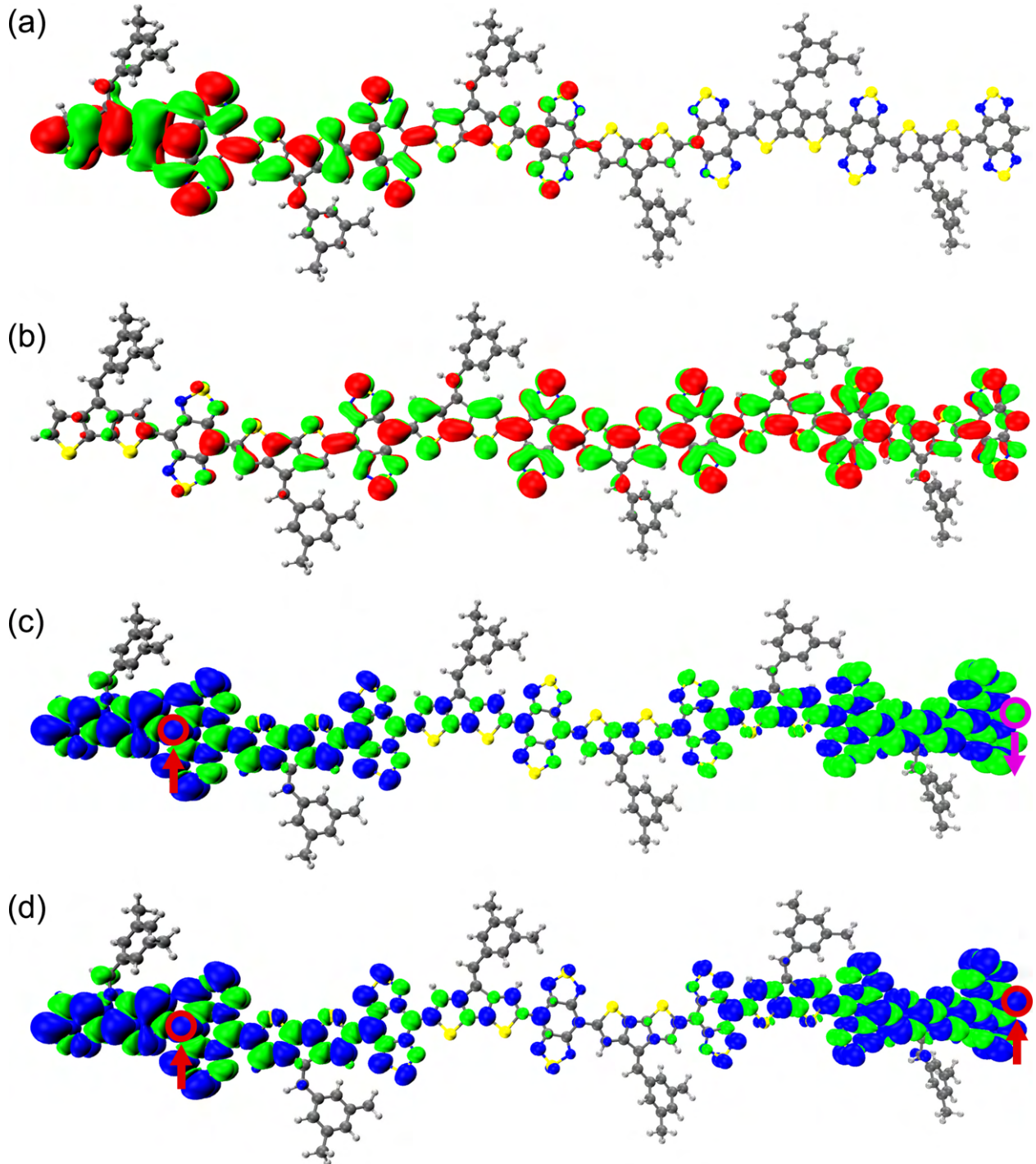


**Figure S27:** Optimized ground-state geometric structures for the CPDT-BBT hexamer ( $N = 6$ ) and pictorial representations of the frontier MOs and spin density distribution. (a)  $\alpha$ -SOMO and (b)  $\beta$ -SOMO of the open-shell singlet ( $S = 0$ ), (c) spin density distribution of the singlet and (d) triplet states ( $S = 1$ ). The green and red surfaces represent positive and negative signs of the MO at isovalue = 0.01 au, respectively. The blue and green surfaces represent positive and negative contributions of the spin density at an isovalue = 0.0002 au. The most probable locations for the unpaired electrons are indicated with up (alpha spin) and down (beta spin) arrows and open circles, respectively. Color codes for the atoms are: gray for C, blue for N, and yellow for S.

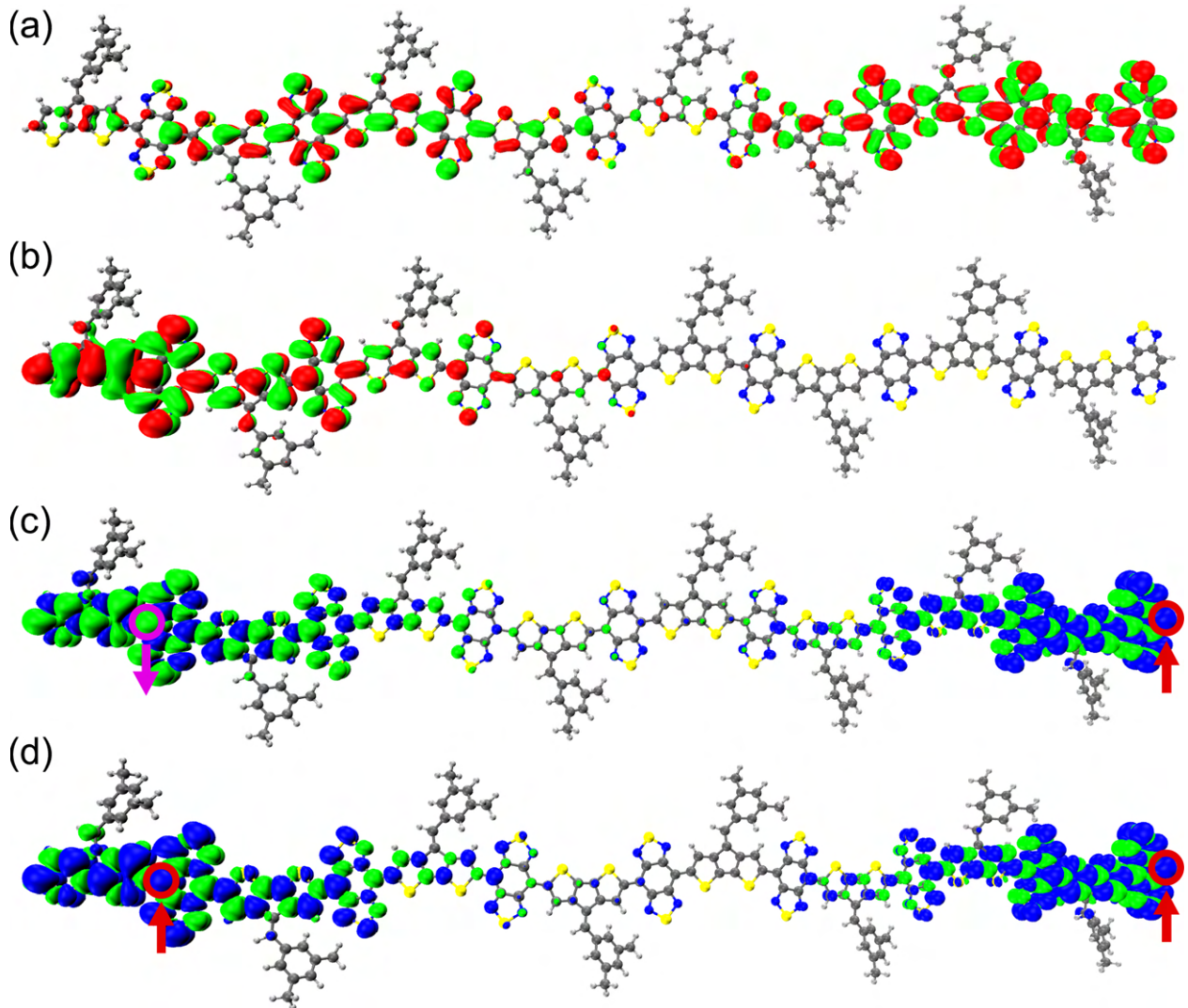


**Figure S28:** Optimized ground-state geometric structures for the CPDT-BBT octamer ( $N = 8$ ) and pictorial representations of the frontier MOs and spin density distribution. (a)  $\alpha$ -SOMO and (b)  $\beta$ -SOMO of the open-shell singlet ( $S = 0$ ), (c) spin density distribution of the singlet and (d) triplet states ( $S = 1$ ). The green and red surfaces represent positive and negative signs of the MO at  $\text{isovalue} = 0.01 \text{ au}$ , respectively. The blue and green surfaces represent positive and negative contributions of the spin density at  $\text{isovalue} = 0.0002 \text{ au}$ . The most probable locations for the unpaired electrons are indicated with up (alpha spin) and down (beta spin) arrows and open circles, respectively. Color codes for the atoms are: gray for C, blue for N, and yellow for S.

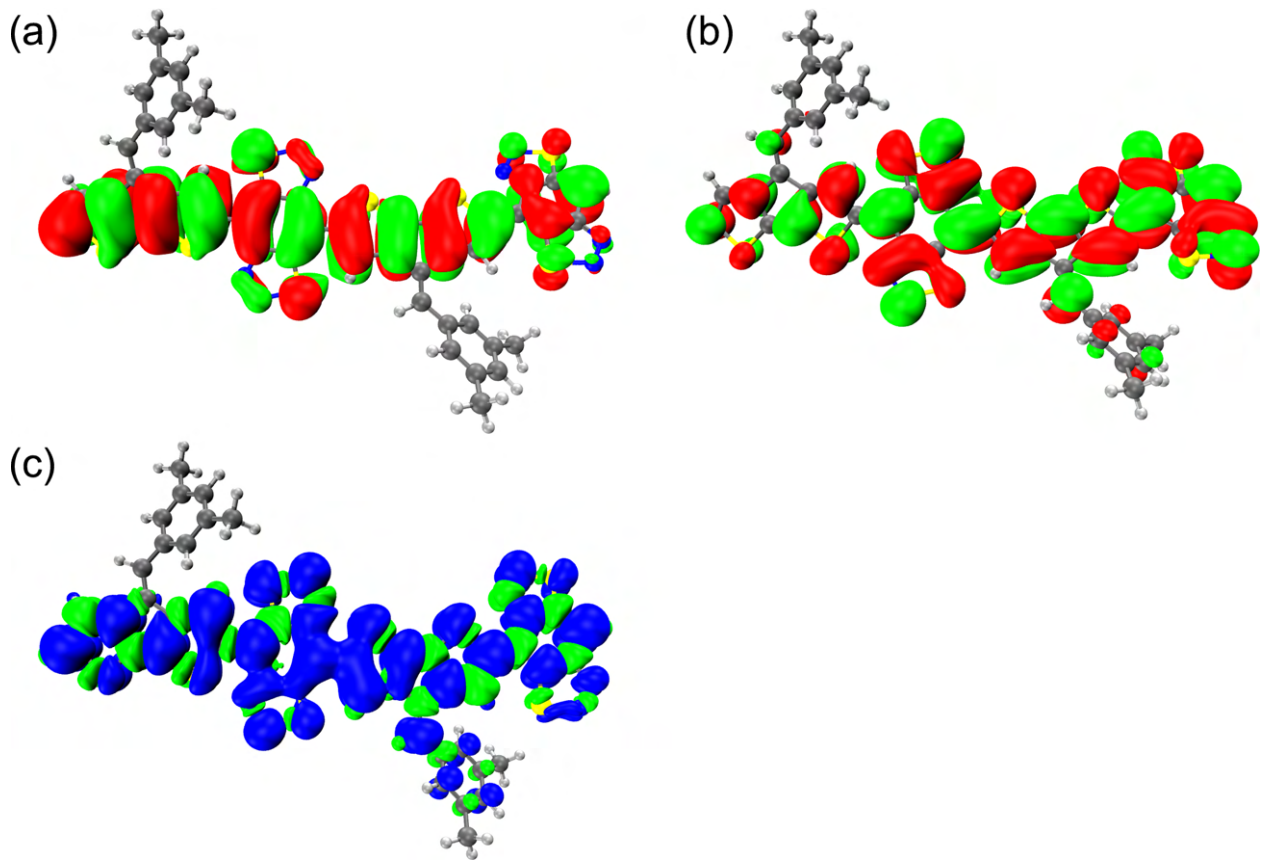


**Figure S29:** Optimized ground-state geometric structures for the CPDT-iso-BBT dimer ( $N = 2$ ) and pictorial representations of the frontier MOs and spin density distribution. (a) HOMO and (b) LUMO of the closed-shell singlet ( $S = 0$ ), (c) spin density distribution of the triplet state ( $S = 1$ ). The green and red surfaces represent positive and negative signs of the MO at isovalue = 0.01 au, respectively. The blue and green surfaces represent positive and negative contributions of the spin density at an isovalue = 0.0002 au. Color codes for the atoms are: gray for C, blue for N, and yellow for S.

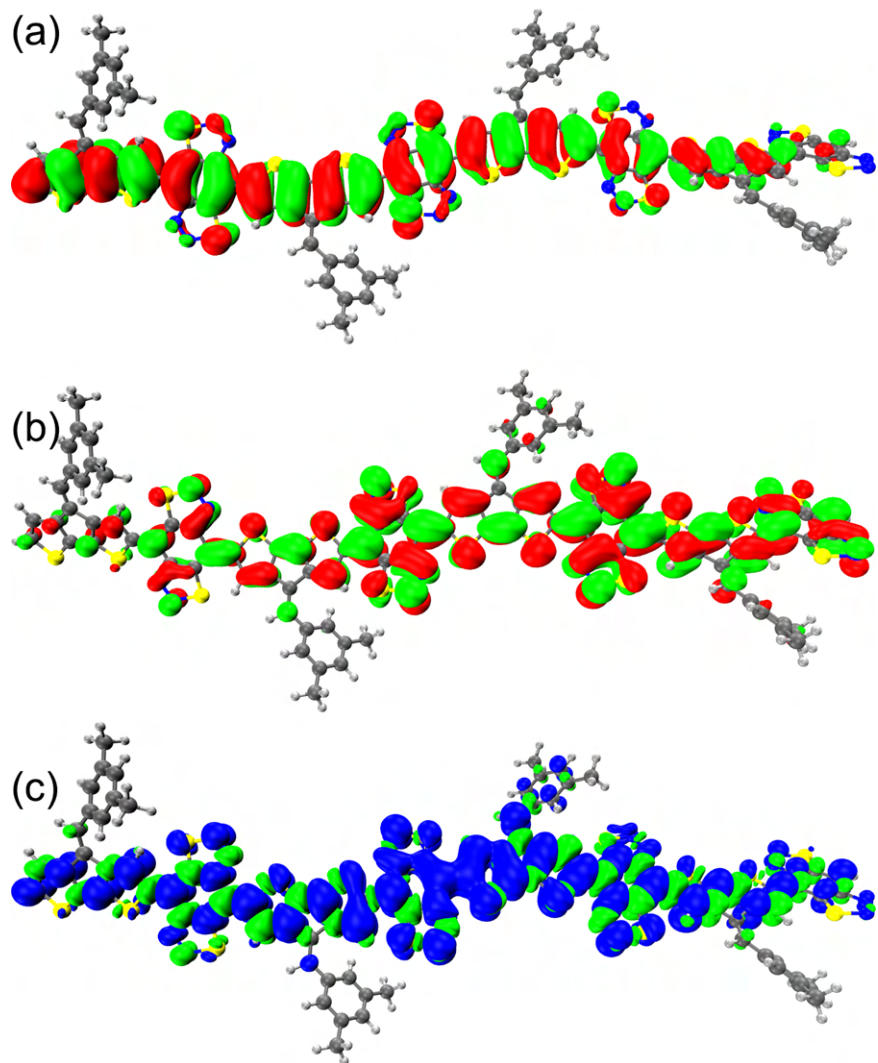


**Figure S30:** Optimized ground-state geometric structures for the CPDT-iso-BBT tetramer ( $N = 4$ ) and pictorial representations of the frontier MOs and spin density distribution. (a) HOMO and (b) LUMO of the closed-shell singlet ( $S = 0$ ), (c) spin density distribution of the triplet state ( $S = 1$ ). The green and red surfaces represent positive and negative signs of the MO at isovalue = 0.01 au, respectively. The blue and green surfaces represent positive and negative contributions of the spin density at an isovalue = 0.0002 au. Color codes for the atoms are: gray for C, blue for N, and yellow for S.

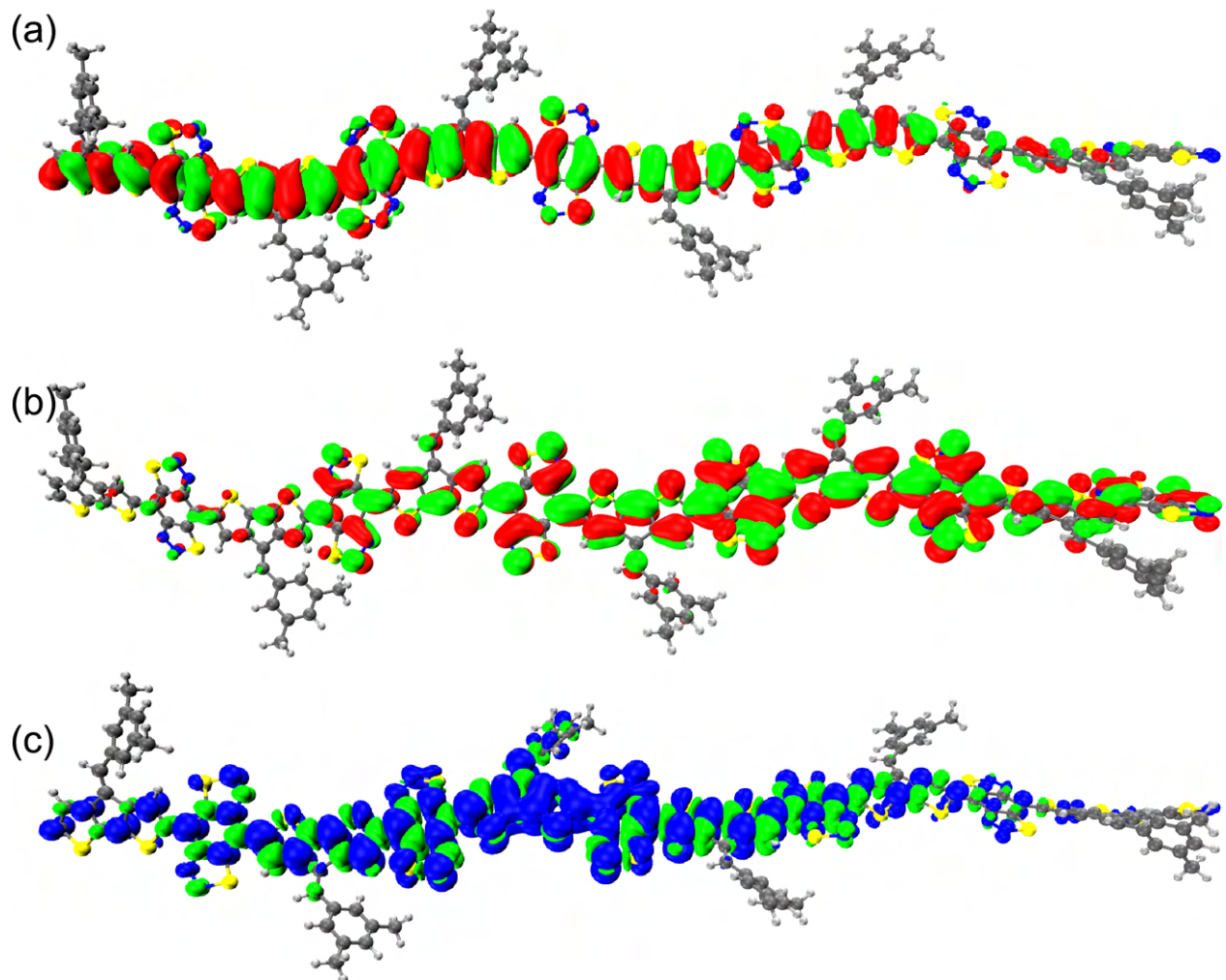


**Figure S31:** Optimized ground-state geometric structures for the CPDT-iso-BBT hexamer ( $N = 6$ ) and pictorial representations of the frontier MOs and spin density distribution. (a) HOMO and (b) LUMO of the closed-shell singlet ( $S = 0$ ), (c) spin density distribution of the triplet state ( $S = 1$ ). The green and red surfaces represent positive and negative signs of the MO at isovalue = 0.01 au, respectively. The blue and green surfaces represent positive and negative contributions of the spin density at an isovalue = 0.0002 au. Color codes for the atoms are: gray for C, blue for N, and yellow for S.

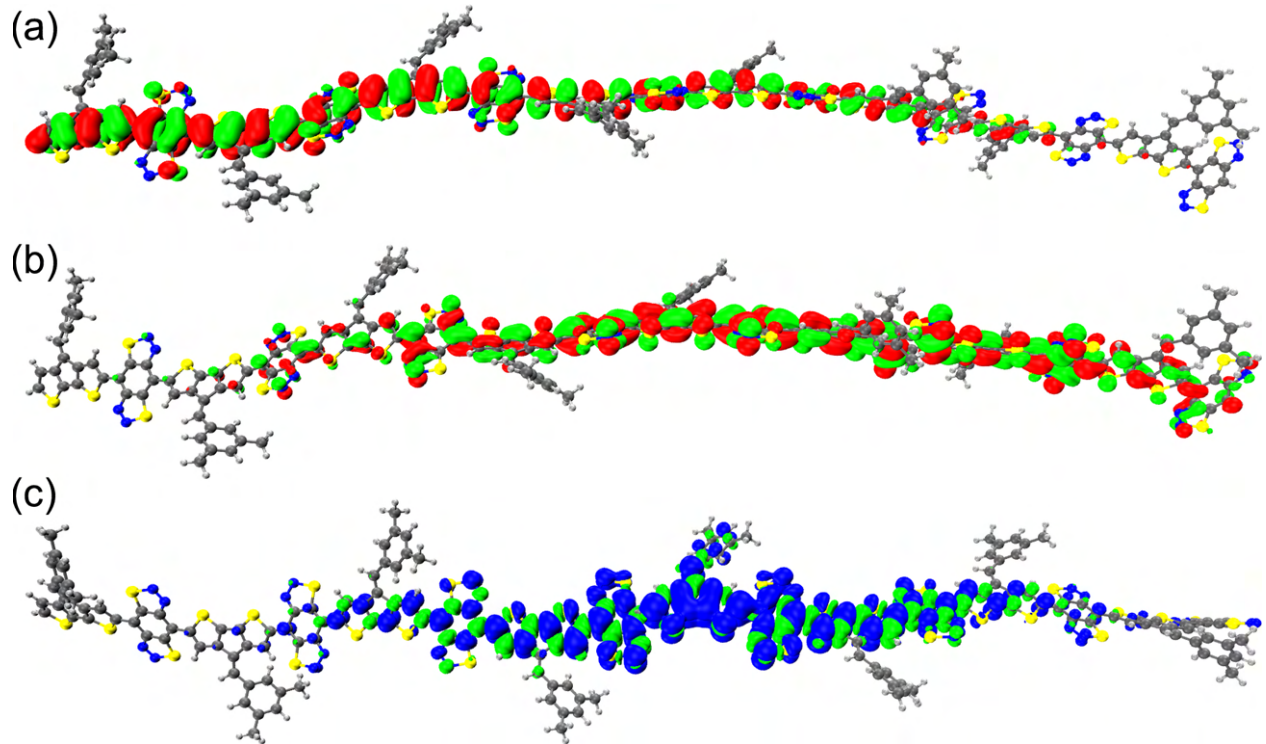


**Figure S32:** Optimized ground-state geometric structures for the CPDT-iso-BBT octamer ( $N = 8$ ) and pictorial representations of the frontier MOs and spin density distribution. (a) HOMO and (b) LUMO of the closed-shell singlet ( $S = 0$ ), (c) spin density distribution of the triplet state ( $S = 1$ ). The green and red surfaces represent positive and negative signs of the MO at isovalue = 0.01 au, respectively. The blue and green surfaces represent positive and negative contributions of the spin density at an isovalue = 0.0002 au. Color codes for the atoms are: gray for C, blue for N, and yellow for S.

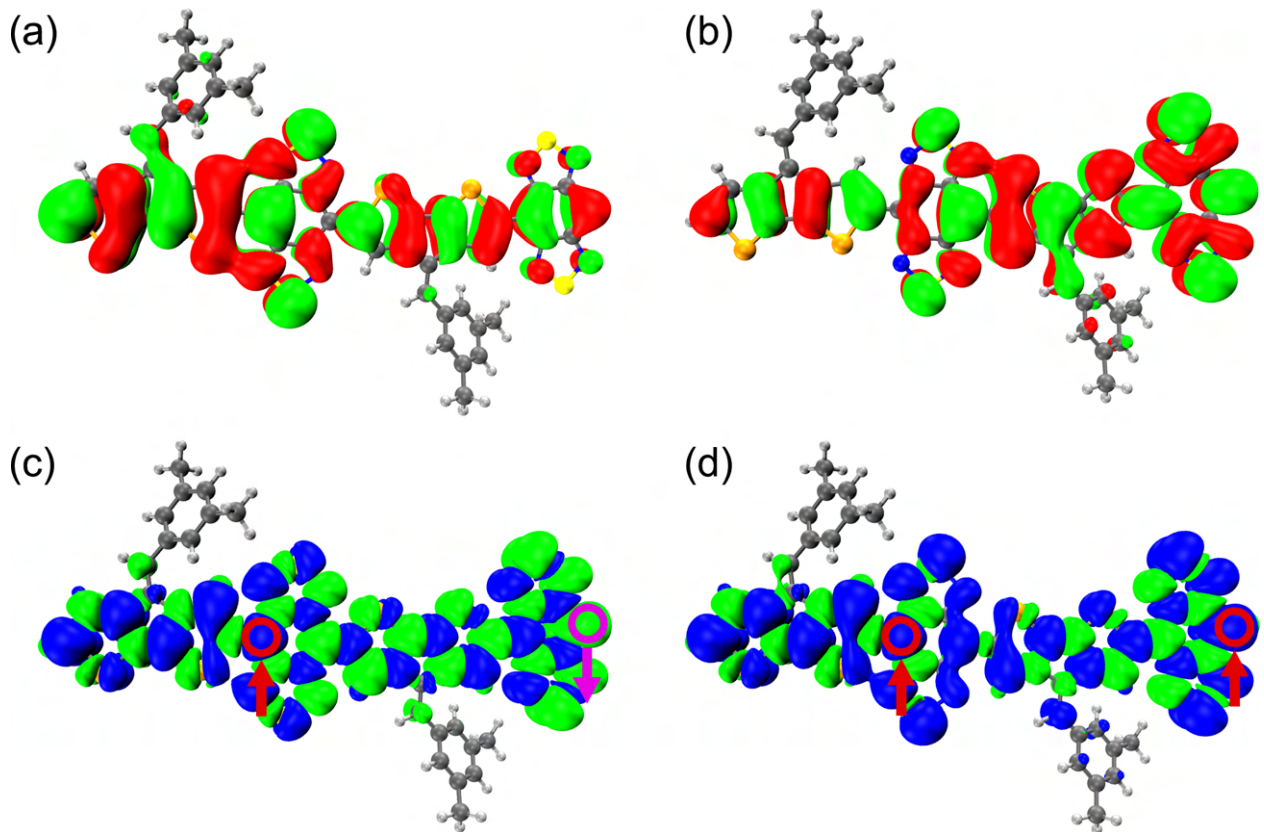


**Figure S33:** Optimized ground-state geometric structures for the CPDS-BBT dimer ( $N = 2$ ) and pictorial representations of the frontier MOs and spin density distribution. (a)  $\alpha$ -SOMO and (b)  $\beta$ -SOMO of the open-shell singlet ( $S = 0$ ), (c) spin density distribution of the singlet and (d) triplet states ( $S = 1$ ). The green and red surfaces represent positive and negative signs of the MO at isovalue = 0.01 au, respectively. The blue and green surfaces represent positive and negative contributions of the spin density at an isovalue = 0.0002 au. The most probable locations for the unpaired electrons are indicated with up (alpha spin) and down (beta spin) arrows and open circles, respectively. Color codes for the atoms are: gray for C, blue for N, yellow for S, and orange for Se.

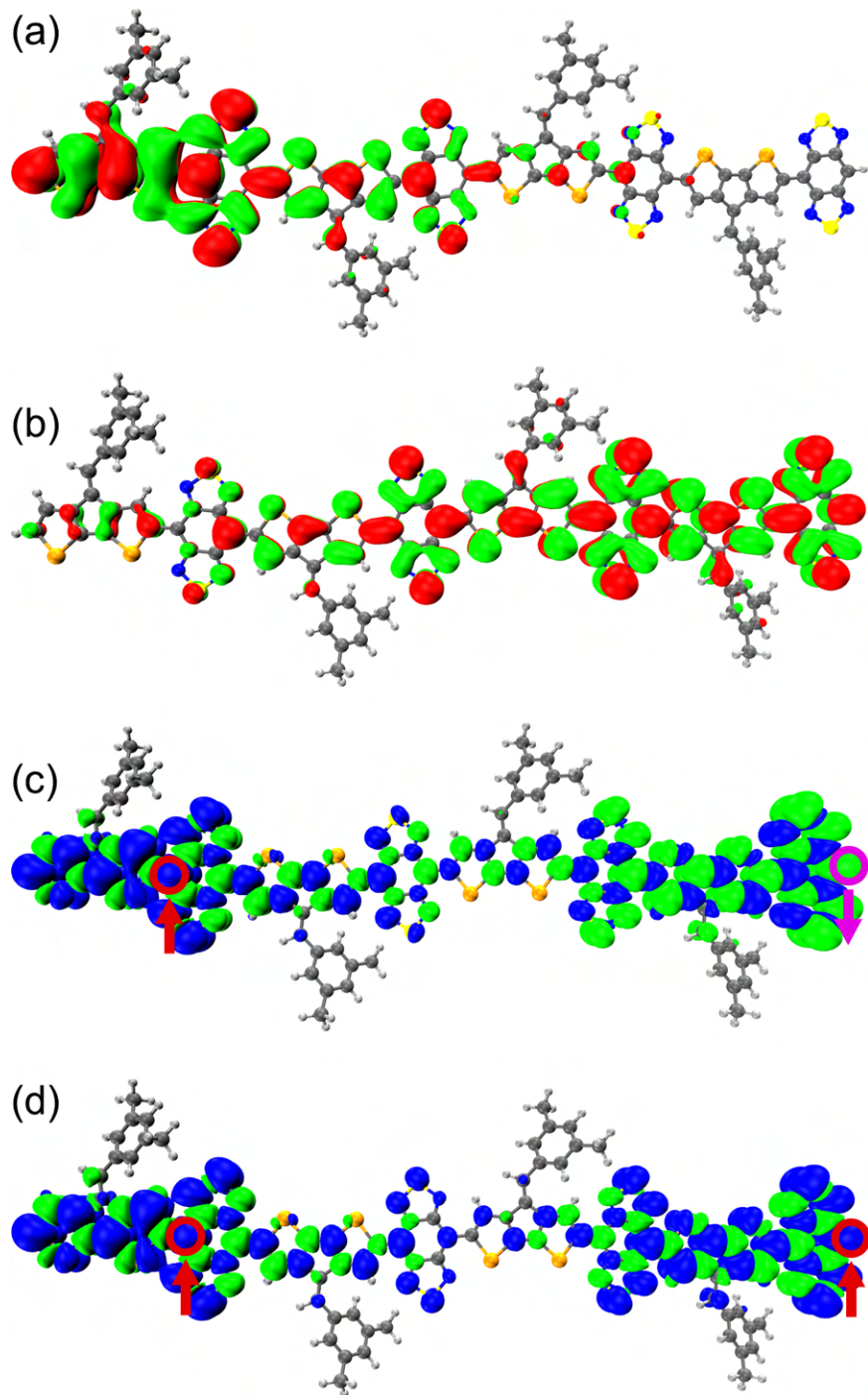


**Figure S34:** Optimized ground-state geometric structures for the CPDS-BBT tetramer ( $N = 4$ ) and pictorial representations of the frontier MOs and spin density distribution. (a)  $\alpha$ -SOMO and (b)  $\beta$ -SOMO of the open-shell singlet ( $S = 0$ ), (c) spin density distribution of the singlet and (d) triplet states ( $S = 1$ ). The green and red surfaces represent positive and negative signs of the MO at isovalue = 0.01 au, respectively. The blue and green surfaces represent positive and negative contributions of the spin density at an isovalue = 0.0002 au. The most probable locations for the unpaired electrons are indicated with up (alpha spin) and down (beta spin) arrows and open circles, respectively. Color codes for the atoms are: gray for C, blue for N, yellow for S, and orange for Se.

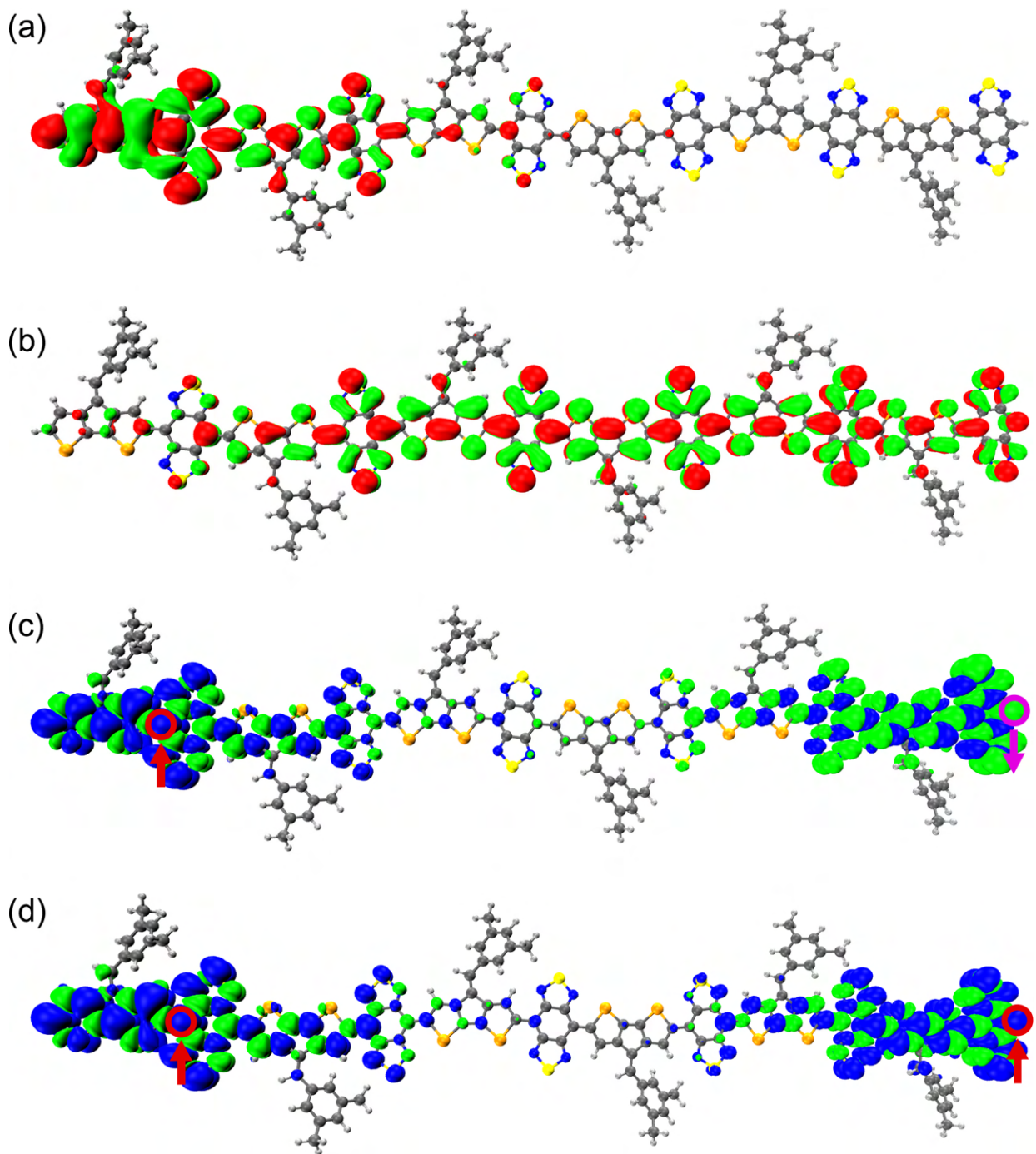


**Figure S35:** Optimized ground-state geometric structures for the CPDS-BBT hexamer ( $N = 6$ ) and pictorial representations of the frontier MOs and spin density distribution. (a)  $\alpha$ -SOMO and (b)  $\beta$ -SOMO of the open-shell singlet ( $S = 0$ ), (c) spin density distribution of the singlet and (d) triplet states ( $S = 1$ ). The green and red surfaces represent positive and negative signs of the MO at isovalue = 0.01 au, respectively. The blue and green surfaces represent positive and negative contributions of the spin density at an isovalue = 0.0002 au. The most probable locations for the unpaired electrons are indicated with up (alpha spin) and down (beta spin) arrows and open circles, respectively. Color codes for the atoms are: gray for C, blue for N, yellow for S, and orange for Se.

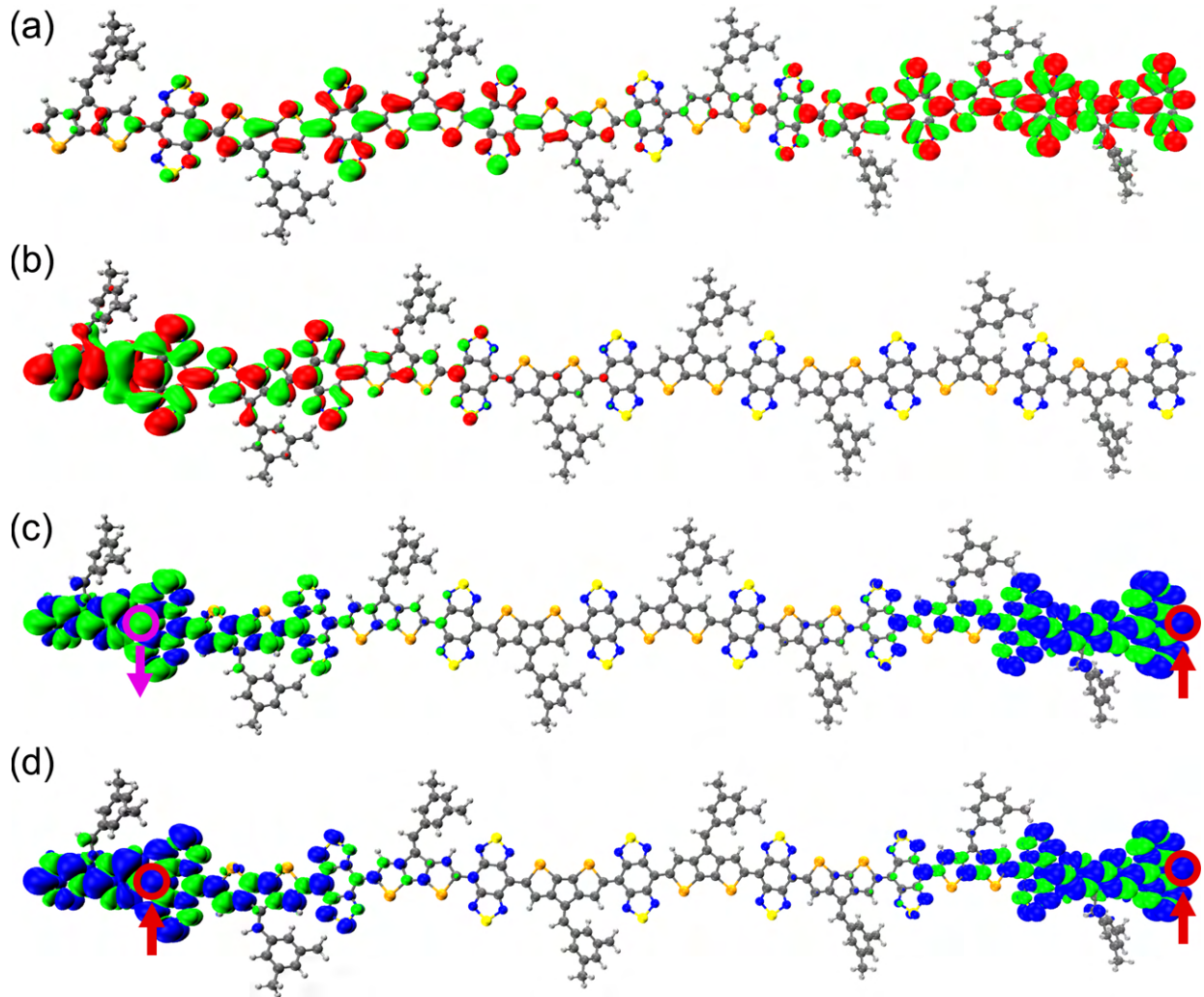


**Figure S36:** Optimized ground-state geometric structures, pictorial representations of the frontier MOs (FMOs), and spin density distribution of the CPDS-BBT ( $N = 8$ ) polymer. (a)  $\alpha$ -SOMO-1 and (b)  $\beta$ -SOMO of the open-shell singlet; (c) spin density distribution of the singlet ( $S = 0$ ) and (d) triplet ( $S = 1$ ) states. The green and red surfaces represent positive and negative signs of the MO at isovalue = 0.01 au, respectively. The blue and green surfaces represent positive and negative contributions of the spin density at an isovalue = 0.0002 au. The most probable locations for the unpaired electrons are highlighted with open circles (red: up-spin and purple: down-spin).

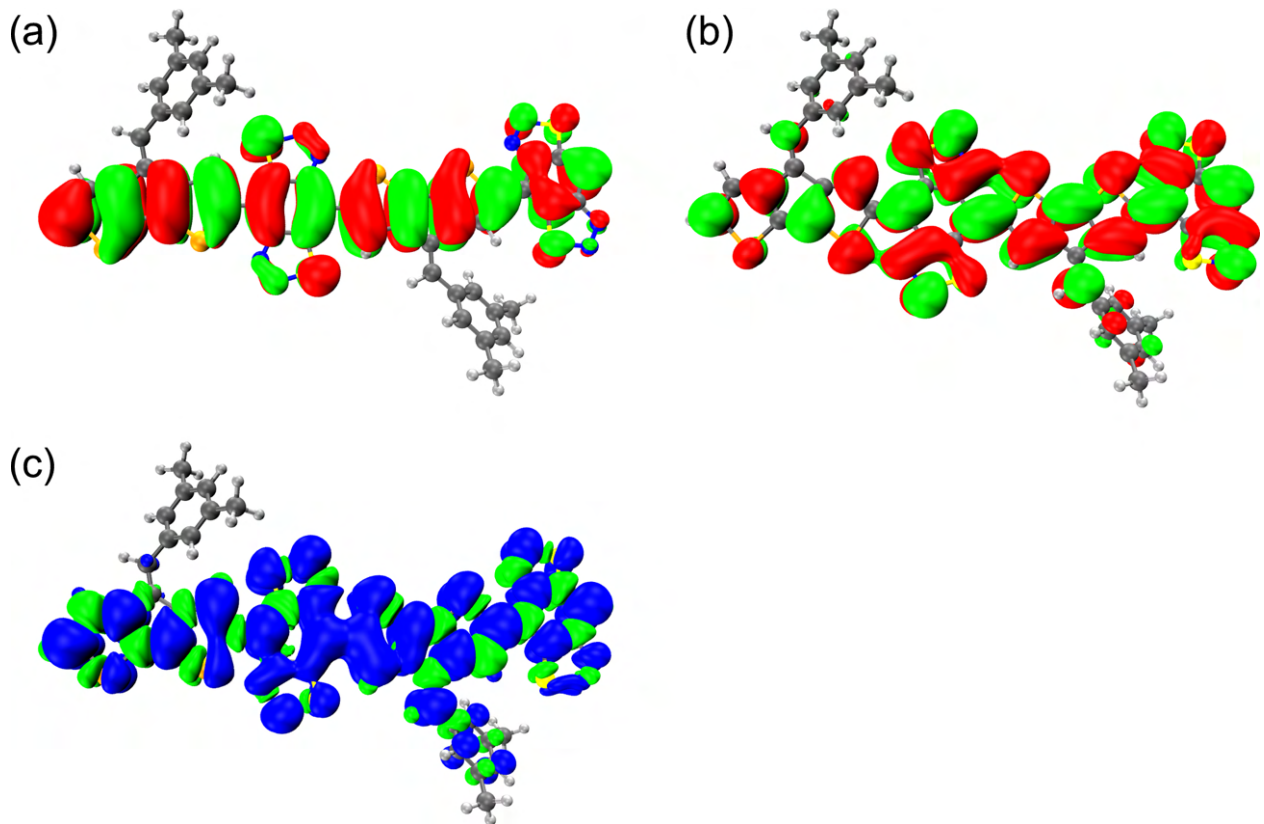


**Figure S37:** Optimized ground-state geometric structures for the CPDS-iso-BBT dimer ( $N = 2$ ) and pictorial representations of the frontier MOs and spin density distribution. (a) HOMO and (b) LUMO of the closed-shell singlet ( $S = 0$ ), (c) spin density distribution of the triplet state ( $S = 1$ ). The green and red surfaces represent positive and negative signs of the MO at isovalue = 0.01 au, respectively. The blue and green surfaces represent positive and negative contributions of the spin density at an isovalue = 0.0002 au. Color codes for the atoms are: gray for C, blue for N, yellow for S, and orange for Se.

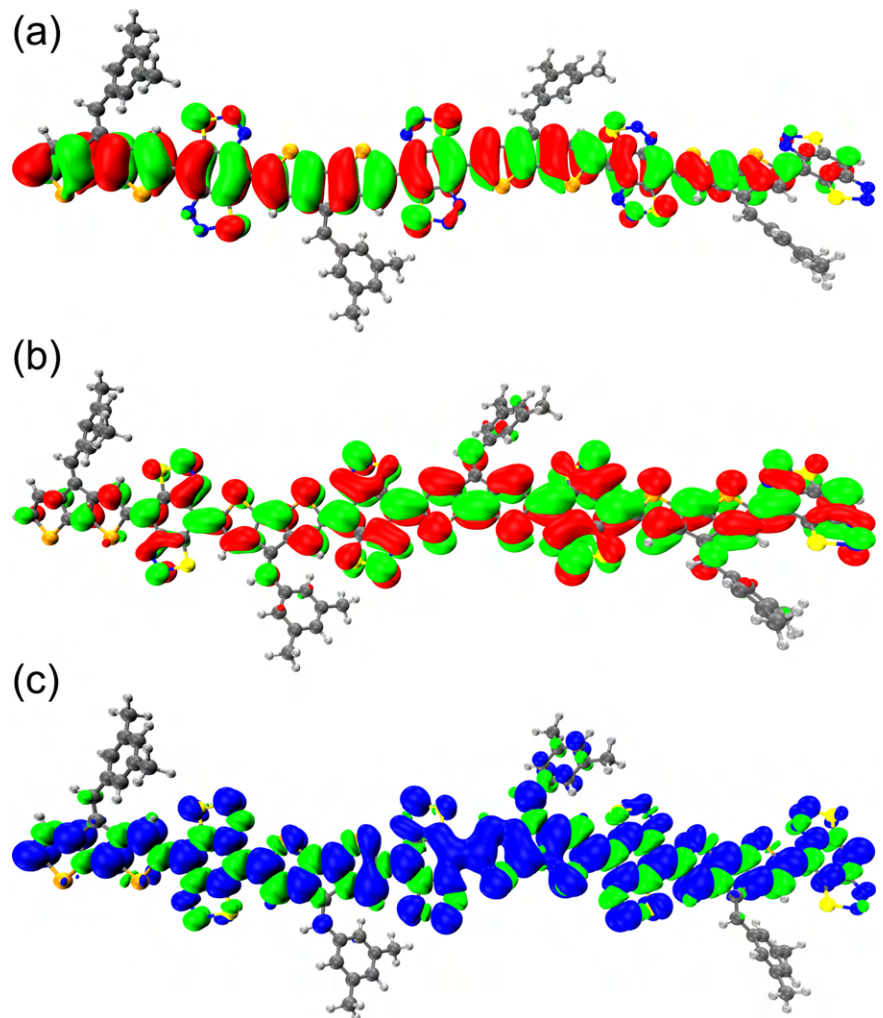


**Figure S38:** Optimized ground-state geometric structures for the CPDS-iso-BBT tetramer ( $N = 4$ ) and pictorial representations of the frontier MOs and spin density distribution. (a) HOMO and (b) LUMO of the closed-shell singlet ( $S = 0$ ), (c) spin density distribution of the triplet state ( $S = 1$ ). The green and red surfaces represent positive and negative signs of the MO at isovalue = 0.01 au, respectively. The blue and green surfaces represent positive and negative contributions of the spin density at an isovalue = 0.0002 au. Color codes for the atoms are: gray for C, blue for N, yellow for S, and orange for Se.

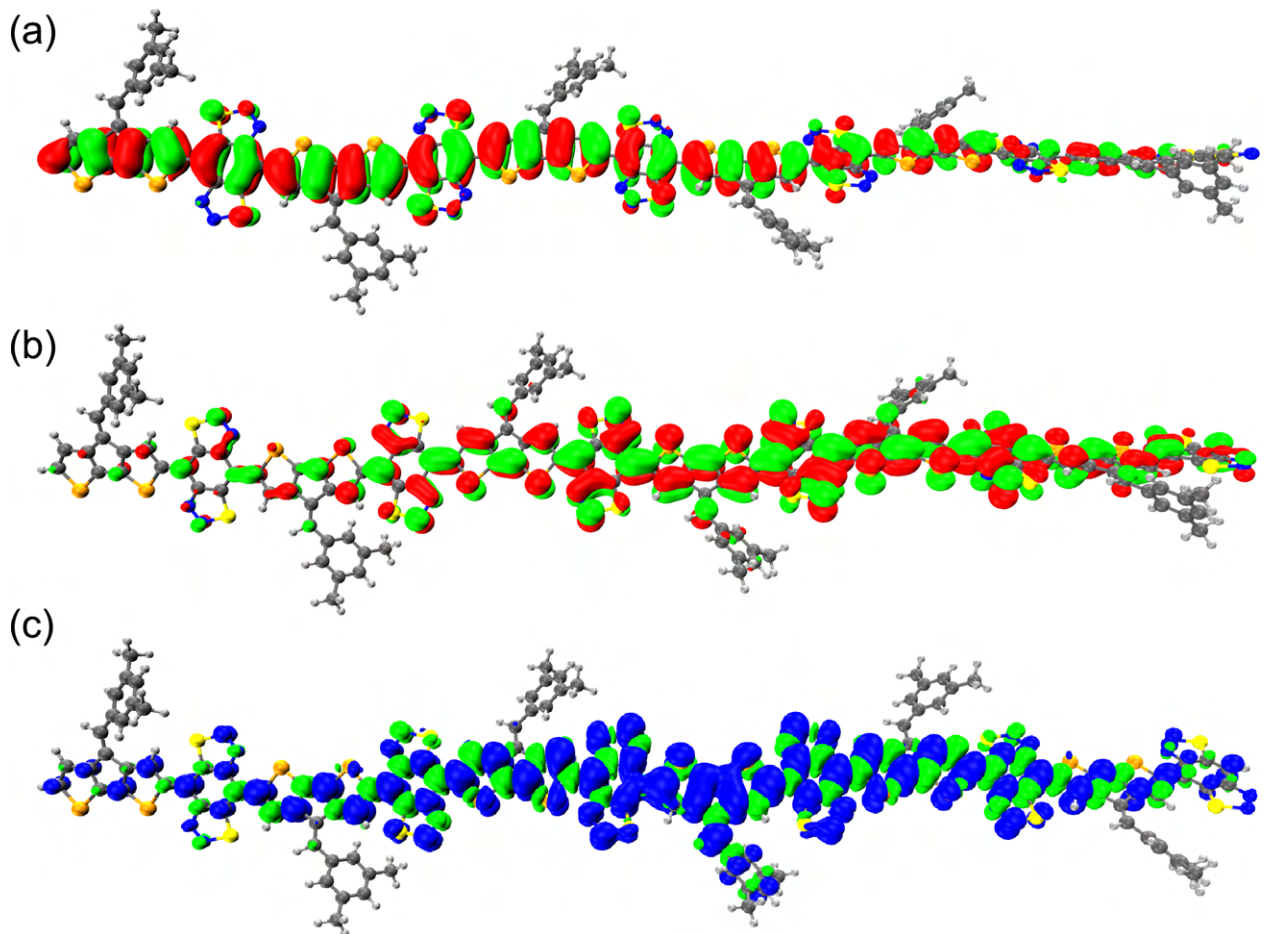


**Figure S39:** Optimized ground-state geometric structures for the CPDS-iso-BBT hexamer ( $N = 6$ ) and pictorial representations of the frontier MOs and spin density distribution. (a) HOMO and (b) LUMO of the closed-shell singlet ( $S = 0$ ), (c) spin density distribution of the triplet state ( $S = 1$ ). The green and red surfaces represent positive and negative signs of the MO at isovalue = 0.01 au, respectively. The blue and green surfaces represent positive and negative contributions of the spin density at an isovalue = 0.0002 au. Color codes for the atoms are: gray for C, blue for N, yellow for S, and orange for Se.

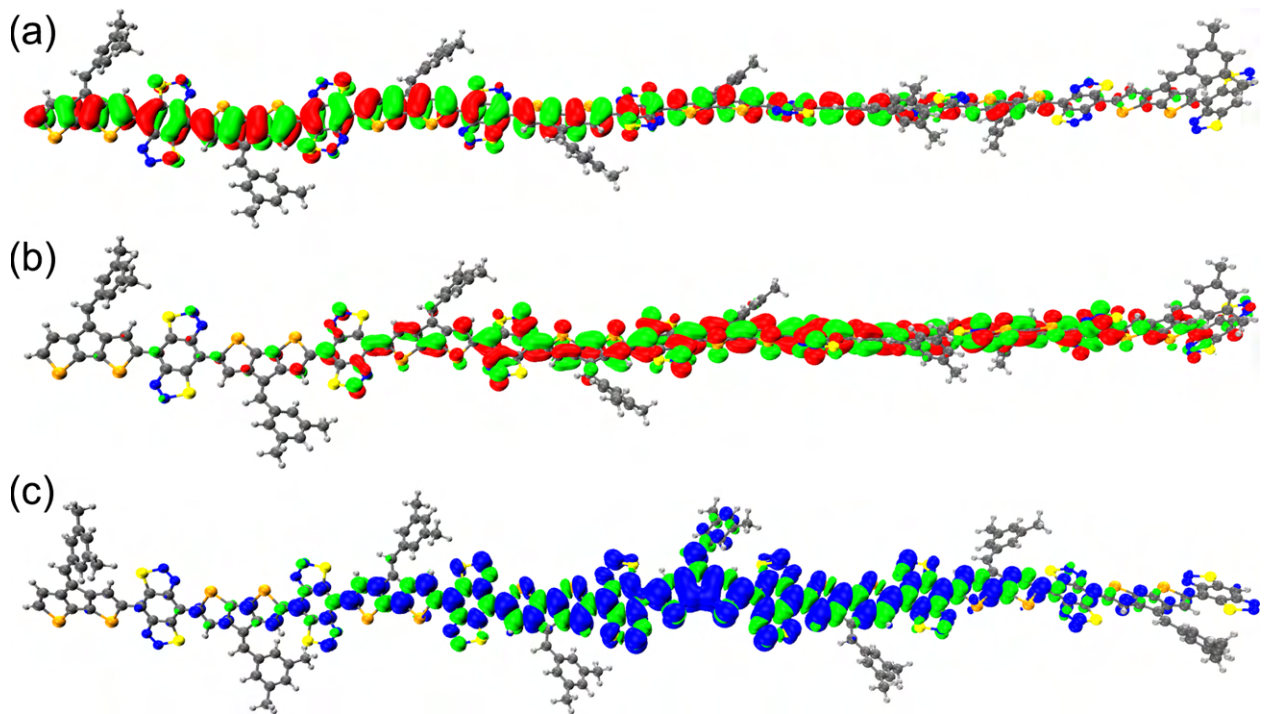


**Figure S40:** Optimized ground-state geometric structures for the CPDS-iso-BBT octamer ( $N = 8$ ) and pictorial representations of the frontier MOs and spin density distribution. (a) HOMO and (b) LUMO of the closed-shell singlet ( $S = 0$ ), (c) spin density distribution of the triplet state ( $S = 1$ ). The green and red surfaces represent positive and negative signs of the MO at isovalue = 0.01 au, respectively. The blue and green surfaces represent positive and negative contributions of the spin density at an isovalue = 0.0002 au. Color codes for the atoms are: gray for C, blue for N, yellow for S, and orange for Se.

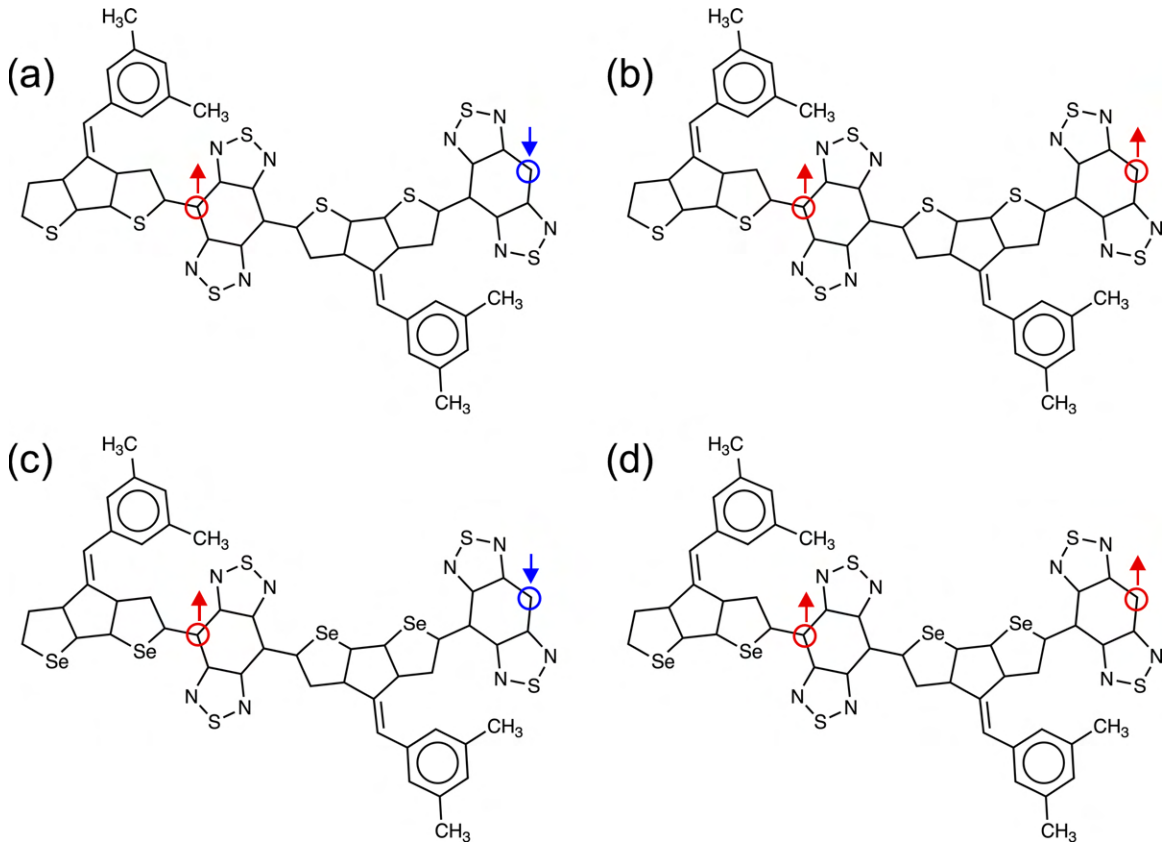


**Figure S41:** Locations of the unpaired electrons for (a) singlet ( $S = 0$ ) and (b) triplet ( $S = 1$ ) states on CPDT-BBT; (c) singlet ( $S = 0$ ) and (d) triplet ( $S = 1$ ) states on CPDS-BBT dimer ( $N = 2$ ) backbone based on the probability of maximum spin density. Color code: Red is for spin-up and Blue is for spin-down.

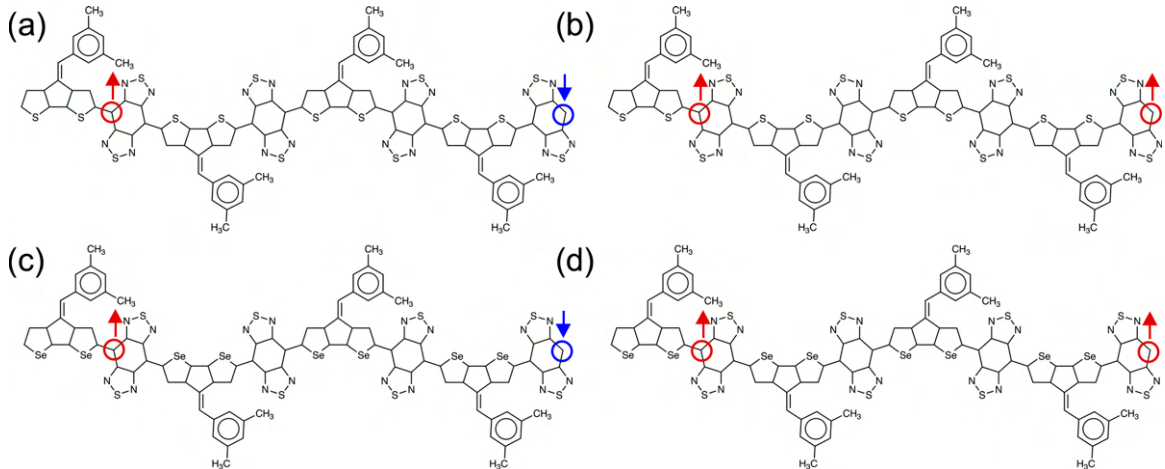


**Figure S42:** Locations of the unpaired electrons for (a) singlet ( $S = 0$ ) and (b) triplet ( $S = 1$ ) states on CPDT-BBT; (c) singlet ( $S = 0$ ) and (d) triplet ( $S = 1$ ) states on CPDS-BBT tetramer ( $N = 4$ ) backbone based on the probability of maximum spin density. Color code: Red is for spin-up and Blue is for spin-down.

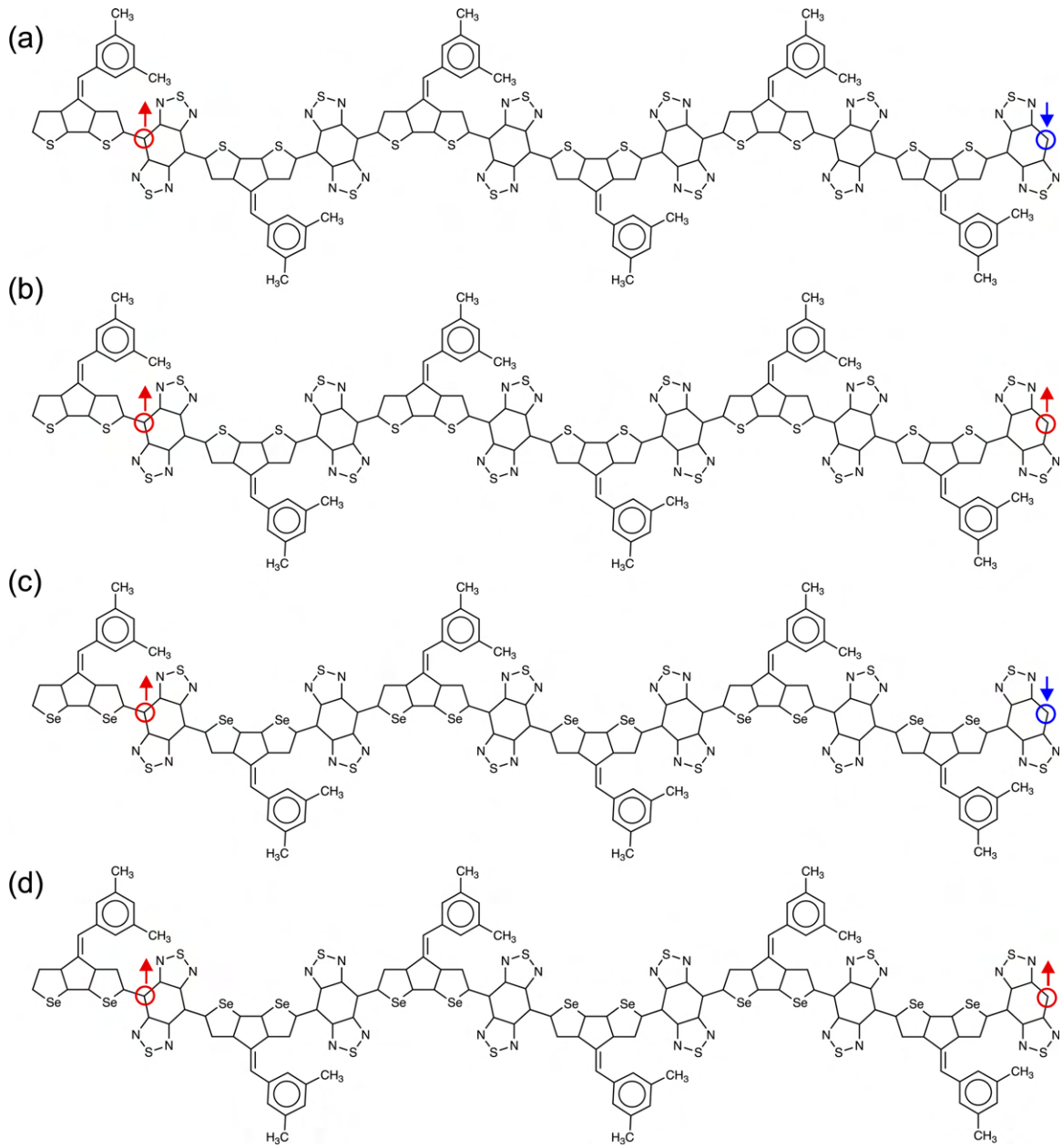


**Figure S43:** Locations of the unpaired electrons for (a) singlet ( $S = 0$ ) and (b) triplet ( $S = 1$ ) states on CPDT-BBT; (c) singlet ( $S = 0$ ) and (d) triplet ( $S = 1$ ) states on CPDS-BBT hexamer ( $N = 6$ ) backbone based on the probability of maximum spin density. Color code: Red is for spin-up and Blue is for spin-down.

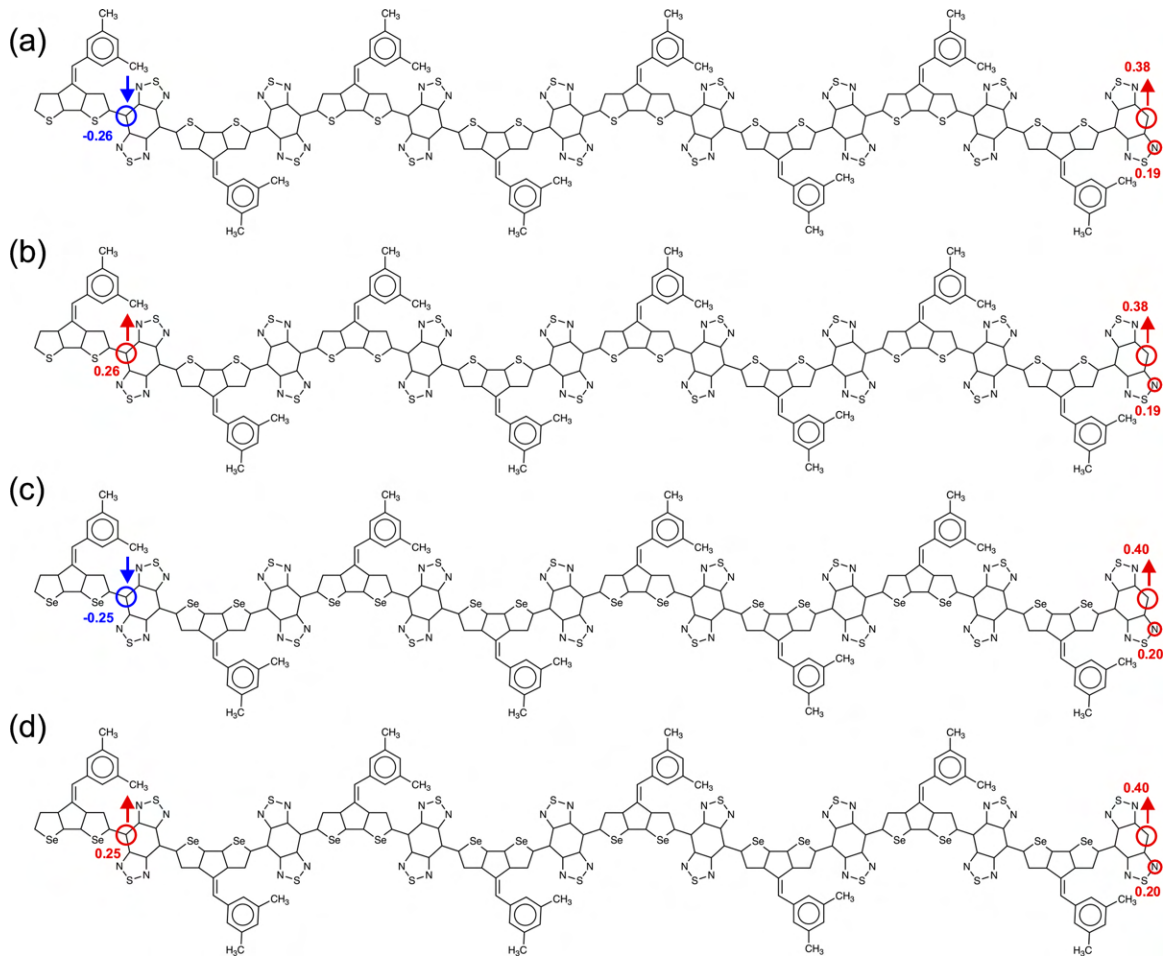


**Figure S44:** Locations of the unpaired electrons for (a) singlet ( $S = 0$ ) and (b) triplet ( $S = 1$ ) states on CPDT-BBT; (c) singlet ( $S = 0$ ) and (d) triplet ( $S = 1$ ) states on CPDS-BBT octamer ( $N = 8$ ) backbone based on the probability of maximum spin density. Color code: Red is for spin-up and Blue is for spin-down.

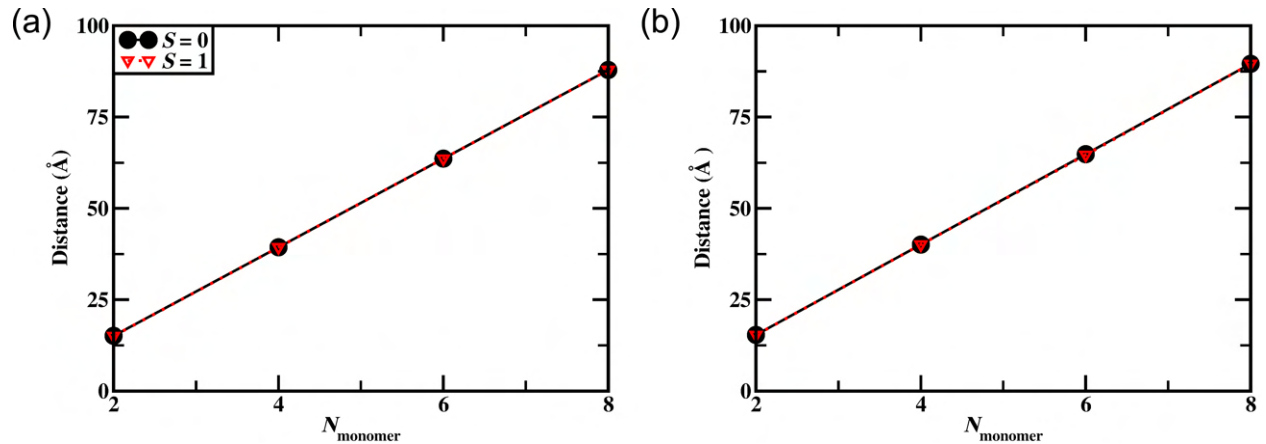


**Figure S45:** Separation between the unpaired electrons as a function of polymer chain length for (a) CPDT-BBT and (b) CPDS-BBT. Black filled circle is for singlet state ( $S = 0$ ) and red triangle is for triplet state ( $S = 1$ ). As a greater number of monomer units are added to the polymer backbone, a rapid increase in the distance between the unpaired electrons is observed.

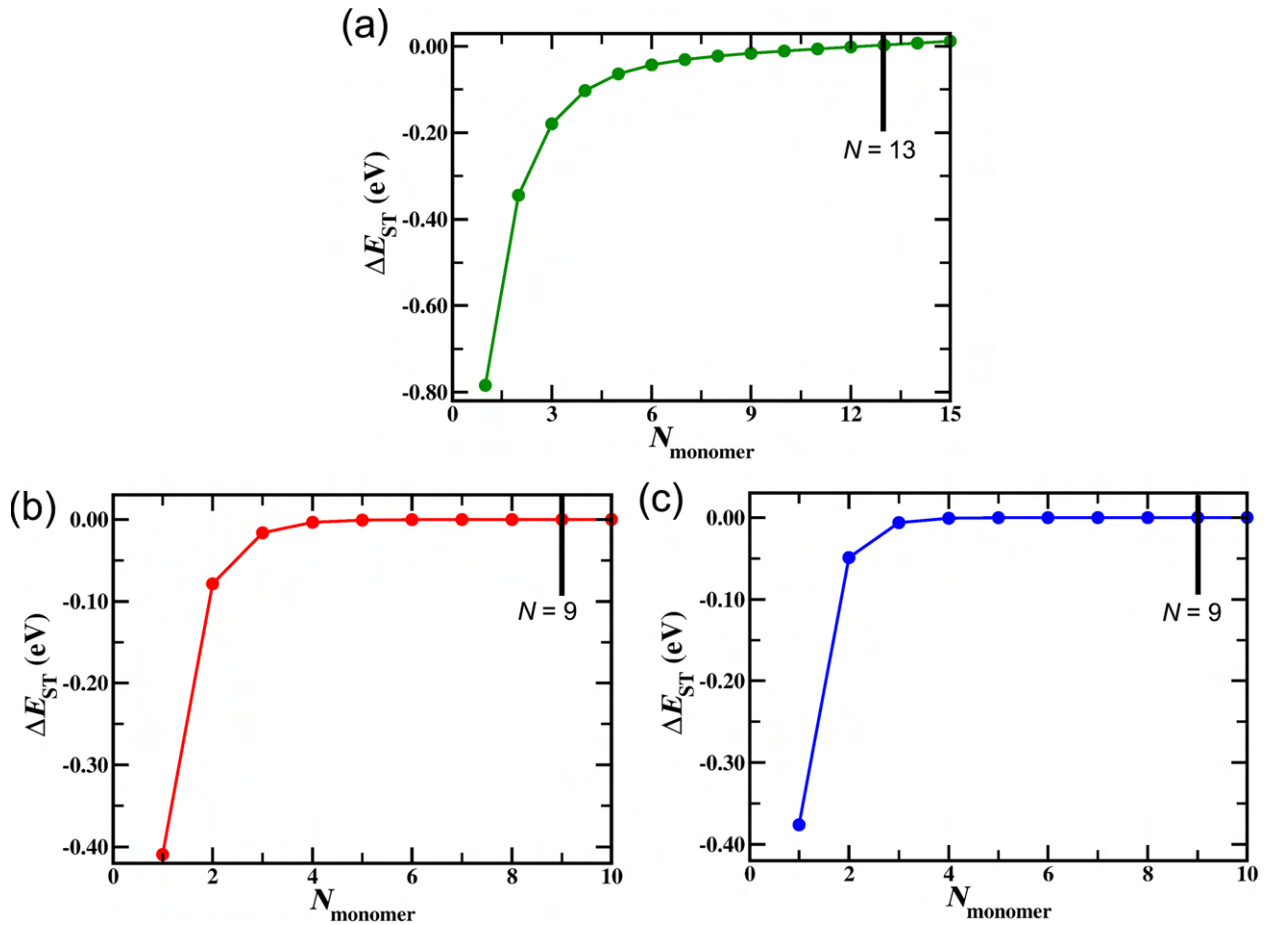


**Figure S46:**  $\Delta E_{\text{ST}}$  of the (a) CPDT-TQ, (b) CPDT-BBT, and (c) CPDS-BBT polymers as a function of  $N$  showing as  $N$  increases,  $\Delta E_{\text{ST}}$  decreases rapidly and become degenerate at  $N = 8$  in the BBT-based polymers. From extrapolation of these data, an inflection point is achieved at  $N = 9$  for both CPDT-BBT and CPDS-BBT polymers, whereas, the CPDT-TQ show an inflection point  $N = 13$  (shown with the vertical line).

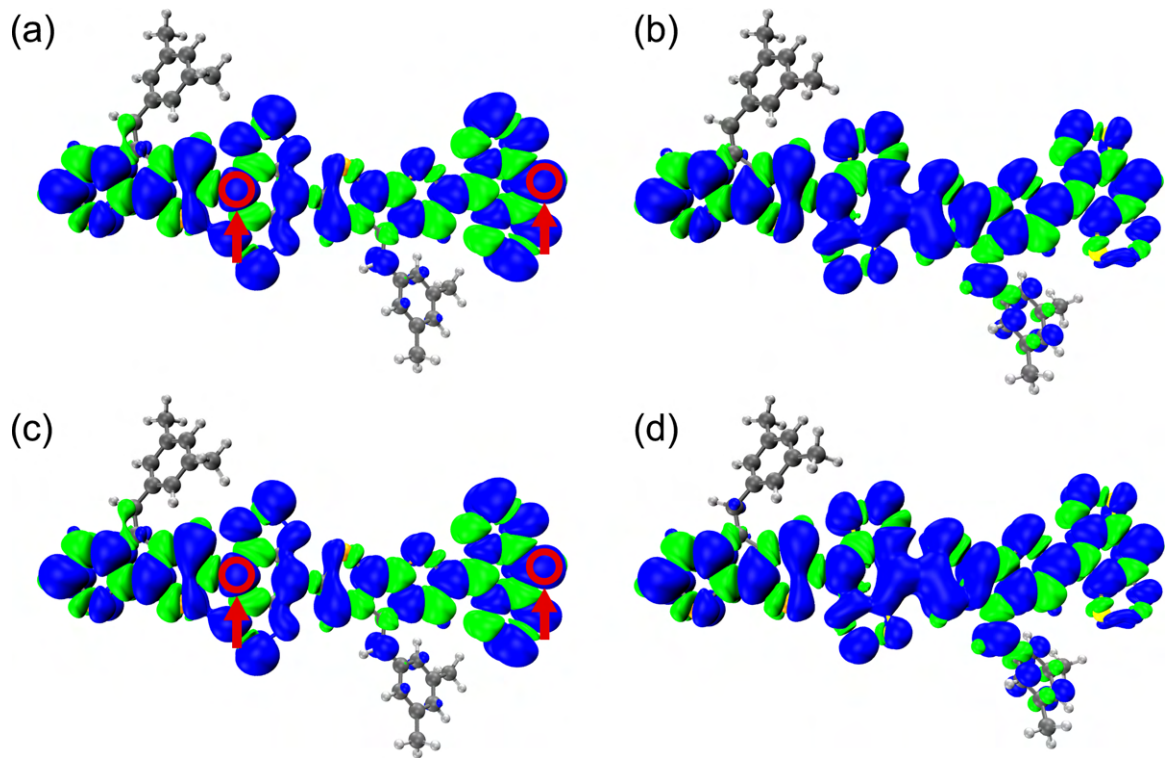


**Figure S47:** Spin density distributions of the (a) CPDT-BBT, (b) CPDT-iso-BBT, (c) CPDS-BBT, and (d) CPDS-iso-BBT ( $N = 2$ ) polymers in their triplet state ( $S = 1$ ). The blue and green surfaces represent positive and negative contributions of the spin density at an isovalue = 0.0002 au. The most probable locations for the unpaired electrons are highlighted with open circles.

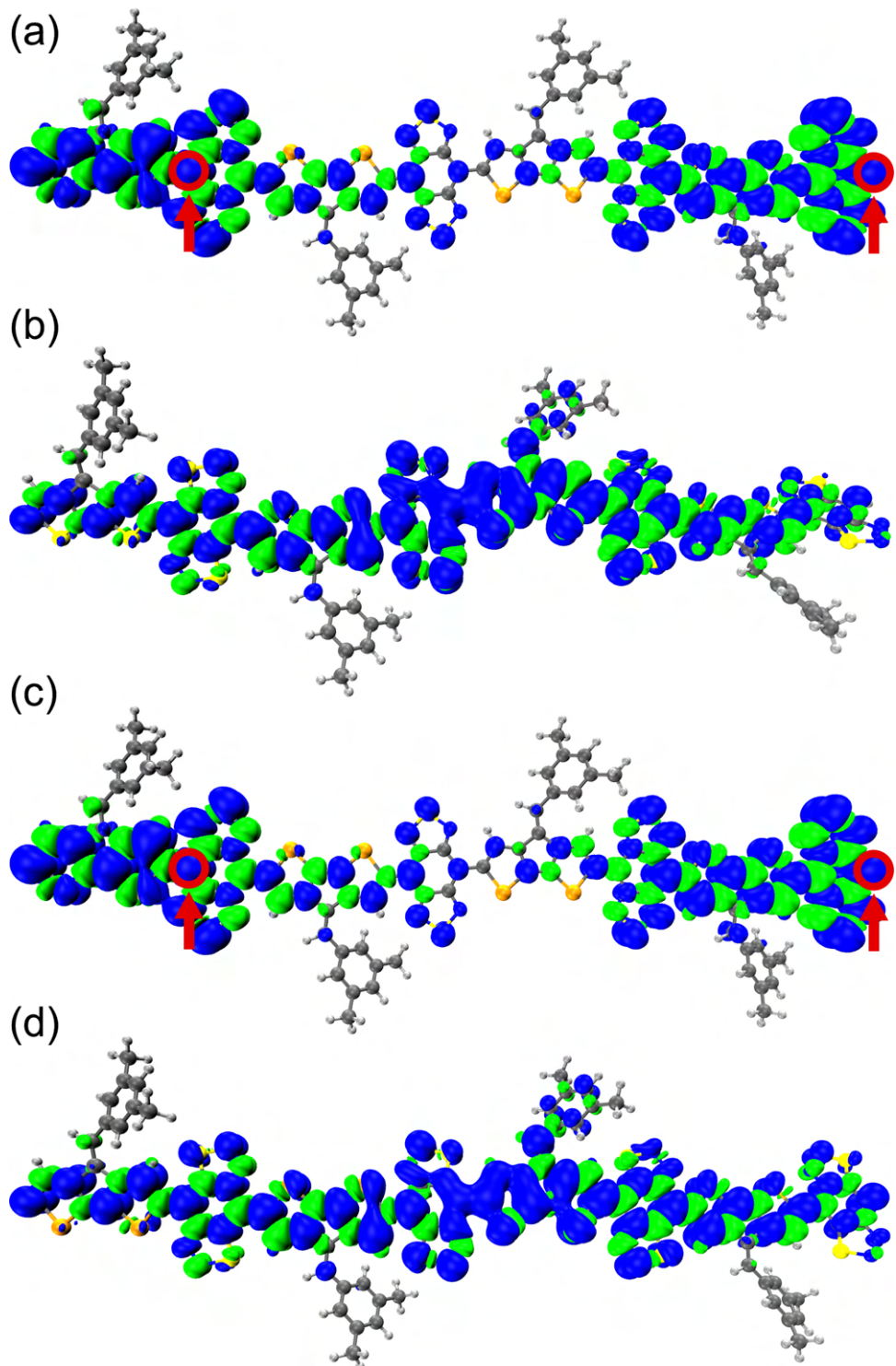


**Figure S48:** Spin density distributions of the (a) CPDT-BBT, (b) CPDT-iso-BBT, (c) CPDS-BBT, and (d) CPDS-iso-BBT ( $N = 4$ ) polymers in their triplet state ( $S = 1$ ). The blue and green surfaces represent positive and negative contributions of the spin density at an isovalue = 0.0002 au. The most probable locations for the unpaired electrons are highlighted with open circles.

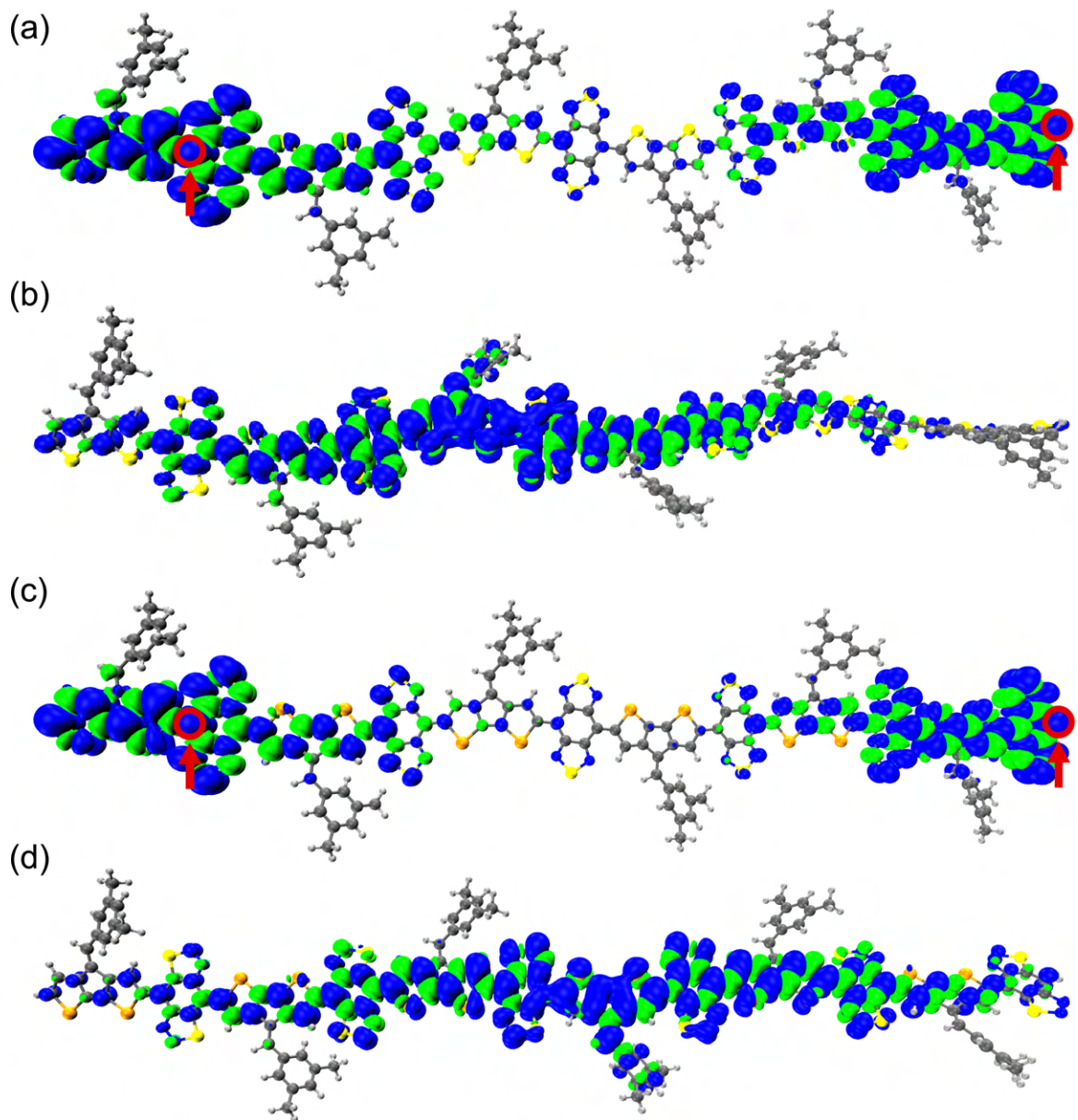


**Figure S49:** Spin density distributions of the (a) CPDT-BBT, (b) CPDT-iso-BBT, (c) CPDS-BBT, and (d) CPDS-iso-BBT ( $N = 6$ ) polymers in their triplet state ( $S = 1$ ). The blue and green surfaces represent positive and negative contributions of the spin density at an isovalue = 0.0002 au. The most probable locations for the unpaired electrons are highlighted with open circles.

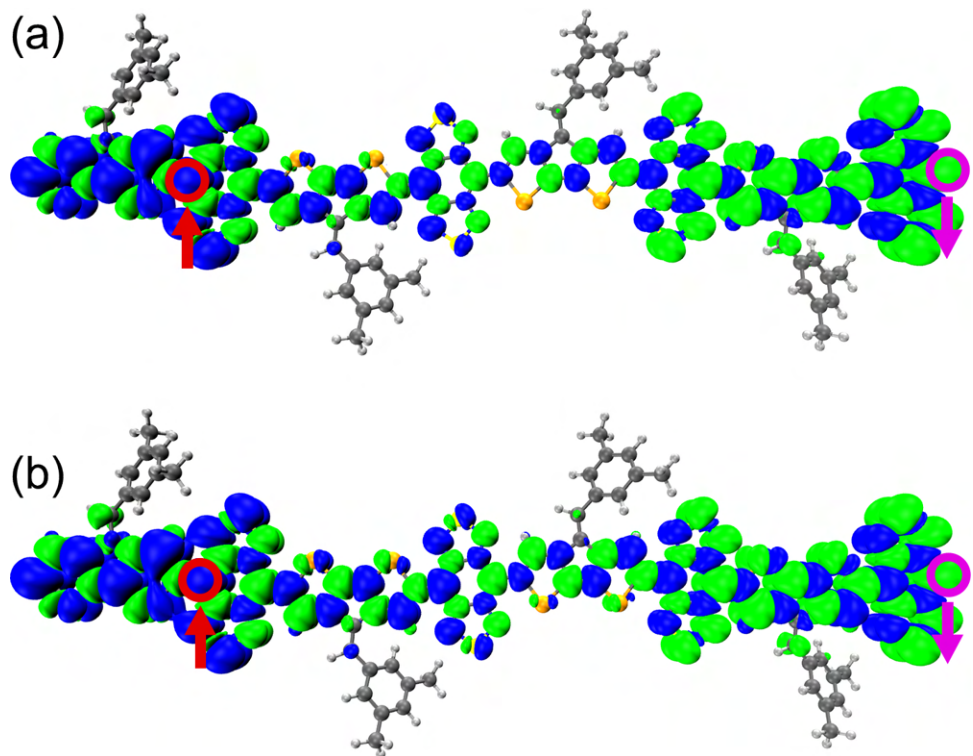


**Figure S50:** Spin density distributions of the CPDS-BBT polymer ( $N = 4$ ) at (a) UB3LYP and (b) ULC- $\omega$ HPBE level of theory and 6-31G(d,p) basis set in the singlet state ( $S = 0$ ). The localization of the unpaired electrons is observed with both methods. The blue and green surfaces represent positive and negative contributions of the spin density at an isovalue = 0.0002 au. The most probable locations for the unpaired electrons are highlighted with open circles.

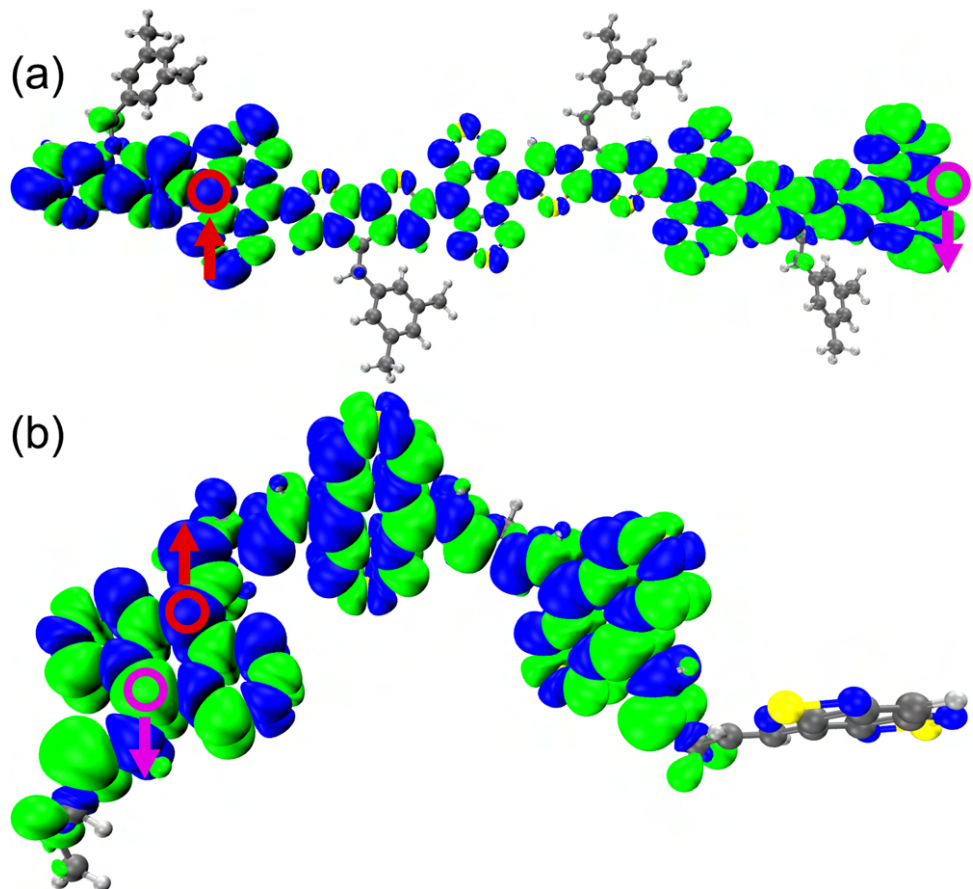


**Figure S51:** Spin density distributions of the (a) CPDT-BBT and (b) pentadiene-BBT polymer ( $N = 4$ ) in the singlet state ( $S = 0$ ). The blue and green surfaces represent positive and negative contributions of the spin density at an isovalue = 0.0002 au. The most probable locations for the unpaired electrons are highlighted with open circles (red: up-spin and purple: down-spin)

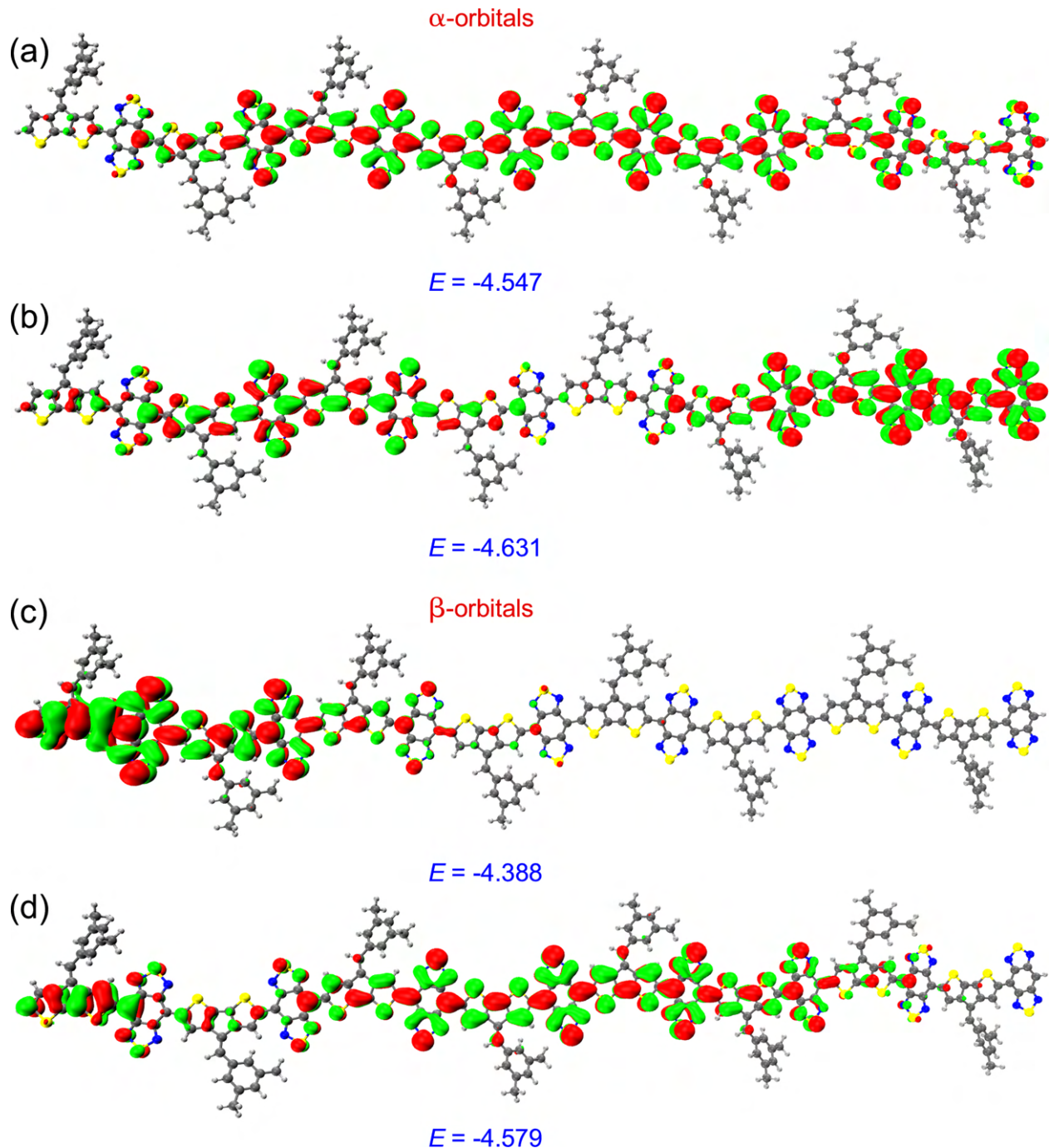


**Figure S52:** The degenerate  $\alpha$ -SOMO ( $E = -4.547$  eV) (a) and  $\beta$ -SOMO-1 ( $E = 4.579$  eV) (d) orbitals indicate significant overlap between these two orbitals. As a consequence, the  $\alpha$ -SOMO-1 ( $E = -4.631$  eV) (b) and  $\beta$ -SOMO ( $E = -4.388$  eV) (c) contribute to the total spin density. MOs are displayed for CPDT-BBT octamer ( $N = 8$ ). The green and red surfaces represent positive and negative signs of the MO at isovalue = 0.01 au, respectively.

**Table S7:** Calculated orbital overlap ( $S^{\alpha\beta}$ ) values between different spin orbitals for CPDT-BBT ( $N = 8$ ) in the singlet state ( $S = 0$ ).

	$\beta$ -SOMO	$\beta$ -SOMO-1
$\alpha$ -SOMO	0.302	0.903
$\alpha$ -SOMO-1	0.234	—

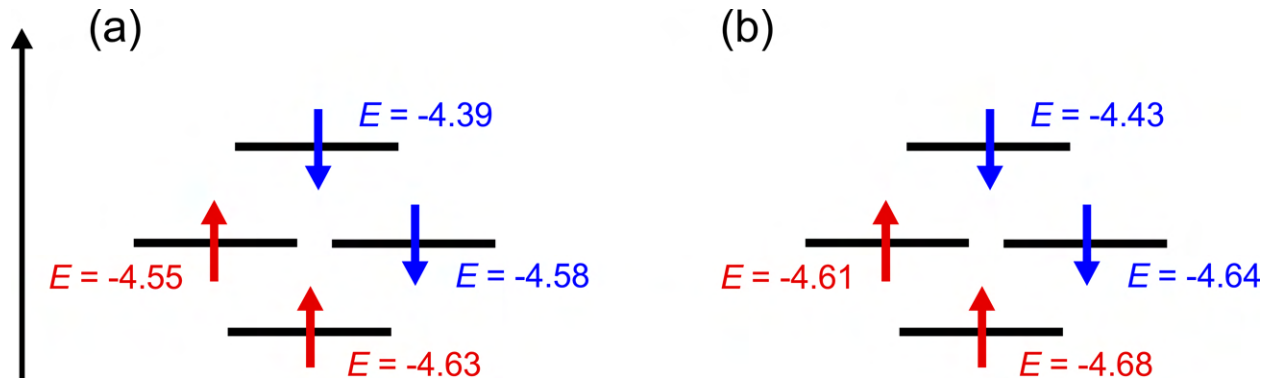


**Figure S53:** Calculated SOMO energies of octamer ( $N = 8$ ) for (a) CPDT-BBT and (b) CPDS-BBT in their singlet state indicate unique orbital topology inherent to the BBT-based polymers.

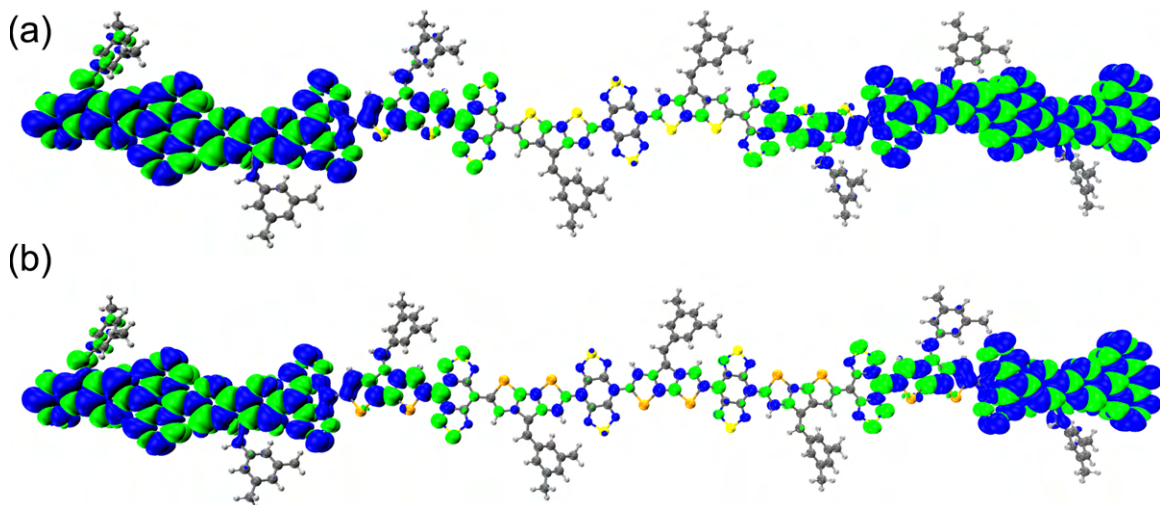


**Figure S54:** Spin density distributions of the (a) CPDT-BBT and (b) CPDS-BBT octamer ( $N = 8$ ) in their triplet states ( $S = 1$ ) with  $\omega$ B97X functional and 6-31G(d,p) basis set on UB3LYP geometry. The blue and green surfaces represent positive and negative contributions of the spin density at an isovalue = 0.0002 au.

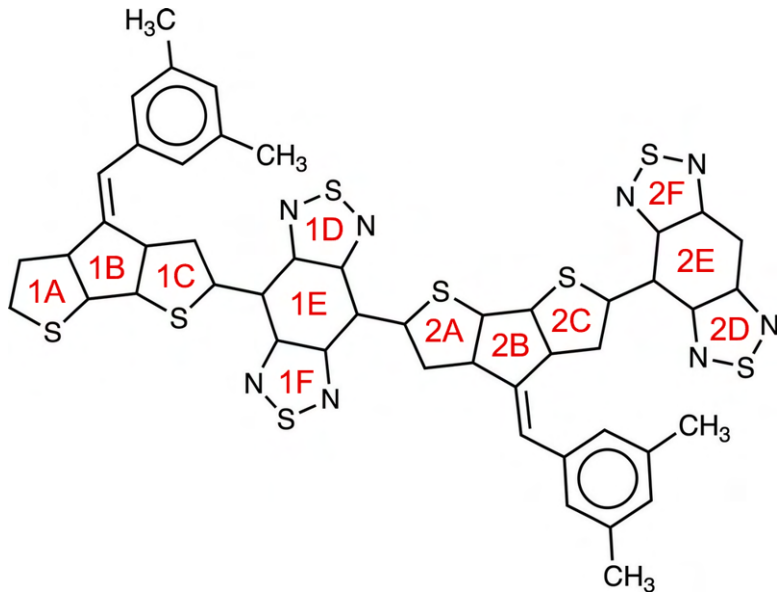


**Table S8:** Calculated NICS<sub>iso</sub>(1) (ppm) of CPDT-BBT dimer ( $N = 2$ ) in the singlet and triplet states.

Ring index	singlet ( $S = 0$ )	triplet ( $S = 1$ )	Ring index	singlet ( $S = 0$ )	triplet ( $S = 1$ )
1A	-7.20	-7.10	2A	-4.35	-3.77
1B	-0.19	-0.29	2B	-1.48	-1.84
1C	-5.28	-5.20	2C	-5.04	-4.69
1D	-10.53	-9.30	2D	-11.40	-10.74
1E	-3.07	-1.14	2E	-5.52	-4.21
1F	-10.59	-9.39	2F	-11.23	-10.57

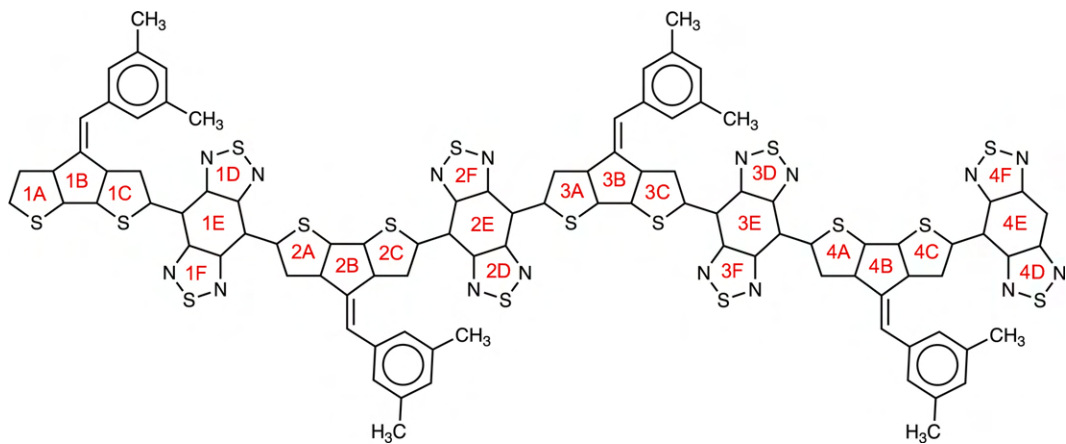


**Table S9:** Calculated NICS<sub>iso</sub>(1) (ppm) of CPDT-BBT tetramer ( $N = 4$ ) in the singlet and triplet states.

Ring index	singlet ( $S = 0$ )	triplet ( $S = 1$ )	Ring index	singlet ( $S = 0$ )	triplet ( $S = 1$ )
1A	-7.15	-7.14	2A	-3.88	-3.85
1B	-0.11	-0.11	2B	-1.91	-1.94
1C	-5.36	-5.35	2C	-4.51	-4.48
1D	-9.95	-9.88	2D	-9.94	-9.88
1E	-2.01	-1.92	2E	-1.30	-1.20
1F	-9.96	-9.91	2F	-9.93	-9.88
3A	-3.75	-3.72	4A	-4.04	-4.01
3B	-1.47	-1.49	4B	-1.71	-1.72
3C	-4.03	-4.01	4C	-4.86	-4.84
3D	-9.93	-9.88	4D	-11.08	-10.90
3E	-1.45	-1.37	4E	-4.88	-4.83
3F	-9.93	-9.89	4F	-10.92	-11.05

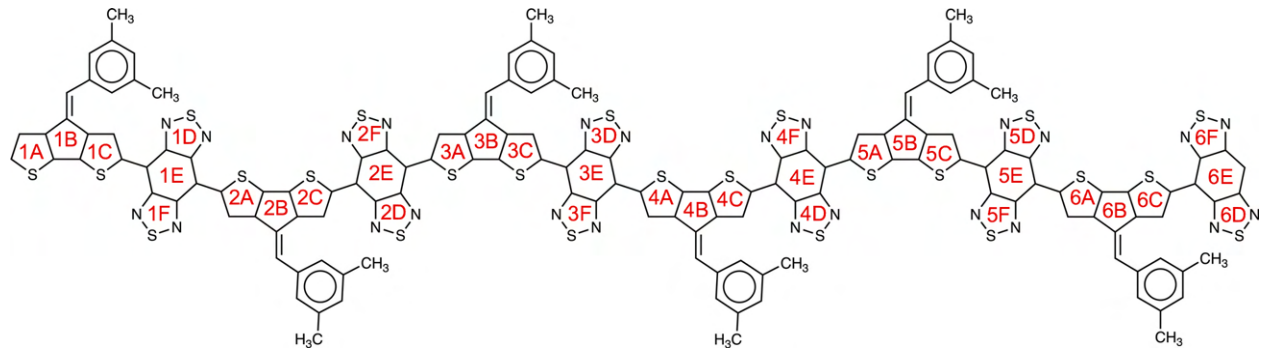


**Table S10:** Calculated NICS<sub>iso</sub>(1) (ppm) of CPDT-BBT hexamer ( $N = 6$ ) in the singlet and triplet states.

Ring index	singlet ( $S = 0$ )	triplet ( $S = 1$ )	Ring index	singlet ( $S = 0$ )	triplet ( $S = 1$ )
1A	-7.16	-7.16	2A	-3.97	-3.97
1B	-0.08	-0.08	2B	-1.90	-1.89
1C	-5.33	-5.33	2C	-4.36	-4.37
1D	-9.88	-9.88	2D	-9.88	-9.88
1E	-1.96	-1.97	2E	-1.22	-1.23
1F	-9.93	-9.94	2F	-9.88	-9.88
3A	-3.81	-3.80	4A	-3.83	-3.84
3B	-1.49	-1.49	4B	-1.96	-1.97
3C	-3.93	-3.93	4C	-4.36	-4.36
3D	-9.81	-9.82	4D	-9.91	-9.91
3E	-1.16	-1.15	4E	-1.20	-1.19
3F	-9.83	-9.83	4F	-9.89	-9.89
5A	-3.77	-3.76	6A	-4.04	-4.03
5B	-1.47	-1.47	6B	-1.71	-1.71
5C	-3.98	-3.98	6C	-4.85	-4.83
5D	-9.89	-9.89	6D	-11.07	-11.07
5E	-1.40	-1.40	6E	-4.85	-4.84
5F	-9.91	-9.91	6F	-10.91	-10.90

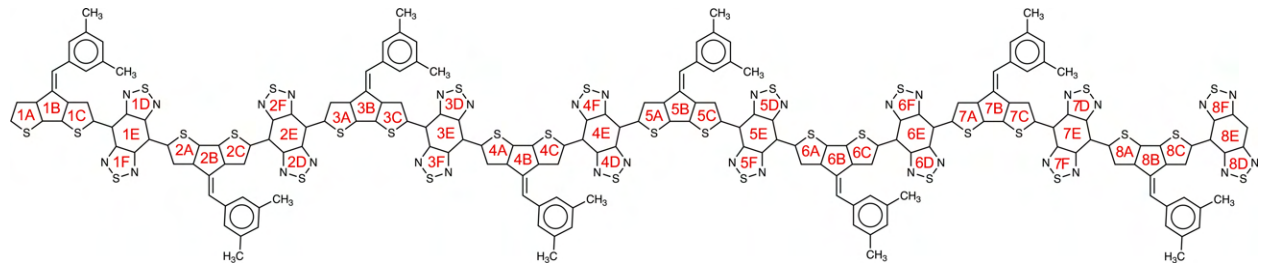


**Table S11:** Calculated NICS<sub>iso</sub>(1) (ppm) of CPDT-BBT octamer ( $N = 8$ ) in the singlet and triplet states.

Ring index	singlet ( $S = 0$ )	triplet ( $S = 1$ )	Ring index	singlet ( $S = 0$ )	triplet ( $S = 1$ )
1A	-7.17	-7.17	2A	-4.04	-4.04
1B	-0.09	-0.09	2B	-1.87	-1.87
1C	-5.31	-5.31	2C	-4.28	-4.29
1D	-9.86	-9.87	2D	-9.89	-9.88
1E	-1.96	-1.96	2E	-1.22	-1.22
1F	-9.95	-9.95	2F	-9.88	-9.88
3A	-3.84	-3.84	4A	-3.91	-3.91
3B	-1.50	-1.50	4B	-1.95	-1.95
3C	-3.87	-3.87	4C	-4.27	-4.27
3D	-9.80	-9.80	4D	-9.89	-9.89
3E	-1.15	-1.15	4E	-1.18	-1.18
3F	-9.83	-9.83	4F	-9.87	-9.88
5A	-3.83	-3.83	6A	-3.84	-3.84
5B	-1.48	-1.48	6B	-1.96	-1.96
5C	-3.91	-3.90	6C	-4.35	-4.35
5D	-9.81	-9.81	6D	-9.91	-9.92
5E	-1.15	-1.15	6E	-1.20	-1.20
5F	-9.84	-9.83	6F	-9.89	-9.90
7A	-3.78	-3.77	8A	-4.05	-4.05
7B	-1.47	-1.47	8B	-1.70	-1.70
7C	-3.97	-3.96	8C	-4.85	-4.84
7D	-9.88	-9.89	8D	-11.08	-11.08
7E	-1.41	-1.41	8E	-4.87	-4.87
7F	-9.91	-9.91	8F	-10.91	-10.93

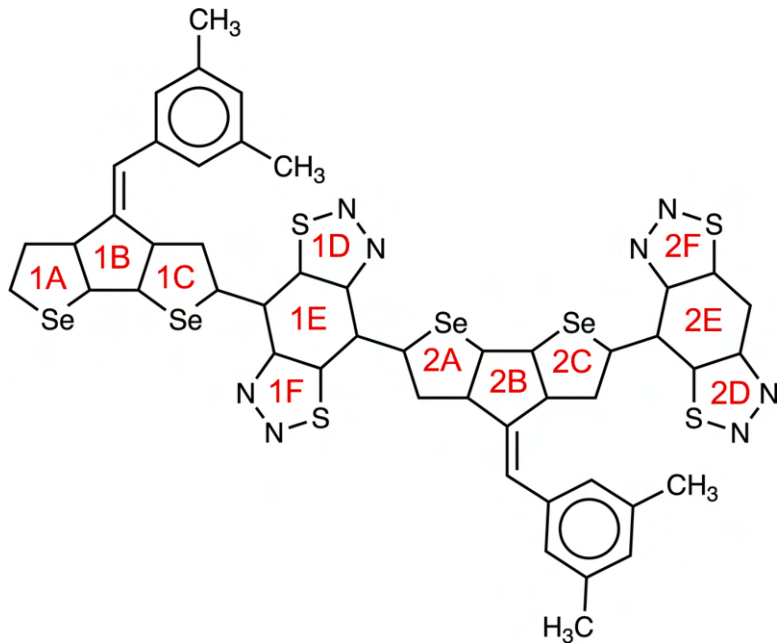


**Table S12:** Calculated NICS<sub>iso</sub>(1) (ppm) of CPDT-iso-BBT dimer ( $N = 2$ ) in the singlet and triplet states.

Ring index	singlet ( $S = 0$ )	triplet ( $S = 1$ )	Ring index	singlet ( $S = 0$ )	triplet ( $S = 1$ )
1A	-7.61	-6.90	2A	-6.59	-3.87
1B	-0.12	-0.03	2B	-0.90	-1.13
1C	-6.00	-5.05	2C	-6.40	-4.84
1D	-10.05	-8.99	2D	-10.19	-10.14
1E	-8.44	-1.38	2E	-10.47	-9.18
1F	-9.83	-9.41	2F	-10.24	-10.05

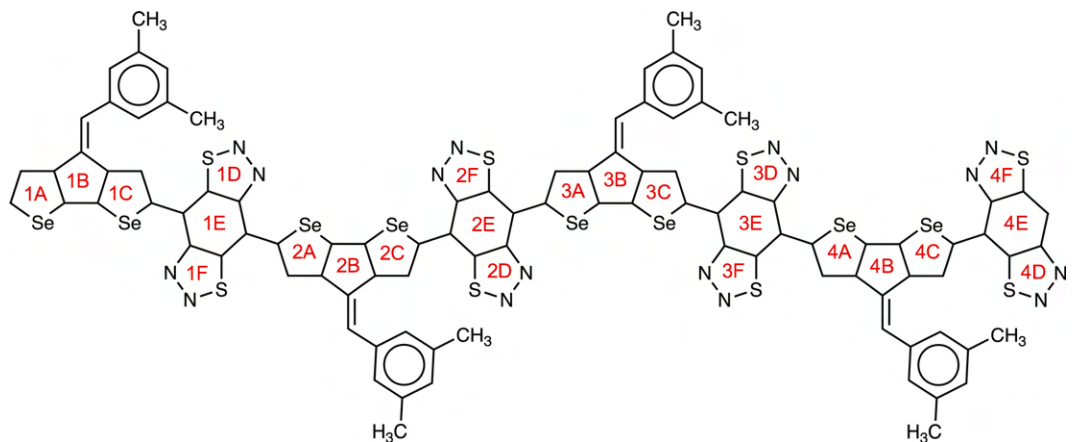


**Table S13:** Calculated NICS<sub>iso</sub>(1) (ppm) of CPDT-iso-BBT tetramer ( $N = 4$ ) in the singlet and triplet states.

Ring index	singlet ( $S = 0$ )	triplet ( $S = 1$ )	Ring index	singlet ( $S = 0$ )	triplet ( $S = 1$ )
1A	-7.78	-7.63	2A	-6.48	-5.35
1B	-0.05	-0.13	2B	-0.90	-1.02
1C	-6.00	-5.87	2C	-6.16	-5.07
1D	-10.02	-9.91	2D	-10.18	-9.49
1E	-8.41	-7.58	2E	-8.70	-2.77
1F	-9.85	-9.91	2F	-9.78	-9.64
3A	-6.31	-3.89	4A	-6.54	-6.09
3B	-0.36	-0.69	4B	-0.93	-0.97
3C	-6.00	-4.44	4C	-6.41	-6.27
3D	-9.99	-9.93	4D	-10.20	-10.19
3E	-8.40	-6.30	4E	-10.51	-10.38
3F	-9.82	-9.60	4F	-10.24	-10.21

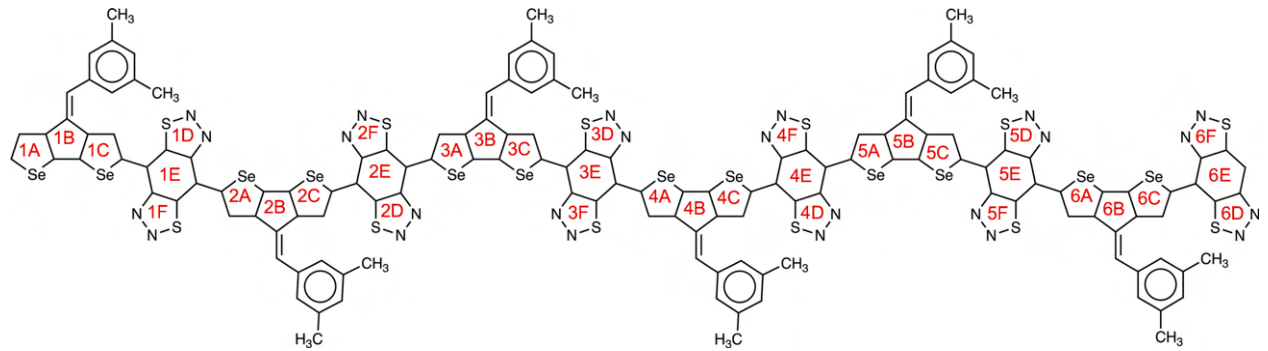


**Table S14:** Calculated NICS<sub>iso</sub>(1) (ppm) of CPDT-iso-BBT hexamer ( $N = 6$ ) in the singlet and triplet states.

Ring index	singlet ( $S = 0$ )	triplet ( $S = 1$ )	Ring index	singlet ( $S = 0$ )	triplet ( $S = 1$ )
1A	-8.37	-7.71	2A	-6.55	-6.14
1B	-0.03	-0.12	2B	-0.88	-0.80
1C	-5.96	-5.91	2C	-6.19	-5.81
1D	-10.02	-10.02	2D	-10.22	-9.89
1E	-8.43	-8.21	2E	-8.68	-5.66
1F	-9.87	-9.86	2F	-9.66	-9.95
3A	-6.38	-3.95	4A	-6.45	-5.38
3B	-0.39	-0.68	4B	-0.86	-1.06
3C	-5.94	-3.80	4C	-6.20	-5.62
3D	-10.02	-9.73	4D	-10.18	-9.75
3E	-8.35	-3.55	4E	-8.75	-8.52
3F	-9.78	-9.34	4F	-9.75	-10.17
5A	-6.31	-6.36	6A	-6.53	-6.54
5B	-0.43	-0.40	6B	-0.94	-0.94
5C	-5.97	-5.97	6C	-6.40	-6.41
5D	-10.00	-10.02	6D	-10.17	-10.18
5E	-8.40	-8.37	6E	-10.51	-10.50
5F	-9.85	-9.83	6F	-10.23	-10.24

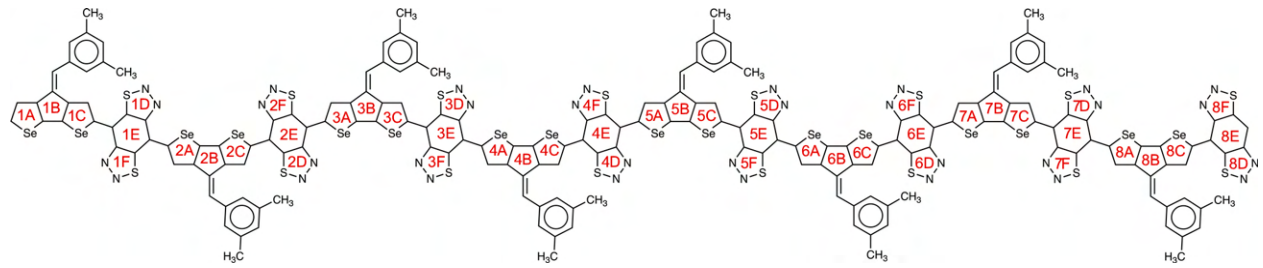


**Table S15:** Calculated NICS<sub>iso</sub>(1) (ppm) of CPDT-iso-BBT octamer ( $N = 8$ ) in the singlet and triplet states.

Ring index	singlet ( $S = 0$ )	triplet ( $S = 1$ )	Ring index	singlet ( $S = 0$ )	triplet ( $S = 1$ )
1A	-8.28	-8.12	2A	-6.53	-6.47
1B	-0.05	-0.05	2B	-0.93	-0.82
1C	-5.84	-5.90	2C	-6.18	-6.19
1D	-10.06	-9.98	2D	-9.87	-9.78
1E	-8.37	-8.44	2E	-9.12	-9.15
1F	-9.84	-9.81	2F	-10.19	-10.17
3A	-6.45	-6.40	4A	-6.43	-5.93
3B	-0.28	-0.32	4B	-0.89	-1.00
3C	-5.99	-5.95	4C	-6.17	-5.62
3D	-9.98	-9.94	4D	-10.19	-9.78
3E	-8.42	-7.95	4E	-8.72	-4.91
3F	-9.76	-9.90	4F	-9.76	-9.85
5A	-6.35	-3.74	6A	-6.47	-5.49
5B	-0.36	-0.75	6B	-0.86	-1.05
5C	-5.92	-3.79	6C	-6.21	-5.82
5D	-10.01	-9.76	6D	-10.18	-10.20
5E	-8.35	-4.27	6E	-8.74	-8.29
5F	-9.82	-9.45	6F	-9.73	-9.80
7A	-6.29	-6.22	8A	-6.67	-6.65
7B	-0.45	-0.45	8B	-0.93	-0.92
7C	-5.99	-5.95	8C	-6.41	-6.41
7D	-9.82	-9.85	8D	-10.17	-10.19
7E	-8.43	-8.37	8E	-10.51	-10.50
7F	-9.99	-10.00	8F	-10.24	-10.25

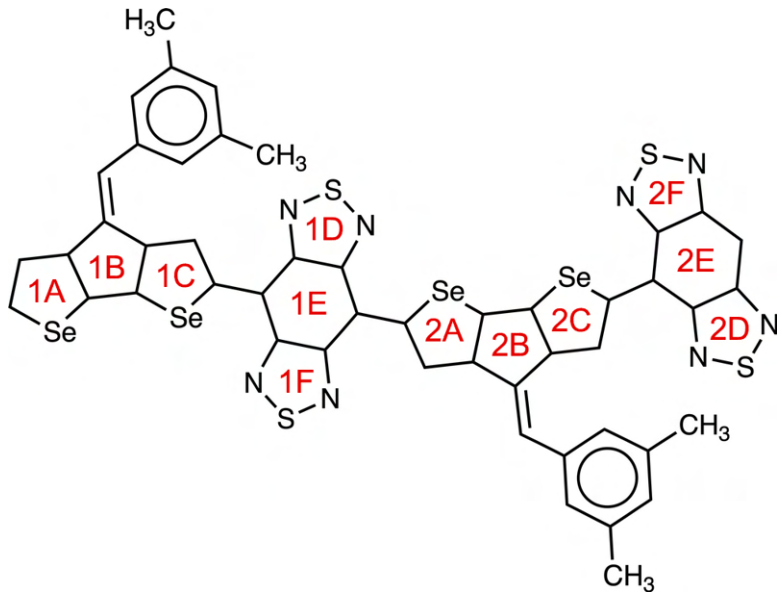


**Table S16:** Calculated NICS<sub>iso</sub>(1) (ppm) of CPDS-BBT dimer ( $N = 2$ ) in the singlet and triplet states.

Ring index	singlet ( $S = 0$ )	triplet ( $S = 1$ )	Ring index	singlet ( $S = 0$ )	triplet ( $S = 1$ )
1A	-7.20	-7.12	2A	-3.86	-3.46
1B	-0.11	-0.18	2B	-1.50	-1.74
1C	-5.46	-5.39	2C	-5.01	-4.76
1D	-10.21	-9.31	2D	-11.27	-10.81
1E	-2.49	-1.20	2E	-4.92	-4.02
1F	-10.27	-9.39	2F	-10.85	-10.37

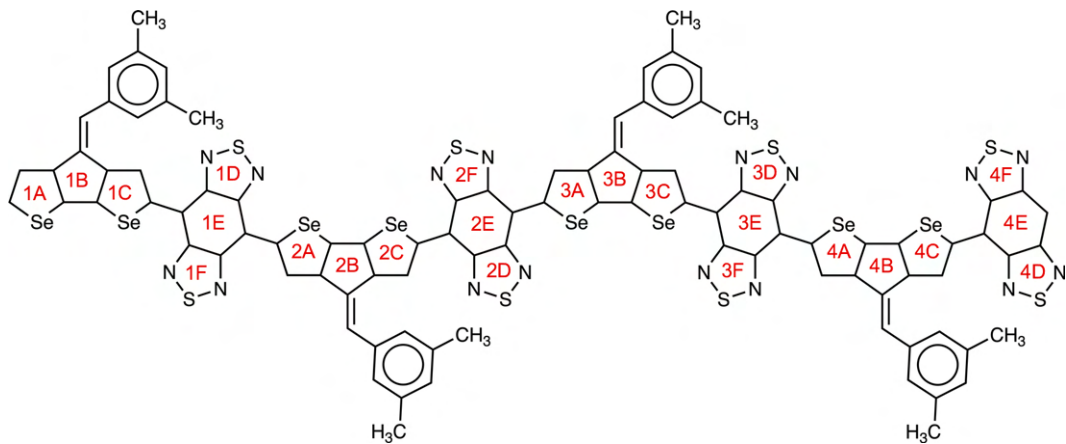


**Table S17:** Calculated NICS<sub>iso</sub>(1) (ppm) of CPDS-BBT tetramer ( $N = 4$ ) in the singlet and triplet states.

Ring index	singlet ( $S = 0$ )	triplet ( $S = 1$ )	Ring index	singlet ( $S = 0$ )	triplet ( $S = 1$ )
1A	-7.16	-7.16	2A	-3.56	-3.55
1B	0.02	0.02	2B	-1.85	-1.85
1C	-5.61	-5.61	2C	-4.61	-4.61
1D	-9.73	-9.72	2D	-9.88	-9.87
1E	-1.67	-1.66	2E	-1.18	-1.15
1F	-9.73	-9.72	2F	-9.81	-9.80
3A	-3.50	-3.50	4A	-3.63	-3.63
3B	-1.30	-1.30	4B	-1.67	-1.67
3C	-4.22	-4.21	4C	-4.86	-4.86
3D	-9.81	-9.80	4D	-11.03	-11.02
3E	-1.22	-1.20	4E	-4.43	-4.42
3F	-9.78	-9.77	4F	-10.59	-10.59

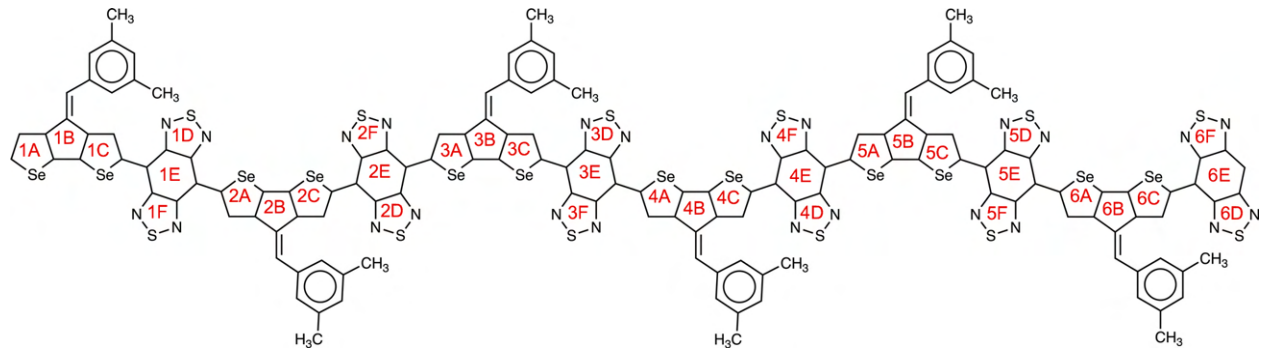


**Table S18:** Calculated NICS<sub>iso</sub>(1) (ppm) of CPDS-BBT hexamer ( $N = 6$ ) in the singlet and triplet states.

Ring index	singlet ( $S = 0$ )	triplet ( $S = 1$ )	Ring index	singlet ( $S = 0$ )	triplet ( $S = 1$ )
1A	-7.15	-7.15	2A	-3.63	-3.63
1B	0.05	0.05	2B	-1.85	-1.84
1C	-5.60	-5.60	2C	-4.55	-4.55
1D	-9.71	-9.72	2D	-9.87	-9.87
1E	-1.68	-1.68	2E	-1.15	-1.15
1F	-9.70	-9.69	2F	-9.79	-9.78
3A	-3.56	-3.56	4A	-3.57	-3.58
3B	-1.30	-1.30	4B	-1.87	-1.88
3C	-4.17	-4.16	4C	-4.57	-4.57
3D	-9.76	-9.76	4D	-9.88	-9.88
3E	-1.07	-1.06	4E	-1.14	-1.14
3F	-9.71	-9.70	4F	-9.80	-9.80
5A	-3.50	-3.50	6A	-3.64	-3.64
5B	-1.29	-1.30	6B	-1.67	-1.67
5C	-4.18	-4.17	6C	-4.86	-4.86
5D	-9.81	-9.80	6D	-11.03	-11.03
5E	-1.22	-1.22	6E	-4.43	-4.43
5F	-9.78	-9.78	6F	-10.60	-10.60

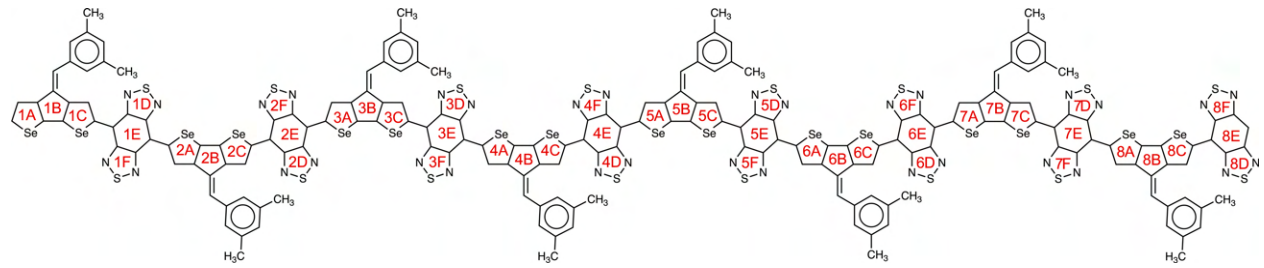


**Table S19:** Calculated NICS<sub>iso</sub>(1) (ppm) of CPDS-BBT octamer ( $N = 8$ ) in the singlet and triplet states.

Ring index	singlet ( $S = 0$ )	triplet ( $S = 1$ )	Ring index	singlet ( $S = 0$ )	triplet ( $S = 1$ )
1A	-7.15	-7.16	2A	-3.68	-3.67
1B	0.07	0.06	2B	-1.85	-1.85
1C	-5.61	-5.60	2C	-4.51	-4.51
1D	-9.71	-9.71	2D	-9.90	-9.88
1E	-1.67	-1.66	2E	-1.15	-1.15
1F	-9.67	-9.68	2F	-9.78	-9.77
3A	-3.58	-3.58	4A	-3.64	-3.64
3B	-1.30	-1.30	4B	-1.87	-1.87
3C	-4.14	-4.15	4C	-4.52	-4.51
3D	-9.76	-9.76	4D	-9.88	-9.88
3E	-1.06	-1.06	4E	-1.13	-1.14
3F	-9.69	-9.69	4F	-9.77	-9.78
5A	-3.56	-3.56	6A	-3.59	-3.59
5B	-1.30	-1.30	6B	-1.87	-1.87
5C	-4.13	-4.13	6C	-4.58	-4.58
5D	-9.76	-9.76	6D	-9.88	-9.89
5E	-1.07	-1.07	6E	-1.14	-1.14
5F	-9.72	-9.71	6F	-9.80	-9.80
7A	-3.50	-3.50	8A	-3.64	-3.64
7B	-1.30	-1.29	8B	-1.67	-1.67
7C	-4.16	-4.16	8C	-4.86	-4.86
7D	-9.80	-9.80	8D	-11.02	-11.03
7E	-1.21	-1.22	8E	-4.43	-4.44
7F	-9.78	-9.78	8F	-10.61	-10.61

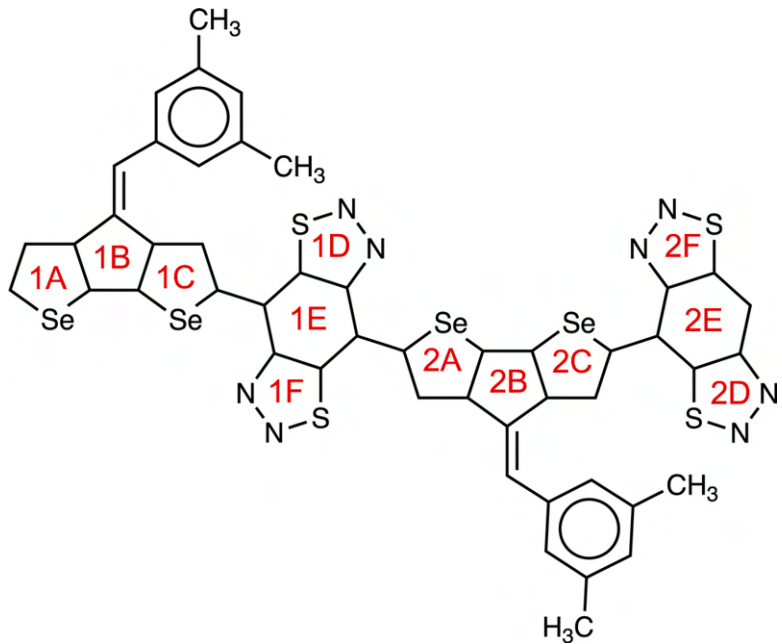


**Table S20:** Calculated NICS<sub>iso</sub>(1) (ppm) of CPDS-iso-BBT dimer ( $N = 2$ ) in the singlet and triplet states.

Ring index	singlet ( $S = 0$ )	triplet ( $S = 1$ )	Ring index	singlet ( $S = 0$ )	triplet ( $S = 1$ )
1A	-7.58	-6.92	2A	-5.85	-3.54
1B	-0.03	0.07	2B	-0.79	-0.98
1C	-5.62	-4.84	2C	-6.07	-4.57
1D	-10.17	-9.13	2D	-10.38	-10.30
1E	-8.19	-1.92	2E	-10.21	-8.95
1F	-9.96	-9.55	2F	-10.30	-10.00

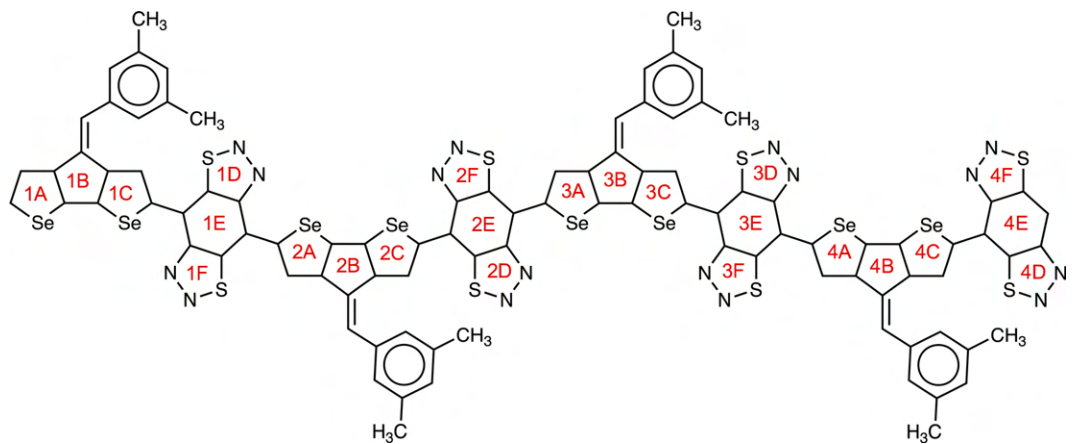


**Table S21:** Calculated  $\text{NICS}_{iso}(1)$  (ppm) of CPDS-iso-BBT tetramer ( $N = 4$ ) in the singlet and triplet states.

Ring index	singlet ( $S = 0$ )	triplet ( $S = 1$ )	Ring index	singlet ( $S = 0$ )	triplet ( $S = 1$ )
1A	-7.60	-7.62	2A	-5.69	-4.94
1B	-0.02	-0.01	2B	-0.76	-0.98
1C	-5.64	-5.52	2C	-5.96	-4.99
1D	-10.11	-10.03	2D	-10.49	-9.69
1E	-8.14	-7.42	2E	-8.68	-3.29
1F	-10.04	-10.06	2F	-10.23	-9.77
3A	-5.85	-3.67	4A	-5.79	-5.52
3B	-0.36	-0.62	4B	-0.84	-0.89
3C	-5.55	-4.08	4C	-6.08	-5.89
3D	-10.09	-10.02	4D	-10.38	-10.36
3E	-8.10	-5.78	4E	-10.23	-10.09
3F	-9.97	-9.74	4F	-10.32	-10.28

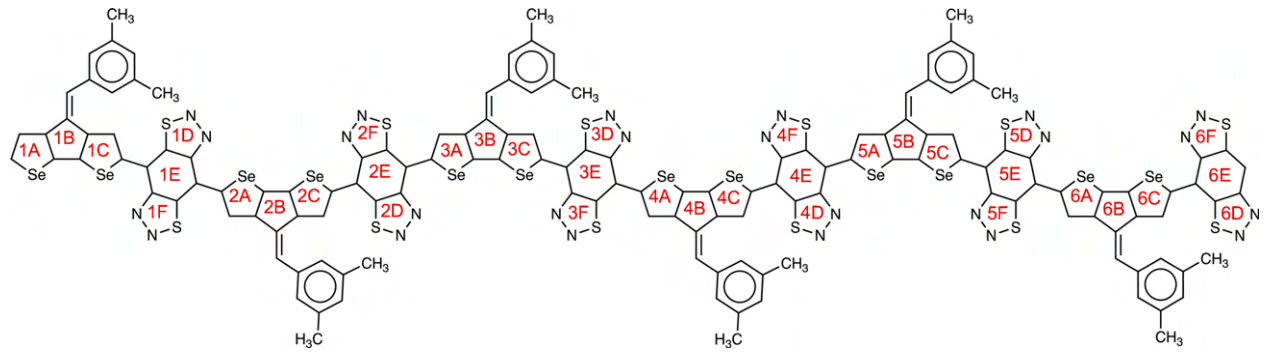


**Table S22:** Calculated NICS<sub>iso</sub>(1) (ppm) of CPDS-iso-BBT hexamer ( $N = 6$ ) in the singlet and triplet states.

Ring index	singlet ( $S = 0$ )	triplet ( $S = 1$ )	Ring index	singlet ( $S = 0$ )	triplet ( $S = 1$ )
1A	-7.61	-7.57	2A	-5.80	-5.64
1B	0.05	0.00	2B	-0.70	-0.70
1C	-5.62	-5.64	2C	-5.98	-5.86
1D	-10.17	-10.11	2D	-10.43	-10.43
1E	-8.14	-8.07	2E	-8.70	-7.96
1F	-9.97	-10.07	2F	-10.29	-10.22
3A	-5.85	-5.24	4A	-5.74	-3.70
3B	-0.31	-0.42	4B	-0.77	-1.13
3C	-5.50	-4.95	4C	-5.93	-4.06
3D	-10.10	-9.62	4D	-10.45	-10.12
3E	-8.03	-3.93	4E	-8.70	-5.08
3F	-9.95	-9.83	4F	-10.28	-9.75
5A	-5.85	-5.19	6A	-5.78	-5.73
5B	-0.39	-0.48	6B	-0.85	-0.86
5C	-5.55	-5.24	6C	-6.08	-6.05
5D	-10.09	-10.10	6D	-10.35	-10.39
5E	-8.10	-7.73	6E	-10.24	-10.20
5F	-9.95	-9.94	6F	-10.31	-10.31

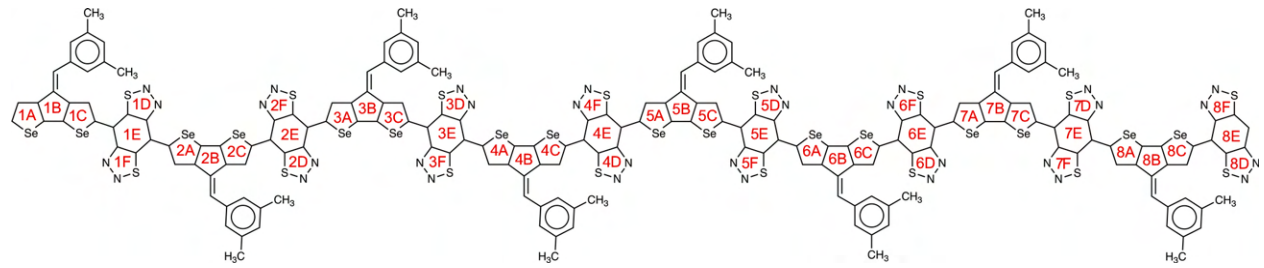


**Table S23:** Calculated NICS<sub>iso</sub>(1) (ppm) of CPDS-iso-BBT octamer ( $N = 8$ ) in the singlet and triplet states.

Ring index	singlet ( $S = 0$ )	triplet ( $S = 1$ )	Ring index	singlet ( $S = 0$ )	triplet ( $S = 1$ )
1A	-7.59	-7.64	2A	-5.72	-5.77
1B	-0.01	0.03	2B	-0.72	-0.71
1C	-5.68	-5.61	2C	-5.94	-5.97
1D	-10.07	-10.20	2D	-10.47	-10.38
1E	-8.17	-8.09	2E	-8.67	-8.66
1F	-10.02	-9.98	2F	-10.24	-10.26
3A	-5.85	-5.79	4A	-5.62	-5.23
3B	-0.35	-0.36	4B	-0.75	-0.94
3C	-5.57	-5.39	4C	-5.99	-5.30
3D	-10.06	-10.06	4D	-10.50	-9.85
3E	-8.05	-7.56	4E	-8.71	-4.50
3F	-10.08	-10.01	4F	-10.24	-9.92
5A	-5.83	-3.65	6A	-5.70	-5.18
5B	-0.36	-0.62	6B	-0.80	-0.93
5C	-5.54	-3.76	6C	-6.01	-5.53
5D	-10.07	-9.91	6D	-10.47	-10.42
5E	-8.05	-4.56	6E	-8.73	-8.16
5F	-9.97	-9.63	6F	-10.28	-10.22
7A	-5.87	-5.73	8A	-5.79	-5.78
7B	-0.37	-0.40	8B	-0.84	-0.85
7C	-5.54	-5.52	8C	-6.07	-6.07
7D	-10.10	-10.10	8D	-10.37	-10.34
7E	-8.08	-8.06	8E	-10.23	-10.24
7F	-9.96	-9.97	8F	-10.30	-10.32

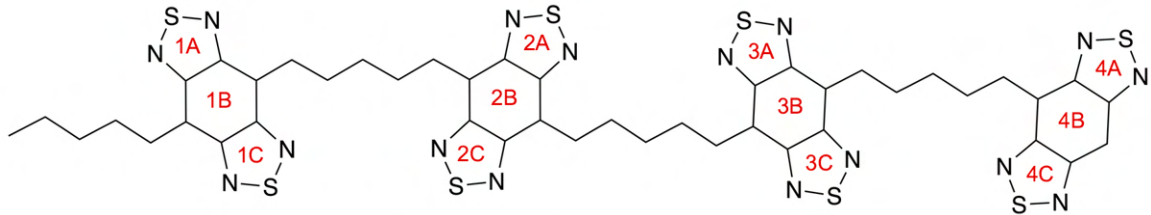


**Table S24:** Calculated NICS<sub>iso</sub>(1) (ppm) of pentadiene-BBT tetramer ( $N = 4$ ) in the singlet state.

Ring index	singlet ( $S = 0$ )	Ring index	singlet ( $S = 0$ )
1A	-12.89	3A	-13.33
1B	-8.43	3B	-8.38
1C	-13.41	3C	-12.77
2A	-13.26	4A	-13.74
2B	-8.33	4B	-10.52
2C	-12.70	4C	-13.97

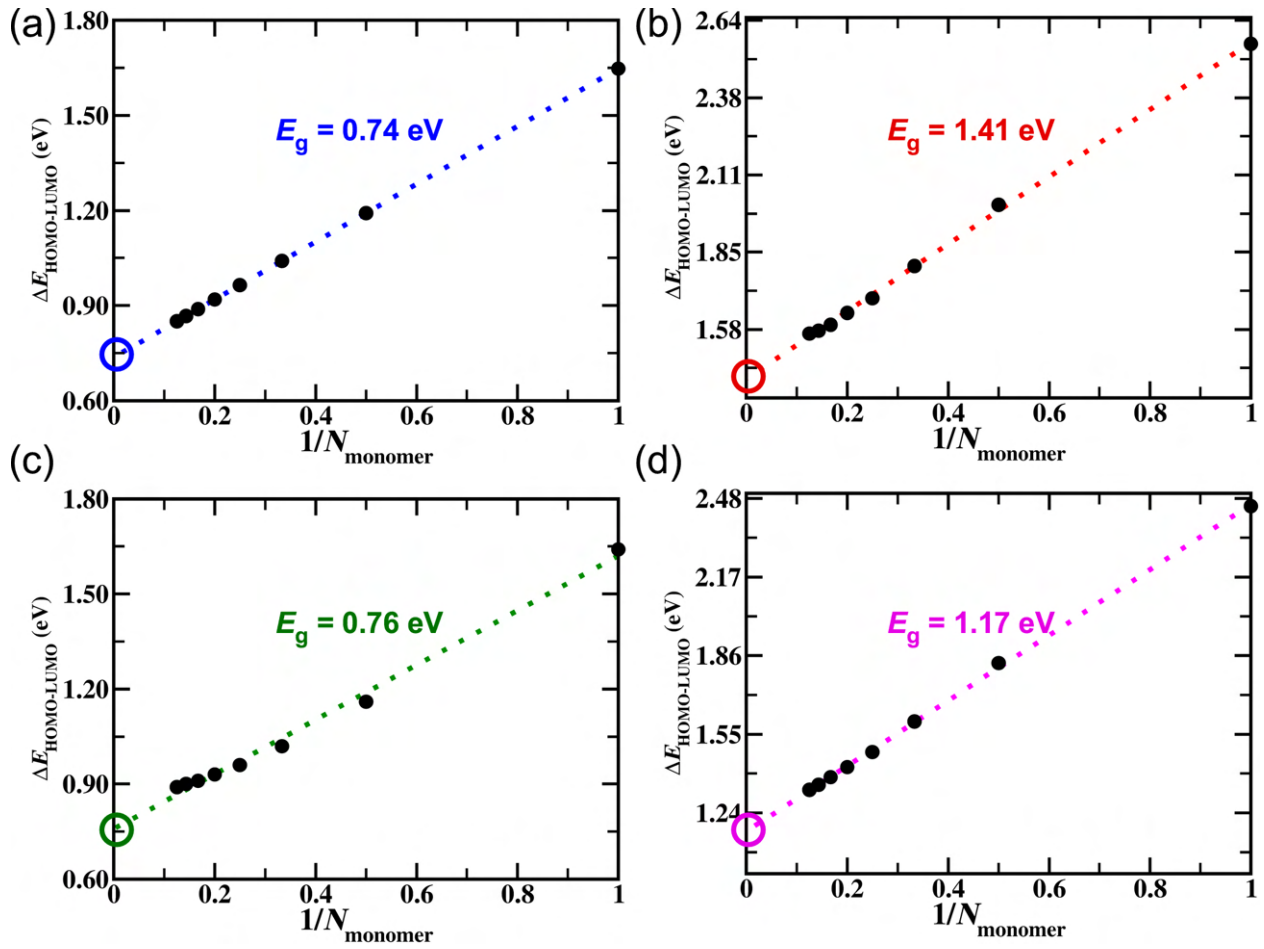


**Figure S55:** Calculated HOMO–LUMO energy gaps as a function of oligomer length ( $N$ ) of (a) CPDT-BBT, (b) CPDT-iso-BBT, (c) CPDS-BBT, and (d) CPDS-iso-BBT polymers. The predicted electrochemical bandgap ( $E_g$ ) is obtained by extrapolation of the calculated HOMO–LUMO gaps to the polymer chain limit ( $N \rightarrow \infty$ ). The calculated HOMO–LUMO gaps are indicated in black filled circles and extrapolated trend is shown in dashed lines.

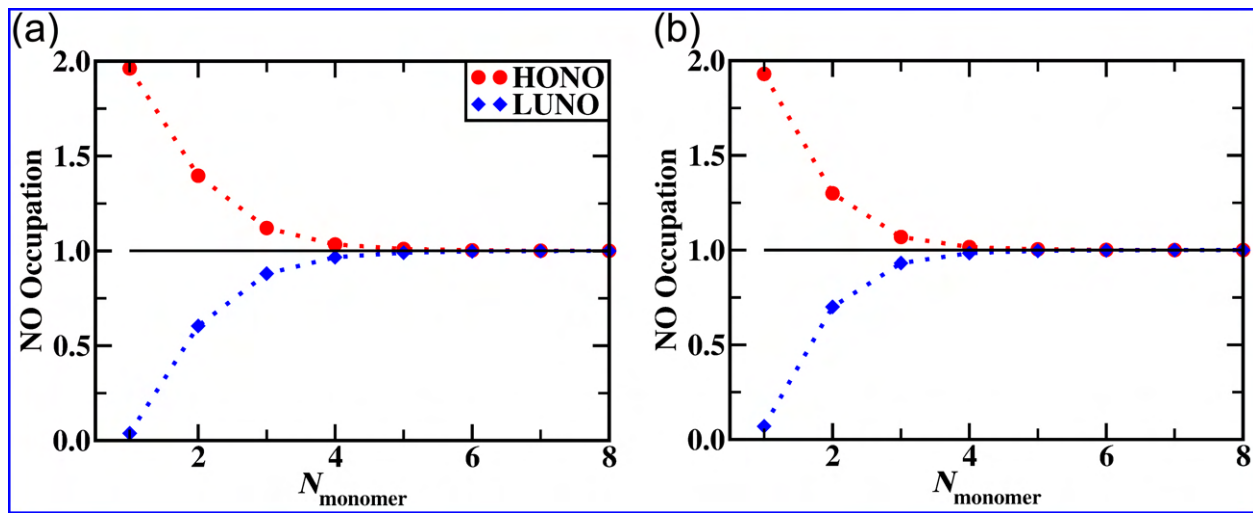


**Figure S56:** Calculated occupation numbers of the highest occupied natural orbital (HONO) and lowest unoccupied natural orbital (LUNO) of (a) CPDT-BBT and (b) CPDS-BBT polymers, obtained as a function of oligomer length ( $N$ ). As more monomers are added to the polymer chain, the HONO decreases, while increasing the LUNO. Both the HONO and LUNO reaches to the saturation (indicated with the solid black lines) for a larger repeat unit, indicating the bond dissociation limit.

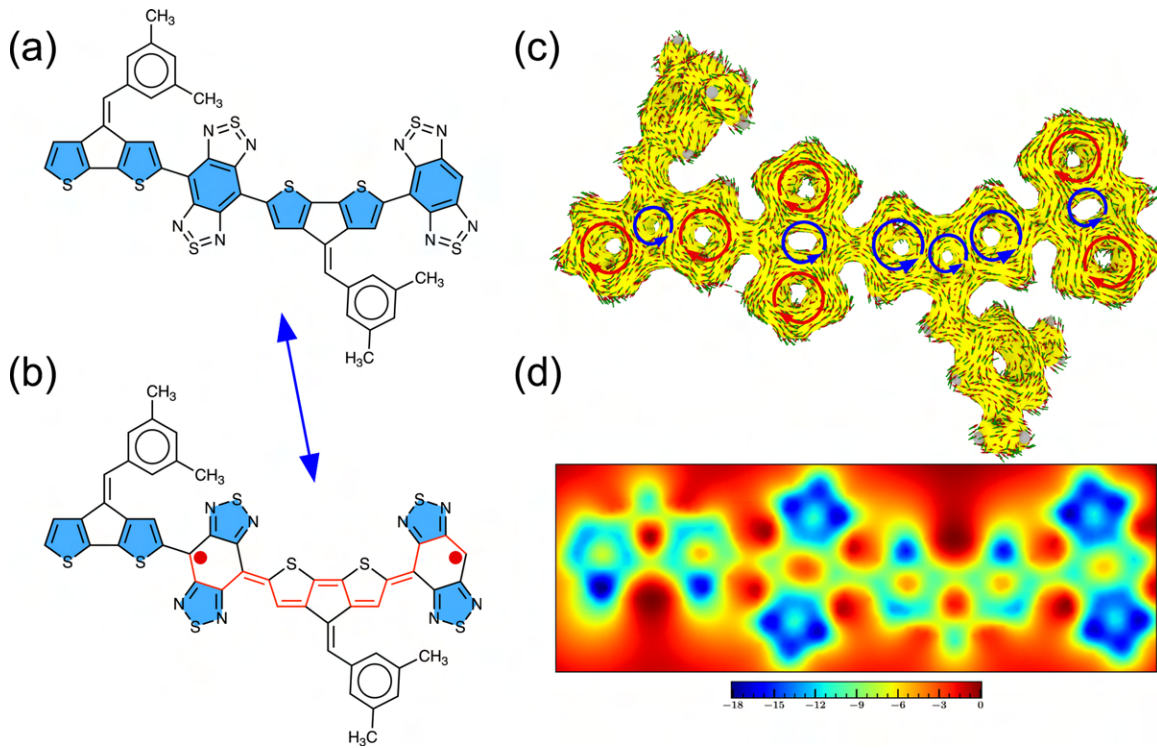


**Figure S57:** Resonance structures and magnetic properties of the CPDT-BBT polymer ( $N = 2$ ) in the singlet ( $S = 0$ ) state. (a–b) The resonance structures indicate regaining aromatic stabilization energy in the thiadiazole units (shaded in blue), (c) ACID plots, and (d) 2D-ICSS (ppm) maps. In the ACID plots, the clockwise (diatropic: aromatic) and counterclockwise (paratropic: quinoidal) ring currents are indicated by red and blue arrows, respectively. The applied magnetic field is perpendicular to the molecular backbone and pointed out through the plane of the molecule. ACID plots were generated with an isovalue = 0.025 a.u.

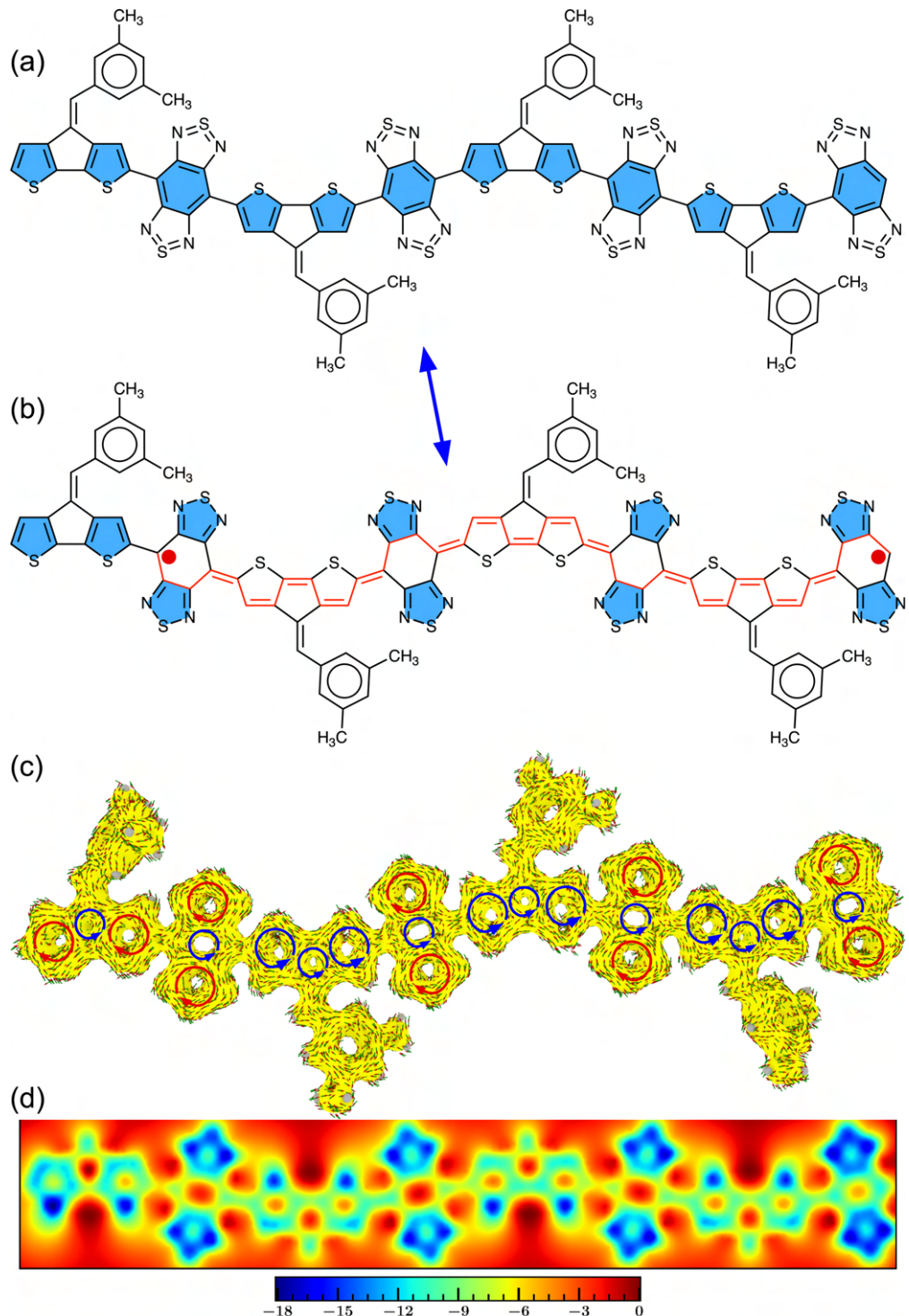


**Figure S58:** Resonance structures and magnetic properties of the CPDT-BBT polymer ( $N = 4$ ) in the singlet ( $S = 0$ ) state. (a–b) The resonance structures indicate regaining aromatic stabilization energy in the thiadiazole units (shaded in blue), (c) ACID plots, and (d) 2D-ICSS (ppm) maps. In the ACID plots, the clockwise (diatropic: aromatic) and counterclockwise (paratropic: quinoidal) ring currents are indicated by red and blue arrows, respectively. The applied magnetic field is perpendicular to the molecular backbone and pointed out through the plane of the molecule. ACID plots were generated with an isovalue = 0.025 a.u.

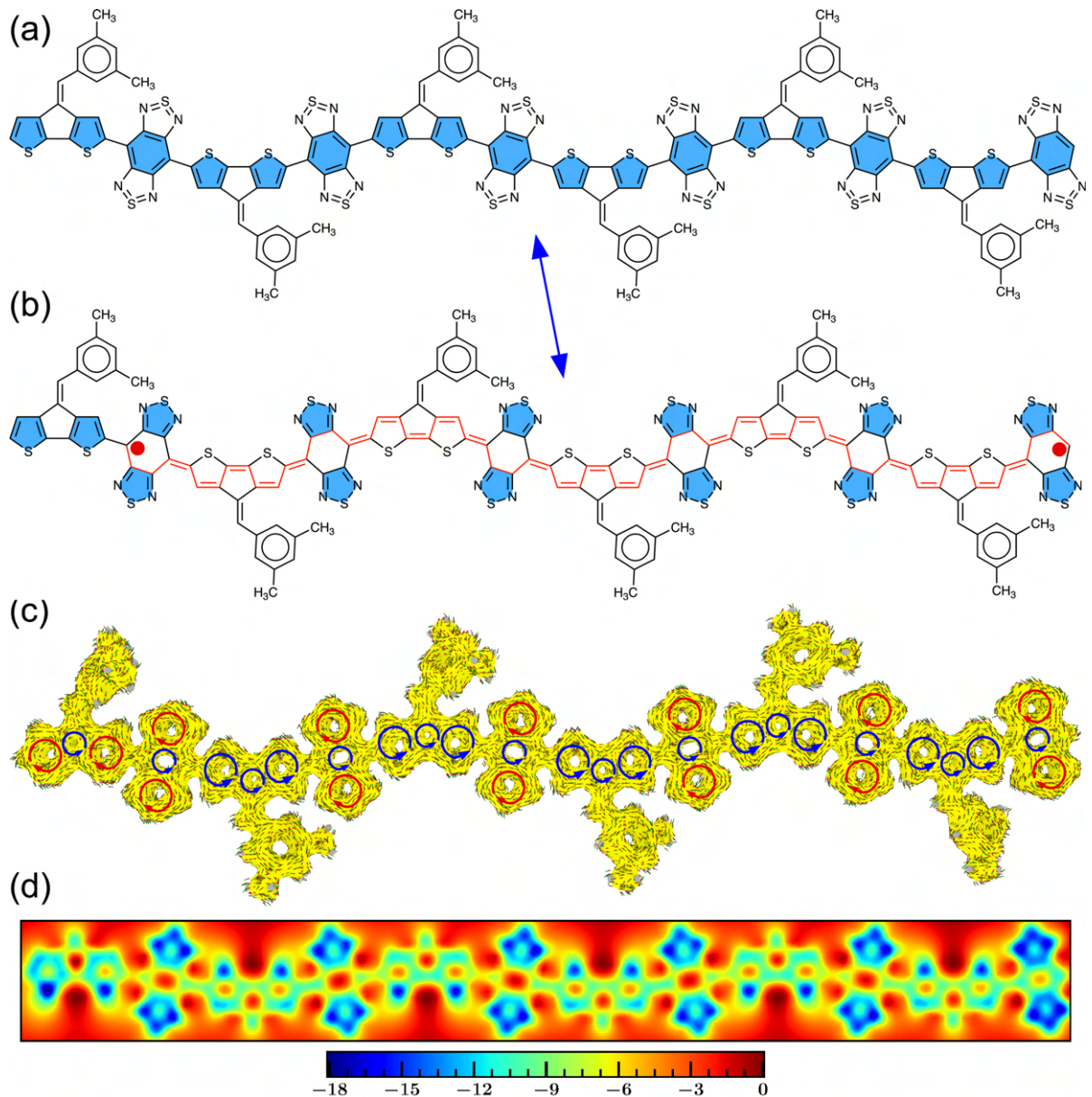


**Figure S59:** Resonance structures and magnetic properties of the CPDT-BBT polymer ( $N = 6$ ) in the singlet ( $S = 0$ ) state. (a–b) The resonance structures indicate regaining aromatic stabilization energy in the thiadiazole units (shaded in blue), (c) ACID plots, and (d) 2D-ICSS (ppm) maps. In the ACID plots, the clockwise (diatropic: aromatic) and counterclockwise (paratropic: quinoidal) ring currents are indicated by red and blue arrows, respectively. The applied magnetic field is perpendicular to the molecular backbone and pointed out through the plane of the molecule. ACID plots were generated with an isovalue = 0.025 a.u.

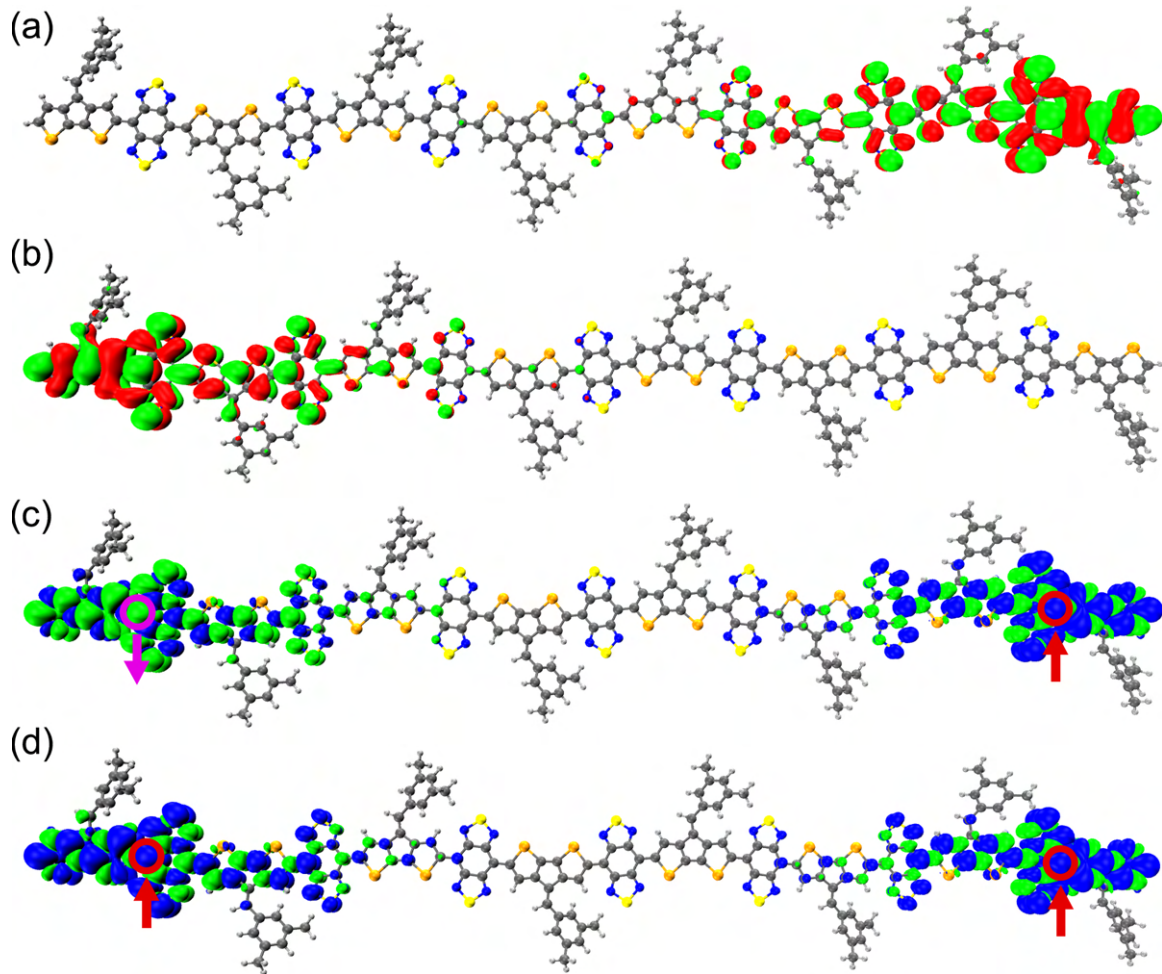


**Figure S60:** Optimized ground-state geometric structures and pictorial representations of the frontier MOs (FMOs) and spin density distribution of CPDS-BBT ( $N = 7$ ) polymer with CPDS donor as the end unit. (a)  $\alpha$ -SOMO and (b)  $\beta$ -SOMO of the open-shell singlet; (c) spin density distribution of the singlet and (d) triplet states. The green and red surfaces represent positive and negative signs of the MO at isovalue = 0.01 au, respectively. The blue and green surfaces represent positive and negative contributions of the spin density at an isovalue = 0.0002 au. The most probable locations for the unpaired electrons are highlighted with open circles (red: up-spin and purple: down-spin).

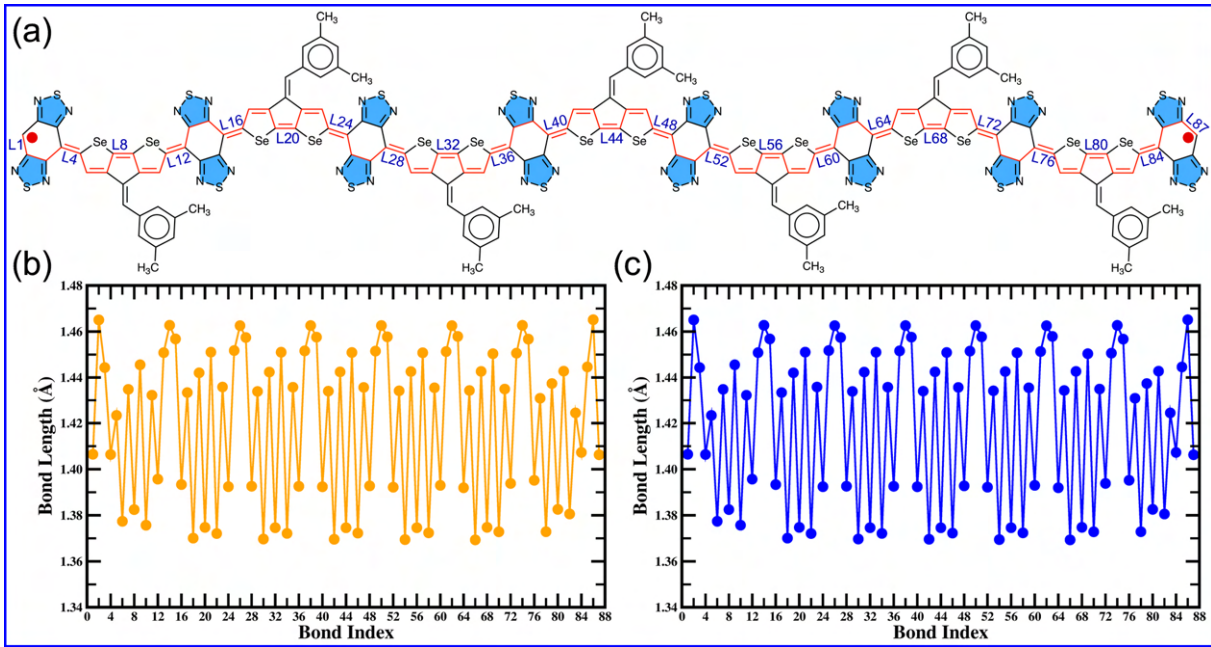


**Figure S61:** Structural and electronic properties of the CPDS-BBT heptamer ( $N = 7$ ) with acceptor end groups in the singlet ( $S = 0$ ) state. (a) Resonance structure show recovery of aromatic stabilizing energy in the acceptor thiadiazole units, calculated bond lengths ( $\text{\AA}$ ) along the conjugation path in the (b) singlet ( $S = 0$ ) and (c) triplet ( $S = 1$ ) states highlighted in red.

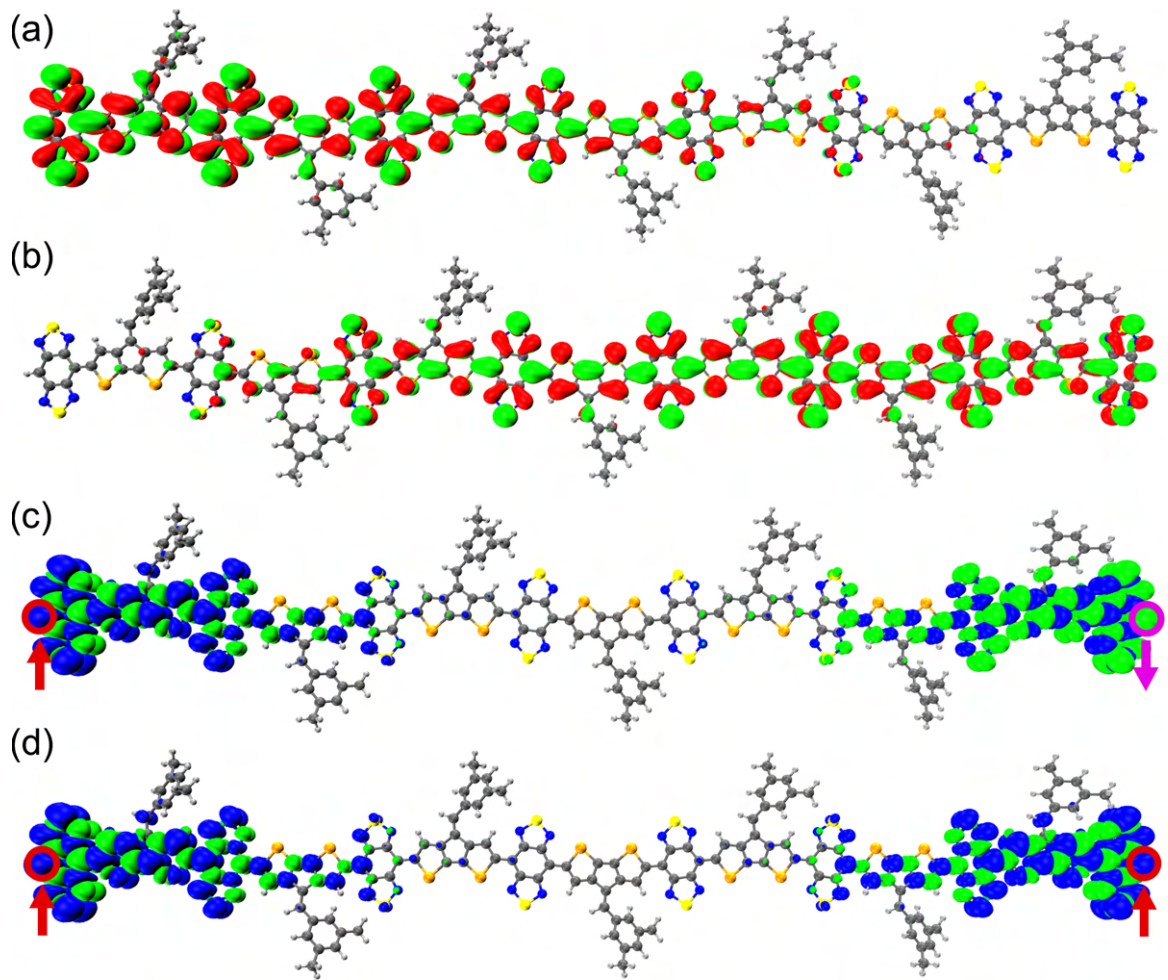


**Figure S62:** Optimized ground-state geometric structures and pictorial representations of the frontier MOs (FMOs) and spin density distribution of CPDS-BBT ( $N = 7$ ) polymer with BBT acceptor as the end unit. (a)  $\alpha$ -SOMO and (b)  $\beta$ -SOMO of the open-shell singlet; (c) spin density distribution of the singlet and (d) triplet states. The green and red surfaces represent positive and negative signs of the MO at isovalue = 0.01 au, respectively. The blue and green surfaces represent positive and negative contributions of the spin density at an isovalue = 0.0002 au. The most probable locations for the unpaired electrons are highlighted with open circles (red: up-spin and purple: down-spin).